TABLE OF CONTENTS

Section		Page
3.1	**General Summary**	**7**
Table 3.1-1	Monticello Unit 1 Core Components Design	8
Table 3.1-2	Design Basis Limits For Fission Product Barriers	10
3.2	**Thermal And Hydraulic Characteristics**	**11**
3.2.1	Design Basis	11
3.2.2	Fuel Damage Limits	11
3.2.3	Design Criteria and Safety Limits	12
3.2.4	Specific Design Characteristics	13
3.2.4.1	Steady-State Limits	13
3.2.4.2	Operating Limit Heat Generation Rate	13
3.2.4.3	CPR Limits for Operation	14
3.2.4.4	Peaking Factors, Flux Tilts and Power Distributions	14
3.2.5	Performance Characteristics for Normal Operation	15
3.2.6	Monticello Operating Map	16
3.2.7	Performance Capability Demonstration	17
3.2.7.1	Steady State Hydraulic Methods	17
3.2.7.2	Transient Core Performance	19
3.3	**Nuclear Characteristics**	**19**
3.3.1.1	Design Basis	19
3.3.2	General Description	20
3.3.3	Nuclear Design Characteristics	20
3.3.3.1	Power Distributions	20
3.3.3.2	Reactivity Coefficients	21
3.3.3.2.1	Doppler Coefficients	22
3.3.3.2.2	Moderator Temperature and Void Coefficients	23
3.3.3.2.3	Power Coefficient	24
3.3.3.3	Reactivity Control	25
3.3.3.4	Control Rod Worth	26
3.3.3.5	Xenon Stability	27
3.3.4	Analytical Methods	28
Table 3.3-1	Physics Data for Typical Fuel Cycle	31

TABLE OF CONTENTS (CONT'D)

Section		Page
Table 3.3-2	Fissionable Isotope Yields	32
3.4	**Fuel Mechanical Characteristics**	**33**
3.4.1	Design Basis	33
3.4.2	Description of Fuel Assemblies	34
3.4.2.1	General	34
3.4.2.2	Fuel Rods	34
3.4.2.3	Water Rods	35
3.4.2.4	Other Fuel Assembly Components	35
3.4.2.5	Channels	36
3.4.3	Design Evaluation	37
3.4.3.1	Material Properties	37
3.4.3.2	Fuel Rod Thermal-Mechanical Design	37
3.4.3.2.1	Cladding Stress Analysis	37
3.4.3.2.2	Cladding Collapse Analysis	38
3.4.3.2.3	Fatigue Analysis	38
3.4.3.2.4	Fuel Cladding Integrity Safety Limit LHGR	38
3.4.3.2.5	Waterlogging	39
3.4.3.2.6	Fretting-Corrosion Wear	39
3.4.3.2.7	Lateral Deflection	39
3.4.3.2.8	Pellet Cladding Interaction	40
3.4.3.2.9	Fuel Densification	40
3.4.3.2.10	Fission Gas Release	41
3.4.3.2.11	Thermal Conductivity Degradation	41
3.4.3.3	Fuel Assembly Structural Design	42
3.4.3.4	Application of the Generic Mechanical Design Evaluation to Reloads	42
3.4.3.5	Overheating of Fuel Pellets	42
3.4.4	Surveillance and Testing	43
3.4.4.1	Unirradiated Fuel	43
3.4.4.2	Irradiated Fuel Rods	43
3.5	**Reactivity Control Mechanical Characteristics**	**44**
3.5.1	Design Basis	44

TABLE OF CONTENTS (CONT'D)

Section		Page
3.5.2	Control Methods	45
3.5.2.1	Description of Control Rods	45
3.5.2.1.1	Standard Control Rods	45
3.5.2.1.2	Advance Design Control Rods	46
3.5.2.2	Mechanical Design of Control Rods	47
3.5.3	Control Rod Drive System	48
3.5.3.1	Rate of Response	48
3.5.3.2	System Description	49
3.5.3.2.1	General Description	49
3.5.3.2.2	Principle of Drive Operation	50
3.5.3.2.2.1	General	50
3.5.3.2.2.2	Control Rod Insertion	51
3.5.3.2.2.3	Control Rod Withdrawal	51
3.5.3.2.2.4	Scram Actuation	52
3.5.3.2.2.5	Mechanical Arrangement	53
3.5.3.2.2.6	Drive Piston and Index Tube	54
3.5.3.2.2.7	Locking Mechanism	55
3.5.3.2.2.8	Piston Tube and Stop Piston	55
3.5.3.2.2.9	Position Indicator	56
3.5.3.2.2.10	Flange and Cylinder Assembly	56
3.5.3.2.2.11	Materials of Construction	57
3.5.3.2.3	Drive Mechanism Tests	58
3.5.3.2.3.1	General	58
3.5.3.2.3.2	Development Drive Tests	58
3.5.3.2.3.3	Production Prototype Tests	59
3.5.3.2.3.4	Factory Quality Control Tests	59
3.5.3.2.3.5	Reactor Pre-Operational Tests	60
3.5.3.3	Control Rod Drive Hydraulic System	60
3.5.3.3.1	System Description	60
3.5.3.3.2	Supply Subsystem	60
3.5.3.3.2.1	General	60
3.5.3.3.2.2	Control Rod Drive (CRD) Pumps	61
3.5.3.3.2.3	Filters	61
3.5.3.3.2.4	Flow Control Station	62

TABLE OF CONTENTS (CONT'D)

Section		Page
3.5.3.3.2.5	Drive Water Pressure Control Station	62
3.5.3.3.2.6	Cooling Water Pressure Control Station	62
3.5.3.3.2.7	Exhaust Header	63
3.5.3.3.2.8	Emergency Source of High-Pressure Water to the Core	63
3.5.3.3.3	Scram Subsystem	63
3.5.3.3.3.1	General	63
3.5.3.3.3.2	Accumulator	64
3.5.3.3.3.3	Scram Pilot Valves	64
3.5.3.3.3.4	Scram Valves	65
3.5.3.3.3.5	Scram Discharge Volumes	65
3.5.3.3.4	Cooling Subsystem	66
3.5.3.3.5	Directional Control	66
3.5.3.3.5.1	General	66
3.5.3.3.5.2	Directional Control Valve Sequencing	67
3.5.4	Control Rod Drive Housing Design	67
3.5.5	Operation and Performance Analysis	68
3.5.5.1	Normal Withdrawal Speed	68
3.5.5.2	Accidental Multiple Operation	69
3.5.5.3	Internal Failures	69
3.5.5.4	Structural and Piping Failures	70
3.5.5.5	Scram Reliability	71
3.5.5.6	Operational Reliability	71
3.6	**Other Reactor Vessel Internals**	**73**
3.6.1	Design Basis	73
3.6.2	Description	74
3.6.2.1	Shroud	74
3.6.2.2	Baffle Plate	74
3.6.2.3	Baffle Plate Support	74
3.6.2.4	Fuel Support Piece	74
3.6.2.5	Control Rod Guide Tubes	75
3.6.2.6	Core Top Guide	75
3.6.2.7	Core Support Plate	75
3.6.2.8	Jet Pumps	75

TABLE OF CONTENTS (CONT'D)

Section		Page
3.6.2.9	Feedwater Sparger	76
3.6.2.10	Core Spray Spargers	76
3.6.2.11	Standby Liquid Control System Sparger	76
3.6.2.12	Steam Separator Assembly	77
3.6.2.13	Steam Dryer Assembly	77
3.6.2.14	Incore Nuclear Instrumentation Tubes	77
3.6.3	Performance Evaluation	78
3.6.3.1	Vibration Measurements	78
3.6.3.1.1	Shroud-Separator Assembly Vibration Measurements	79
3.6.3.1.2	Jet Pump Riser Pipe Vibration Motion (Tangential)	80
3.6.3.1.3	Jet Pump Vibration Motion (Radial at the Top)	81
3.6.3.1.4	In-Core Guide Tube Housing Vibration Motion	81
3.6.3.1.5	Control Rod Guide Tubes	81
3.6.3.1.6	Evaluation of Reactor Internals Flow Induced Vibration	82
3.6.3.2	Pressure Forces During Blowdown	83
3.6.3.2.1	Analytical Model	83
3.6.3.2.2	Recirculation Line Rupture	84
3.6.3.2.3	Steam Line Rupture	85
3.6.3.3	Performance of Reactor Internals	86
3.6.4	Inspection and Testing	88
Table 3.6-1	Reactor Internal Pressure Differentials (psid)	89
3.7	**References**	**90**
FIGURES		**98**
Figure 3.2-1	Power Flow Operating Map	99
Figure 3.3-1	Envelope of Doppler Coefficient Versus Temperature, E= 200 MWd/t	100
Figure 3.3-2	Envelope of Doppler Coefficient Versus Temperature, E= 15,000 MWd/t	101
Figure 3.3-3	Moderator Void Reactivity Coefficient as a Function of Void Percentage and Time of Life	102
Figure 3.3-4	Xenon Reactivity Buildup After Shutdown, Beginning of Life	103
Figure 3.4-1	Typical Core Cell	104
Figure 3.4-2	Schematic of Four Bundle Cell Arrangement	105

TABLE OF CONTENTS (CONT'D)

Section		Page
Figure 3.4-3	Typical GE BWR Fuel Assembly	106
Figure 3.4-4	AREVA 10XM Fuel Assembly	107
Figure 3.5-1	Control Rod Assembly Isometric	108
Figure 3.5-1a	Duralife - 230 Control Blade	109
Figure 3.5-2	Control Rod Assembly and Drive Coupling Isometric	110
Figure 3.5-2a	Hybrid I Control Rod (D-160) Assembly	111
Figure 3.5-3	Control Rod Drive Mechanism Isometric	112
Figure 3.5-4	Control Rod Drive Simplified Component Illustration	113
Figure 3.5-7	Hydraulic Control Unit Isometric	114
Figure 3.6-1	Reactor Vessel Internals	115
Figure 3.6-2	Reactor Vessel and Internal Components Schematic	116
Figure 3.6-5	Dresden-2 Shroud Support Plate Segment Fatigue Analysis	117

3.1 General Summary

This section includes descriptions of the mechanical, thermal-hydraulic and nuclear characteristics of the current fuel load of the reactor. In addition, a functional description of the reactor control systems and reactor vessel internal components is given.

The first of the following subsections (Section 3.2) presents a summary of design performance data for the core. In particular, the thermal-hydraulic characteristics are compared to the design criteria to demonstrate compliance. The thermal-hydraulic operating limits are described in Section 3.2.4. Performance data are presented in Section 3.2.5 for the various modes of operation. The safety limit and the boundaries on the Monticello operating range are discussed in Section 3.2.6. The results of transient analyses show a high degree of effectiveness of the protection system in preventing approach to levels of safety concern. Section 3.2.7 describes core performance capability.

Section 3.3 describes the nuclear aspects of the fuel. Included in this section are analyses for the fuel cycle, reactivity control, and control rod worths. Also included are discussions of the reactivity coefficients and spatial xenon characteristics of the core.

Section 3.4 describes the mechanical aspects of the fuel material (uranium dioxide), the fuel cladding, the fuel rods, and the arrangement of fuel rods in bundles. Section 3.5 describes the mechanical aspects of the movable control rods. These are provided to control reactivity. The control rod drive hydraulic system is designed so that sufficient energy is available to force the control rods into the core under conditions associated with abnormal operational transients and accidents. Control rod insertion speed is sufficient to prevent fuel damage as a result of any abnormal operational transient. Section 3.6 describes both the arrangement of the supporting structure for the core and reactor vessel internal components which are provided to properly distribute the coolant delivered to the reactor vessel. The reactor vessel internals are designed to allow the control rods and core standby cooling systems to perform their safety functions during abnormal operation transients and accidents.

Detailed analytical comparisons of the thermal-hydraulic behavior for normal operation with typical and end-of-cycle power distributions respectively are provided. Data for development of the safety limit, the maximum safety system settings, and the limiting conditions for operation are included in the Technical Specifications.

The physical description of the core, principal core design features and performance parameters for operation at 2004 MWt are presented in Table 3.1-1.

The Design Basis Limits for Fission Product Barriers are located in Table 3.1-2 below.

Table 3.1-1 Monticello Unit 1 Core Components Design

(Page 1 of 2)

Fuel Assembly

Number of fuel assemblies: 484

Movable Control Rods

Number	121
Shape	Cruciform
Pitch	12.0 inches
Stroke	144 inches
Width	9.75 inches
Control Length	143 inches
Control Material	B_4C granules in stainless steel tubes and sheath, and hafnium[1]
Number of Control Material Tubes per Rod	84 (original design, D-120 and D-140A), 72 (D-160 and D-230), or 56 (Marathon and Ultra)
Tube Dimensions[2]	0.188 inch OD x 0.025 inch wall (original design, D-120, D-140A and D-160) 0.220 inch OD x 0.020 inch wall (D-230) 0.298 inch OD x 0.024 inch wall (Marathon)

Core

Equivalent Core Diameter	149.0 inches
Circumscribed Core Diameter	160.1 inches
Core Lattice Pitch	12 inches

THERMAL-HYDRAULIC[3]

General Operating Conditions	Typical Power Distribution
Design Thermal Output	2004 MWt
Reactor Dome Pressure	1025 psia
Steam Flow Rate	8.389×10^6 lb/h
Core Flow Rate	57.6×10^6 lb/h
Fraction of Power Appearing as Heat Flux	0.965
Power Density	48.3 KW/liter
Maximum UO_2 Temperature	2750°F
Volumetric Average Fuel Temperature (typical)	925°F
Power to Flow Ratio at 100% Power and 99 % Core Flow	<50 MWt/Mlbm/hr

[1] For Hybrid I Control Rods (D-160) see Figure 3.5-2a; for D-230 Control Blade see Figure 3.5-1a.
[2] For proprietary Ultra control rod tube dimensions, See Reference 133
[3] This data is for typical 100% power and flow condition and does not reflect data for reduced core flows in the MELLLA+/EFW operating domain.

Table 3.1-1 Monticello Unit 1 Core Components Design

(Page 2 of 2)

Inlet Enthalpy	523.7 Btu/lb
Core Average Exit Void Fraction	0.67 - 0.74 (varies with cycle exposure)
Reactor Average Exit Quality	0.149

NUCLEAR DESIGN DATA

Average Fuel Enrichment

Bundle Type[4]	Wt% U-235	Cycle Loaded	
*DNAB386-16GZ	3.86	27	60400000333
*DNAB387-16GZ	3.87	28	
*DNAB389-11GZ	3.89	28	
*DNAB384-15GZ	3.84	28	
*DNAB374-16GZ	3.74	28	
**XMLC-3966B-14GV75	3.966	29	
**XMLC-3973B-12GV75	3.973	29	
**XMLC-3990B-13GV50	3.990	29	
**XMLC-4052B-12GV75	4.052	30	60400000333
**XMLC-4057B-12GV65	4.057	30	
**XMLC-3958B-12GV75	3.958	30	

Excursion Parameters

λ Prompt Neutron Lifetime	36 microseconds
β Effective Delayed Neutron Fraction	5.29×10^{-3}

* Includes 6 inches of natural UO_2 at bottom and 12 inches of natural UO_2 at top of the fuel column.

** Includes 6 inches of natural UO_2 at bottom and 7.24 inches of natural UO_2 at the top of the fuel column (Reference 114).

[4] The same bundle type identifier below does not necessarily indicate that the fuel pin enrichment layout or Gadolinia Pin enrichment and layout are the same.

Table 3.1-2 Design Basis Limits For Fission Product Barriers

Monticello

Boundary	Design Bases Parameter	Limit	Reference
Fuel Cladding	MCPR	99.9% of fuel rods are prevented from experiencing transition boiling during abnormal operational transient	USAR 3.2.4.3
	Linear Heat Generation Rate	GE14: 13.4 kW/ft during normal ops ATRIUM 10XM : 14.1 kW/ft during normal ops	Core Operating Limits Report (use current revision)
	Fuel Enthalpy	Not more than 280 cal/gram deposited during a reactivity accident.	USAR 3.3.3.4
	Cladding Strain	Not more than 1% plastic strain during an anticipated operational occurrence	USAR 3.4.3.2
	Fuel Burnup - peak pellet	GE14: 70 GWD/MTU ATRIUM 10XM: 74.4 GWD/MTU	Core Operating Limits Report (use current revision)
	Fuel Centerline Temperature	2780°F	USAR 3.4.3.5
	Clad Temperature*	Not more than 2200 °F during a Loss of Coolant Accident	10 CFR 50.46
	Clad Oxidation*	Not more than 17% local oxidation during a Loss of Coolant Accident.	10 CFR 50.46
RCS Boundary	Pressure*	1332 psig steam dome pressure. (Higher pressures allowed at lower elevations. See TS.)	TS 2.1.2
	Stresses*	ASME or ANSI B31.1 Code compliance for normal, upset, faulted conditions, etc., as appropriate for the accident.	10CFR50.55a
	Heat-up/Cool-down*	Applicable ASME Code stress limits.	10CFR50.55a
Primary Containment	Pressure	62 psig maximum, 56 psig design. (ASME Code rating)	USAR 5.2.1.1

*Limits controlled by 10CFR50.46, 10CFR50.55a and/or specific technical specifications require NRC approval to exceed or alter and would not be subject to evaluation under 10CFR50.59(c)(2)(vii).

Notes on selection of Monticello DBLFPBs:

1. Fuel centerline melt is not a DBLFPB for GE fuel in BWRs because it is permitted in certain transients provided the cladding does not exceed 1% plastic strain as a result. See GNF Report NEDE-24011-P-A (Reference 51) “GE Standard Application for Reactor Fuel (GESTAR)” Section 4.2.1.2.4 in the US supplement.

2. The 10CFR 50.46 limit of 1% overall clad oxidation in a LOCA is related to hydrogen generation and does not pertain to cladding integrity.

3. Reference MNGP Calc 01-082, “Basis for Monticello DBLFPB for 10CFR50.59 Criterion 7”.

3.2 Thermal And Hydraulic Characteristics

3.2.1 Design Basis

The design basis employed for the thermal-hydraulic characteristics incorporated in the core design, in conjunction with the plant equipment characteristics, nuclear instrumentation, and the reactor protection system, is to ensure that no fuel damage occurs in normal operation or during operational transients caused by reasonably expected single operator error or equipment malfunction.

The principle inherent in the above statement has been the guide for core design and is also the guide for defining future operating limits.

3.2.2 Fuel Damage Limits

Fuel damage is defined for design purposes as perforation of the cladding which would permit release of fission products to the reactor coolant. The mechanisms which could cause fuel damage in abnormal transients are:

a. Severe overheating of the fuel cladding caused by inadequate cooling. For design purposes, critical power (the onset of the transition from nucleate boiling to film boiling) is conservatively defined as the limit, although fuel damage is not expected to occur until well into the film boiling region.

b. Fracture of the fuel cladding due to strain caused by relative expansion of the UO_2 pellet. A value of 1 percent plastic strain of zircaloy cladding is identified as the safety limit below which fuel damage due to overstraining of the fuel cladding is not expected to occur. Appropriate exposure-dependent LHGR limits are provided in the cycle specific Core Operating Limits Report (COLR) for the various fuel types loaded in that core.

c. Fuel centerline melt is conservatively assumed to lead to fuel failure due to clad overheating or pellet-clad interaction. Appropriate exposure-dependent LHGR limits are provided in the cycle specific COLR for the various fuel types loaded in the core.

The above fuel damage limits are also employed in the development of operating limits to control reactor operation.

3.2.3 Design Criteria and Safety Limits

The fuel cladding integrity limit is set such that no calculated fuel damage would occur as a result of an abnormal operational transient. Because fuel damage is not directly observable, a step-back approach is used to establish a Safety Limit Minimum Critical Power Ratio (SLMCPR). This limit represents a conservative margin relative to the conditions required to maintain fuel cladding integrity. The fuel cladding is one of the physical barriers which separate radioactive materials from the environs. The integrity of this cladding barrier is related to its relative freedom from perforations or cracking. Although some corrosion or use related cracking may occur during the life of the cladding, fission product migration from this source is incrementally cumulative and continuously measurable. Fuel cladding perforations, however, can result from thermal stresses which occur from reactor operation significantly above design conditions and the protection system safety settings. While fission product migration from cladding perforation is just as measurable as that from use related cracking, the thermally caused cladding perforations signal a threshold, beyond which still greater thermal stresses may cause gross rather than incremental cladding deterioration. Therefore, the fuel cladding Safety Limit is defined with margin to the conditions which would produce onset of transition boiling (MCPR of 1.0). These conditions represent a significant departure from the condition intended by design for planned operation. The concept of MCPR, as used in the Global Nuclear Fuel/General Electric GETAB and GEXL14 critical power analysis, is discussed in References 51 and 88.

AREVA methods also recognize that a rapid decrease in heat removal capacity associated with boiling transition could result in high cladding temperatures and subsequent cladding degradation with a loss of fuel integrity. An overview of the AREVA methodology for thermal limits is provided in References 130 and 115. The ACE/ATRIUM 10XM critical power correlation (Reference 117) is used to evaluate the thermal margin for the ATRIUM 10XM fuel. The SPCB critical power correlation (Reference 116) is used in the thermal margin evaluations for the GE14 fuel. The application of the SPCB correlation to GE14 fuel follows the indirect process described in Reference 118. The methodology used by AREVA to calculate SLMCPR is described in Reference 129. Additional information about the calculation of SLMCPR is provided in Section 14.2.

3.2.4 Specific Design Characteristics

3.2.4.1 Steady-State Limits

For purposes of maintaining adequate thermal margin during normal steady-state operation, the minimum critical power ratio must not be less than the required Operating Limit Minimum CPR (OLMCPR) and the maximum linear heat generation rate must be maintained below the design LHGR for the plant. This does not specify the operating power nor does it specify peaking factors. These parameters are determined subject to a number of constraints including the thermal limits given previously. The core and fuel design basis for steady-state operation, i.e., MCPR and LHGR limits, have been defined to provide margin between the steady-state operating condition and any fuel damage condition to accommodate uncertainties and to assure that no fuel damage results even during the worst anticipated transient condition at any time in life. Specifically, the OLMCPR is specified such that at least 99.9% of the fuel rods in the core are expected not to experience boiling transition during the most severe abnormal operational transient. No fuel damage would be expected to occur even if a fuel rod actually experienced a boiling transition.

3.2.4.2 Operating Limit Heat Generation Rate

The peak linear heat generation limits for normal steady-state operation are listed in the Core Operating Limits Report (COLR) for the respective fuels present in that cycle's core. Since the peak cladding temperature following a postulated loss-of-coolant accident is primarily a function of the average heat generation rate of all the rods of a fuel assembly at any axial location, the average planar linear heat generation rate (APLHGR) limits for all fuel types are established during power operation in order to assure that the cladding temperature does not exceed the limit specified in 10CFR50.46. 60400000333

3.2.4.3 CPR Limits for Operation

Onset of transition boiling results in a decrease in heat transfer from the clad and, therefore, elevated clad temperature and the possibility of clad failure.

However, the existence of critical power, or boiling transition, is not a directly observable parameter in an operating reactor. Therefore, the margin to boiling transition is calculated from plant operating parameters such as core power, core flow, feedwater temperature, and core power distribution. The margin for each fuel assembly is characterized by the Critical Power Ratio (CPR) which is the ratio of the bundle power which would produce the onset of transition boiling divided by the actual bundle power. The minimum value of this ratio for any bundle in the core is the Minimum Critical Power Ratio (MCPR). It is assumed that the plant operation is controlled to the nominal protective setpoints via the instrumented variables. The Safety Limit minimum CPR (SLMCPR) has sufficient conservatism to assure that in the event of an abnormal operational transient initiated from the OLMCPR, per Technical Specification, more than 99.9% of the fuel rods in the core are expected to avoid boiling transition. An overview of the AREVA methodology for thermal limits is provided in References 130 and 115. The critical power performance for ATRIUM 10XM fuel is established by means of an empirical correlation based on the results of full scale testing over a wide range of conditions (Reference 117). The critical power performance calculated by AREVA for GE14 fuel, which is not in the AREVA correlation database, is established using the SPCB critical power correlation described in Reference 116 and the methodology for co-resident fuel described in Reference 118. The methodology used by AREVA to calculate SLMCPR is described in Reference 129. The SLMCPR is determined using a statistical analysis that employs a Monte Carlo process that perturbs key input parameters used in the MCPR calculation. The set of uncertainties used in the statistical analyses includes both fuel-related and plant-related uncertainties. The effects of fuel channel bow on the critical power performance are accounted for in the SLMCPR analysis.

Because the boiling transition correlation is based on a large quantity of full scale data, there is a very high confidence that operation of a fuel assembly at the SLMCPR would not produce boiling transition. Thus, although it is not required to establish the Safety Limit, additional margin exists between the Safety Limit and the actual occurrence of loss of cladding integrity. Even if boiling transition were to occur, clad perforation would not be expected.

60400000333

3.2.4.4 Peaking Factors, Flux Tilts and Power Distributions

The design power distribution is divided into several components: the radial peaking factor, the local peaking factor, and the axial peaking factor. The radial peaking factor for a particular fuel assembly is defined as the total power produced in the fuel assembly divided by the core average fuel assembly power. The local peaking factor is defined as the highest heat flux for an individual fuel rod in a node divided by the average heat flux for all the fuel rods in the same node. The axial peaking factor for a particular fuel assembly is defined as the maximum nodal heat flux along the length of that fuel bundle divided by the average nodal heat flux of that bundle.

Peaking factors vary throughout an operating cycle, even at steady-state power operation, because they are affected by withdrawal of control rods to compensate for fuel burnup. The capability of achieving and maintaining an optimum power distribution is directly related to the economics of nuclear power. Thus, limiting assumptions are made in the core sizing process. To demonstrate that the design peaking factors are appropriate, the components are discussed individually.

The design power distribution is used in conjunction with flow and pressure drop distribution computations to determine the thermal conditions of the fuel and the enthalpy conditions of the coolant throughout the core.

The design power distribution is based on detailed calculations of the neutron flux distribution. The analyses have been correlated and verified by operating data and experience.

The limiting constraints in the design of the reactor are stated in terms of the nuclear heat generation rate limit and the OLMCPR operating limit for the plant. The design philosophy used to assure that these limits are met involves the selection of one or more power distributions which are more limiting than expected operating conditions and subsequent verification that under these more stringent conditions, the design limits are met. Therefore, the “design power distribution” is an extreme condition of power. It is certainly not the most extreme condition that could be thought of by employing operating methods contrary to common sense. It is, however, a fair and stringent test of the operability of the reactor as designed to comply with the aforesaid limits. Expected operating conditions are less severe than those represented by a design power distribution which gives the maximum allowable LHGR and the OLMCPR for the plant. However, operation with a less severe power distribution is not a necessary condition for the safety of the reactor.

Since there is an infinite number of operating reactor states which can exist with variations in rod patterns, time in cycle, power level, distribution, flow, etc., which are within the design constraints, it is not possible to determine them all. Constant monitoring of operating conditions using the available plant measurements is the method to ensure compliance with the design objective.

3.2.5 Performance Characteristics for Normal Operation

Variable recirculation flow control provides limited manual load following capability for a BWR. A BWR must operate, however, within certain restrictions due to pump NPSH, overall plant control characteristics, and core thermal power limits. The operating map for Monticello for the normal range of operation is shown in the Monticello Technical Specifications Core Operating Limits Report (COLR).

Assuming the unit to be initially at cold zero power, full power is attained by the following steps. First, the reactor recirculation pumps are started and brought to 30% speed. Control rods are withdrawn until the reactor is critical. Control rod withdrawal then continues to compensate for reactor heatup and then to increase reactor power until feedwater flow is greater than the Low FW Protection Line. Above this feedwater flow, full power is obtained by a combination of flow changes and control rod withdrawals.

3.2.6 Monticello Operating Map

The normal operating range for the Monticello reactor is shown on the operating map in the COLR and Figure 3.2-1. The equipment, nuclear instrumentation, and the reactor protection system in conjunction with the operating procedures maintain operations in allowed regions for normal operating conditions. The boundaries on this map are discussed in the following paragraphs.

1. Natural Circulation - The reactor power and flow would increase along this line as control rods were withdrawn with no recirculation pumps operating.

2. 30% Pump Speed - This line shows the relation between reactor thermal power and total core flow, assuming that the recirc pump speed is held at 30%. 30% pump speed is the runback setpoint for pump cavitation protection. During normal plant shutdowns, recirc pump speed must be maintained at about 30% until shutdown cooling is placed in service.

3. MELLLA Boundary - For core flows less than 57.4%, this line defines the highest allowable power for a given total core flow that has been analyzed and is not to be exceeded for planned operations. Continued operation above the MELLLA Boundary resulting from plant disturbances is not allowed. Immediate action is taken to exit the region above the MELLLA Boundary (Reference 108). In some instances when Extended Flow Window (EFW) operation is prohibited, the MELLLA Boundary, extended to above 57.4% core flow, may define the limit for planned operations.

4. Low FW Protection/Minimum Power - This line provides protection from operating in a region of the Power-Flow Map where there is a potential for pump cavitation damage. An interlock automatically runs the recirculation pumps back to 30% speed when operating below the feedwater flow rate sufficient to provide adequate subcooling for pump NPSH.

5. Scram Region (Region I) (Reference 104) - Operation is not allowed in the Scram Region of the power-flow map when the CDA OPRM upscale trip is inoperable. Immediate manual scram is required upon entry into the Scram Region when the CDA OPRM upscale trip is inoperable. Entry into this region when the CDA OPRM upscale trip is operable is determined by plant procedures.

6. Controlled Entry Region (Region II) - Power distribution controls or continuous monitoring are required for planned entry into the Controlled Entry region when the CDA OPRM upscale trip is inoperable. Immediate exit is required upon entry when the CDA OPRM upscale trip is inoperable. Entry into this region when the CDA OPRM upscale trip is operable is determined by plant procedures.

7. Increased Core Flow (ICF) - Core flow is limited to 105% between a power level of 2004 MWt and 1670 MWt. Below 1670 MWt core flow limit is based on a constant pump speed down to a power level of 751 MWt. Below 751 MWt, core flow is limited to 100% of rated core flow or 57.6×10^6 lbm/hr. (Reference 56 and Attachment 3, Figure 1-1 of Reference 104).

8. Extended Flow Window (EFW) Boundary - The Extended Flow Window (EFW) domain extends from 57.4% to 99% rated core flow. This line defines the highest allowable power for a given total core flow that has been analyzed and is not to be exceeded during planned operations. The MELLLA boundary over the full core flow range represents the highest allowable power for a given total core flow during Single Loop Operations (SLO). Continued operation above the Extended Flow Window (EFW) Boundary resulting from plant disturbances is not permitted. Immediate action is taken to exit the region above the Extended Flow Window (EFW) Boundary. (Reference 104)

9. ARTS Region Boundary – These lines define a boundary where there are step changes in the thermal limits with changes in power and flow. See USAR sections 14.3.1.2 and 14.3.2 for additional description of ARTS.

3.2.7 Performance Capability Demonstration

3.2.7.1 Steady State Hydraulic Methods

The core steady-state hydraulic analysis is performed to establish flow, pressure, enthalpy, void, and quality distributions within the core. This analysis also establishes initial reactor coolant conditions for reactor physics calculations and the analysis of anticipated operational transients. The hydraulic model of the reactor core includes descriptions of the orifices, lower tie plates, fuel rods, fuel assembly spacers, upper tie plates, fuel channels and core bypass flow paths. The core steady-state hydraulic model is composed of separate effects models, which simulate various pressure loss characteristics, and composite models, which simulate the channel-by-channel and core bypass flow paths.

The separate effects hydraulic models of the core and channel components consider frictional, local, elevation, and acceleration hydraulic pressure loss characteristics. The frictional characteristics of the core components are modeled by use of the single phase frictional pressure drop equation with a two-phase multiplier. GE has correlated these multipliers, on a best estimate basis, to a significant amount of multi-rod geometry data (Reference 51), that are representative of modern BWR fuel bundles. The largest collection of this data was acquired from the ATLAS loop during development testing for the GEXL correlation. The data for these correlations cover the range of BWR conditions.

The local pressure drop characteristics have been established in a manner similar to the formulation used for the frictional pressure drop characteristics. It differs to the extent that a local pressure loss coefficient is substituted for the product of friction factor and characteristic length-to-diameter ratio. This is a common hydraulic analysis procedure. This modeling has also been verified (Reference 51) experimentally throughout the range of conditions by the ATLAS loop tests for the GEXL correlation (Reference 2). This modeling technique is used to simulate the pressure losses of the orifice, lower tie plate, spacer, upper tie plate, and lower tie plate bypass flow holes.

The acceleration pressure drop has two components, i.e., area change and density variation. The area change is modeled similar to the local pressure drop. Since an area change is generally treated in this manner, this modeling approach is acceptable. The density variation uses the same formulation as the elevation pressure drop characteristic, except that it accounts for density variations along the fluid channel. This is also a standard hydraulic analysis practice, and is acceptable.

These separate effects hydraulic characteristics are utilized to simulate the hydraulic conditions through the orifices, lower tie plates, fuel rods, water rods, fuel rod spacers, upper tie plates and fuel channel. The core bypass flow paths have been modeled from experimental (Reference 2) results and verified by analytical techniques. These tests were previously reviewed and were found to be acceptable for this use (Reference 5).

The above separate effects hydraulic models, which simulate reactor core component pressure losses and flow paths, permit a composite model of a single fuel channel to be simulated. The fuel channel is then categorized into a fuel “channel type” in order to reduce the number of nodes in the analysis. The fuel channels are grouped by “channel type” and modeled as a single typical channel of that type. Thus, the flow distribution of a particular fuel channel is assumed to be the same as the typical channel for that fuel channel type.

A channel type is classified by five characteristics: (1) orificing type (central or peripheral), (2) fuel geometry, (3) relative bundle power (high power or average), (4) lower tie plate type (drilled or undrilled), and (5) bypass type (finger springs or no finger springs).

With regard to the core relative bundle power distribution, sensitivity studies show (Reference 51) that classification by high power and average power density channels adequately models the core flow distribution. This is due to the fact that average channel characteristics are dominant in establishing the core pressure drop. Therefore, categorization as a function of channel power density need not be broken down into additional sub-channels. The other characteristics completely cover the range of channel type possibilities.

In order to perform channel type categorizations, each fuel channel must have the same pressure drop across its length. This is a major assumption of the steady-state hydraulic analysis. This has been shown to be valid by flow distribution and pressure drop measurements in several operating BWRs (References 6, 7 and 8). These tests further show that the pressure drop across any fuel channel or bypass flow path in the core is the same as for any other fuel channel or bypass flow path in the core. The reports on measurements at Monticello and Quad Cities 1 have been previously accepted (Reference 9) for justification of this assumption.

The steady-state hydraulic analysis uses a digital computer code to calculate the hydraulic characteristics of the core. The code utilizes a trial and error iteration for flow rate, pressure drop, enthalpy, quality, and void distribution for each channel type. It equates the total plenum-to-plenum differential pressure across each flow path, and matches the sum of the flows to the total core flow. For General Electric methods, comparison (Reference 51) of analytical predictions to tests performed in the ATLAS test facility as a function of pressure drop, mass flux, and bundle power show reasonably good agreement, i.e., <6% error for the range of interest.

The steady-state hydraulic methods used by AREVA are described in References 127 and 128. ATRIUM 10XM fuel assemblies have been determined to be hydraulically compatible with the coresident GE14 fuel design in the Monticello reactor for the entire range of the licensed power-to-flow operating map (Reference 119). Detailed calculation results supporting this conclusion are provided in Reference 119 including results for coresident GE14 and ATRIUM 10XM fuel in a representative first transition core, a representative second transition core and for a full core of ATRIUM 10XM fuel.

The ATRIUM 10XM fuel design is geometrically different from the coresident GE14 fuel design, but the designs are hydraulically compatible and satisfy criteria for flow compatibility between the fuel types.

Core bypass flow (defined as leakage flow through the lower tie plate (LTP) flow holes, channel seal, core support plate, and LTP-fuel support interface) is not adversely affected by the introduction of the ATRIUM 10XM fuel design. Analyses at rated conditions show acceptably small core bypass flow variations for core configurations ranging from a full core of GE14 fuel to a full core of ATRIUM 10XM, respectively.

Thermal-hydraulic design and compatibility criteria are satisfied for the Monticello transition cores consisting of GE14 and ATRIUM 10XM fuel for the expected core power distributions and core power/flow conditions encountered during operation.

3.2.7.2 Transient Core Performance

Reactor core performance during abnormal operational transients is analyzed for every core reload to ensure that the minimum critical power ratio of any fuel assembly and the linear heat generation rate along any fuel rod, in the core, are within the safety limits. Summaries of the results of these evaluations are presented in Section 14A.

3.3 Nuclear Characteristics

3.3.1.1 Design Basis

The nuclear characteristics of the core are designed to provide a nuclear dynamic response which:

a. has a strong negative reactivity feedback under severe transient conditions consistent with the requirements of overall plant nuclear-hydrodynamic stability, and

b. has a reactivity response which regulates or damps changes in power level and spatial distribution of power production in the core to a level consistent with safe and efficient operation.

Commensurate with these dynamic characteristics the reactor is designed to operate at full power and to achieve the design exposure.

Characteristic (a) is a major factor in providing shutdown mechanisms in the event of a reactivity excursion. Characteristic (b) assures along with other parameters that there is no inherent tendency for undamped oscillations.

3.3.2 General Description

The Monticello plant utilizes a light-water moderated reactor fueled with slightly enriched uranium dioxide. At operating conditions the moderator is permitted to boil producing a spatially variable density of steam voids within the core. The use of a water moderator produces a neutron energy spectrum such that the fissions are produced principally by thermal neutrons.

The presence of U-238 in uranium dioxide fuel leads to the production of significant quantities of plutonium during core operation. This plutonium contributes both to fuel reactivity and power production of the reactor. In addition, direct fissioning of U-238 by fast neutrons yields approximately seven percent of the total power and contributes to an increased fraction of delayed neutrons in the core. Typical values of neutron lifetime and delayed neutron fraction are given in Table 3.1-1. The U-238 contributes a strong negative Doppler coefficient of reactivity and limits the peak power in excursions. The BWR is not susceptible to xenon-induced instabilities due to the strong negative void reactivity coefficient.

A particular reload core can generally contain a mixture of fuel bundle designs. It is a general characteristic of a BWR core, however, that the individual fuel bundles are loosely coupled; thus, the nuclear characteristics of an individual fuel bundle are not strongly affected by adjacent bundles. Therefore, it is possible to divide the analysis into a “lattice analysis,” the calculation of parameters of an infinite lattice of one bundle type and exposure, and a “core analysis”, the calculation of the parameters of an actual core, using the infinite-lattice parameters as input. Reference 51 describes the lattice analysis for the various bundles and also describes the analysis methods for a reload core licensing analysis using GE/GNF (General Electric/Global Nuclear Fuel) methodology. The results for a specific reload are documented in a Supplemental Reload Licensing Report. Section 3.3 of Reference 115 lists AREVA lattice and core analysis methods. Results from an AREVA analysis for a specific reload are documented in a reload licensing analysis report.

Some design details of the various fuel bundle types are presented in Table 3.1-1.

3.3.3 Nuclear Design Characteristics

3.3.3.1 Power Distributions

The limits on power distribution are determined by the specified acceptable fuel design limits (SAFDL) and by the accident and transient analyses. These limits are reflected in the Technical Specifications as limits on the linear heat generation rate (LHGR), average planar linear heat generation rate (APLHGR) and critical power ratio (CPR). This criterion is met by monitoring the gross radial and axial power distributions and by pre-calculating the local power distributions.

Local power distributions and local peaking factors for the various bundle designs have been pre-calculated as a function of exposure and void fraction as part of the lattice analysis for uncontrolled and controlled configurations.

Because an actual reload core will contain a mixture of fuel assembly exposures, and since local peaking varies with exposure, the new bundles will not necessarily have the lowest local peaking factors at any given time during the reload cycle.

Exposures will be tracked by the plant computer for each six-inch segment of each fuel bundle. Thus in principle, the local peaking factor can be calculated on-line anywhere in the core at any time.

Gross power distributions (radial and axial) will be monitored by periodic Traversing Incore Probe (TIP) scans, which will be updated between scans as necessary by means of the Local Power Range Monitor (LPRM) detectors. This basic method is unaffected either by a core reload or a new fuel design. The calculational method used to transform detector signal to neutron flux and power is discussed in Reference 90. An iterative technique is used to obtain self-consistent axial power and void distributions. This calculational method provides the power distribution in individual bundles in an acceptable manner.

Although the gross radial and axial power distributions will change due to the change in void feedback (and radial self-flattening) this is not a major effect. Since incore methods are used to monitor APLHGR, LHGR, and CPR, the assurance of operating limits is independent of changes in gross power distribution and, therefore, the changes in gross power are not of direct safety significance.

3.3.3.2 Reactivity Coefficients

Reactivity coefficients, the differential changes in reactivity produced by differential changes in core conditions, are useful in calculating relative stability and evaluating response of the core to external disturbances. The base initial condition of the system and the postulated initiating event determine which of the several defined coefficients are significant in evaluating the response of the reactor.

There are three primary reactivity coefficients which characterize the dynamic behavior of boiling water reactors over all operating states. These are the Doppler reactivity coefficient, the moderator temperature reactivity coefficient, and the moderator void reactivity coefficient. Also associated with the BWR is a power reactivity coefficient which is generally associated with xenon stability. However, this coefficient is just a combination of the Doppler and void reactivity coefficients in the power operating range.

In BWRs the Doppler reactivity feedback is more negative with increasing fuel temperature primarily due to the Doppler broadening caused by the resonance absorption broadening of uranium-238 at beginning of cycle and a combination of uranium-238 and plutonium-240 in exposed fuel. Although other heavy metal isotopes (e.g., U-235, Pu-239, etc.) are inherently included in the Doppler model, their importance is negligible for current BWR fuel designs.

Both the moderator temperature and void reactivity coefficients are associated with a change in the moderator density, or, more specifically, the hydrogen- to-fuel ratio. The moderator temperature coefficient is a result of decreasing moderator density with increasing temperature and generally is applied in the start-up or heat-up range. The void coefficient is a result of decreasing moderator density in-channel due to increasing in-channel void fractions.

Characteristically the overall void coefficient is always negative during the complete operating cycle since BWR lattice designs are undermoderated in-channel. The moderator temperature coefficient is negative for most of the operating cycle; however, near the end of cycle the overall moderator temperature coefficient becomes slightly positive. This is due to the fact that the uncontrolled BWR lattice is slightly overmoderated near the end of cycle. This, combined with the fact that more control rods must be withdrawn from the reactor core near the end of cycle to establish criticality, results in the slightly positive overall moderator temperature coefficient.

Limits on reactivity coefficients are set by the transients, accidents, and thermal-hydraulic stability considerations, and General Design Criterion 11 which requires that in the power operating range the net effect of the prompt inherent nuclear feedback characteristics tend to compensate for rapid increases in reactivity. Section 3 of Reference 115 describes Design Criteria and Bases for reactivity coefficients in the AREVA licensing methodology, including any SER restrictions on the applicable models and computer programs that are used. Note that the fundamental behavior of reactivity coefficients is the same for AREVA fuel as it is for other fuel vendors' designs.

3.3.3.2.1 Doppler Coefficients

The Doppler coefficient is of prime importance in reactor safety. The Doppler coefficient is a measure of the reactivity change associated with an increase in the absorption of resonance-energy neutrons caused by a change in the temperature of the material in question. The Doppler reactivity coefficient provides instantaneous negative reactivity feedback to any rise in fuel temperature, on either a gross or local basis. The magnitude of the Doppler coefficient is inherent in the fuel design and does not vary significantly among BWR designs having low fuel enrichment. For most structural and moderator materials, this effect is not significant, but in U-238 and Pu-240 an increase in temperature produces a comparatively large increase in the absorption cross-section. The resulting absorption of neutrons causes a significant loss in reactivity. In BWR fuel, in which approximately 96% of the uranium in UO_2 is U-238, the Doppler coefficient provides an immediate reactivity response that opposes fuel fission rate changes.

Although the reactivity change caused by the Doppler effect is small compared to other power-related reactivity changes during normal operation, it becomes very important during postulated rapid power excursions in which large fuel temperature changes occur. The most severe power excursions are those associated with rod drop accidents. A local Doppler feedback associated with a 3000°F to 5000°F temperature rise is available for terminating the initial excursion.

The Doppler reactivity decrement is derived directly from the lattice calculations by performing two calculations at different fuel temperatures. The results are used to determine the proportionality constant, CDOP, from

$$\frac{\Delta k}{k} = \text{CDOP} \left(\sqrt{T} - \sqrt{T_o}\right)$$

CDOP is fit as a function of lattice exposure and relative water density.

The Doppler coefficient is then generated using

$$\left[\frac{1}{k}\frac{dk}{dT}\right]_{DOP} = \frac{CDOP}{(1 + CDOP(\sqrt{T} - \sqrt{T_o}))2(\sqrt{T})}$$

Maximum and minimum calculated Doppler coefficients as a function of fuel temperature and exposure are shown in Figures 3.3-1 and 3.3-2 for typical fuel central lattices. Uncertainty in the nominal Doppler coefficient application of the point model to three-dimensional analyses and effect of exposure on the Doppler coefficient are discussed in detail in Reference 10 and Reference 11.

3.3.3.2.2 Moderator Temperature and Void Coefficients

Because of the large negative moderator coefficients of reactivity, the BWR has a number of inherent advantages, such as (a) the use of coolant flow as opposed to control rods for load following, (b) the inherent self-flattening of the radial power distribution, (c) the ease of control, and (d) spatial xenon stability.

These coefficients are partial derivatives of the infinite multiplication factor, neutron leakage, and control system worth with respect to the variables of temperature or void content with the reactor near critical. Mathematically these coefficients are represented as follows:

Void Coefficient:

$$\frac{1}{keff}\frac{dkeff}{dV} = \frac{(1\text{-}C)}{keffL}\frac{dkinf^{uc}}{dV} + \frac{C}{keffL}\frac{dkinf^{c}}{dV} + \frac{[k^{uc}(1\text{-}C) + kinf^{c}(C)]}{keff}\frac{d}{dV}\left[\frac{1}{L}\right]$$

Temperature Coefficient:

$$\frac{1}{keff}\frac{dkeff}{dT} = \frac{(1\text{-}C)}{keffL}\frac{dkinf^{uc}}{dT} + \frac{C}{keffL}\frac{dkinf^{c}}{dT} + \frac{[kinf^{uc}(1\text{-}C) + kinf^{c}(C)]}{keff}\frac{d}{dT}\left[\frac{1}{L}\right]$$

where

V = in-channel void fraction

T = average moderator temperature

C = control fraction

L = neutron leakage term

kinf = infinite multiplication factor

keff = effective multiplication factor

uc = uncontrolled fuel

c = controlled fuel

The in-channel void fraction is defined as the volumetric ratio of vapor to liquid and vapor found in the fuel channels.

During normal power operation, constant reactor pressure is maintained by pressure regulators. Consequently, the coolant bulk temperature remains essentially constant and is independent of power level except for minor variations in the subcooled region. Power input to the coolant produces steam voids; therefore, the core steam void fraction depends directly on power level and recirculation flow rate. In the power operating range, boiling is the primary mechanism for moderator density variations, and the void coefficient is most useful as input to stability and transient response calculations.

The only design criterion placed on the void coefficient is the overall void coefficient be negative at every point in the operating cycle. No distinction is made between intra- and inter-assembly moderator coefficients. To verify that the coefficient does not become positive during the complete operating cycle, the coefficient is evaluated at end of cycle as well as beginning of cycle conditions. Figure 3.3-3 presents values for the moderator void reactivity coefficient as a function of void percentage and time of life. As seen from Figure 3.3-3 the moderator void reactivity coefficient is always negative.

The range of values of moderator temperature coefficients encountered in current BWR lattices does not include any that are significant from the safety point of view. Typically, the temperature coefficient may range from $+4x10^{-5}$ Δk/k/°F to $-14x10^{-5}$ Δk/k/°F, depending on base temperature and core exposure. The small magnitude of this coefficient, relative to that associated with steam voids and combined with the long time-constant associated with transfer of heat from the fuel to the coolant, makes the reactivity contribution of moderator temperature change insignificant during rapid transients.

For the reasons stated above, current core design criteria do not impose limits on the value of the temperature coefficient, and effects of minor design changes on the coefficient in members of the same class of core usually are not calculated. A measure of design control over the temperature coefficient is exercised, however, by applying a design limit to the void coefficient. This constraint implies control over the water-to-fuel ratio of the lattice; this, in turn, controls the temperature coefficient. Thus, imposing a quantitative limit on the void coefficient effectively limits the temperature coefficient.

3.3.3.2.3 Power Coefficient

The power coefficient is determined from the composite of all of the significant individual sources of reactivity change associated with a differential change in reactor thermal power assuming xenon reactivity remains constant. Typically the power coefficient at full power is about -0.04 Δk/k per ΔP/P at the beginning of life and decreases in magnitude to -0.03 Δk/k per ΔP/P at 10,000 MWd/t. Such values are well within the range required for adequately damping power and spatial-xenon disturbances. Due to the techniques that are used to derive these coefficients the spatial weighting is part of the calculational model, and therefore is not evaluated.

3.3.3.3 Reactivity Control

Control rods are used during fuel burnup, partly to balance the power distribution effect of steam voids as indicated by the in-core flux monitors. In combination, the control rod and void distributions are used to flatten gross power. The design provides considerable flexibility to control the gross distribution. This permits control of fuel burnup and isotopic composition throughout the core to the extent necessary to counteract the effect of voids on axial power distribution at the end of a fuel cycle, when few control rods remain in the core.

The control rod system is designed to provide adequate control of the maximum excess reactivity during the equilibrium fuel cycle operation. The negative reactivity worth of the gadolinia-containing fuel rods decreases with the depletion of the gadolinia in a nearly linear manner so that it closely matches the depletion of fissile material. Because fuel reactivity is a maximum and control is a minimum at ambient temperature, the shutdown capability is evaluated assuming a cold, xenon-free core. Safety design basis requires that the core, in its maximum reactivity condition, be subcritical with the control rod of highest worth fully withdrawn and all others fully inserted. This limit allows control rod testing at any time in core life and assures that the reactor can be made subcritical by control rods alone.

To assure that the safety design basis is satisfied, an additional design margin is adopted: at any time in the fuel cycle the core can be made subcritical with a margin with the highest worth rod fully withdrawn. The required margin is specified in Technical Specification 3.1.1 “SHUTDOWN MARGIN (SDM).

In addition to the control rod shutdown requirements, the standby liquid control system provides sufficient reactivity control to shut down the reactor from equilibrium full power at any time independent of control rod action. The Supplemental Reload Report (GE/GNF methods) or the reload licensing analysis (AREVA methods) documents that the standby liquid control system can provide adequate shutdown margin for each operating cycle.

Current bundle designs incorporate the use of gadolinia as a burnable poison. With burnable poison in the reload core, fuel reactivity initially decreases, as samarium builds in, then increases to a peak as the burnable poison burns out, then finally decreases until EOC, as fissile nuclide depletion becomes dominant. Thus, the point of maximum core reactivity is generally not BOC but occurs later in the cycle. Burnable poison depletion also causes some control cells to increase in worth, while others may decrease, thus causing the location of the strongest rod to change. The effective multiplication factor in a core configuration with the strongest control rod out, under a cold, xenon-free condition, is calculated for each reload core. This calculation gives shutdown margin directly. The calculations are performed for various exposures during the cycle, with a search for the strongest control rod at each exposure. To ensure conservatism, a sensitivity study is done on exposure for the previous cycle. The Supplemental Reload Licensing Report or the reload licensing analysis for each cycle identifies the minimum shutdown margin for all cycle exposures assuming the strongest worth control rod is completely withdrawn. This information will adequately demonstrate that the Technical Specification shutdown margin requirements are met.

The plant-specific scram reactivity versus time (scram curve) is calculated for EOC (and at the end of an exposure interval) conditions.

The shutdown margin capability of the standby liquid control system is calculated for every core reload. These calculations demonstrate that the Standby Liquid Control System has the capability of bringing the reactor, at any time in cycle, to a sub-critical condition under the most reactive xenon-free state with all of the control rods in the full-out condition. The results to be given in the Supplemental Reload Licensing Report or the reload licensing analysis are necessary to demonstrate that the Standby Liquid Control System Technical Specification requirements are satisfied. See Section 14A for the current cycle standby liquid control shutdown margin capability.

3.3.3.4 Control Rod Worth

In an operating reactor there is a spectrum of possible control rod worths, depending on the reactor state and on control rod patterns chosen for operation. Control rod withdrawal sequences and patterns are selected prior to operation to achieve optimum core performance, and simultaneously, low individual rod worths.

Control rod withdrawal and insertion sequences are established to assure compliance with Banked Position Withdrawal Sequence (BPWS) requirements (References 91 and 92). The requirement that an operator follow these sequences is backed up by the operation of the Rod Worth Minimizer (RWM).

In the reload licensing analysis, the maximum deposited enthalpy is reported each cycle.

Section 2.2.13.2 of Reference 115 describes the CRDA analysis:

"In a severe reactivity initiated accident (RIA), large and rapid deposition of energy in the fuel could result in melting, fragmentation, and dispersal of the fuel. The AREVA methodology complies with the fission product source term guideline in Regulatory Guide 1.77 and the Standard Review Plan that restricts the radially-averaged energy deposition.

The limiting RIA (Reactivity Insertion Accident) for AREVA fuel in a BWR is the control rod drop accident (CRDA). AREVA calculates the maximum radially averaged enthalpy for the CRDA for each reload core in order to assure that the maximum calculated enthalpy is below the 280 cal/gm limit. The control rod drop calculation methodology approved by the NRC is described in Reference 127. The parameterized AREVA control rod drop methodology determines maximum deposited enthalpy as a function of dropped rod worth, effective delayed neutron fraction, Doppler coefficient, and four-bundle local peaking factor.

The CRDA analysis is not part of the normal fuel assembly mechanical analysis but is part of the cycle specific safety analysis performed for each BWR by AREVA."

When the reactor is in the startup or run mode at or below 10% rated thermal power, no control rod shall be moved unless the rod worth minimizer is operable, or an operator or engineer is being used in place of the rod worth minimizer. The RWM provides automatic supervision to assure that out-of-sequence control rods will not be withdrawn or inserted; i.e., it limits operator deviations from planned withdrawal sequences (Section 7.8). It serves as an independent backup of the normal withdrawal procedure followed by the operator. In the event that the RWM fails after withdrawal of at least 12 control rods, or if verified by administrative methods that starup with RWM inoperable has not been performed in the last 12 months, a second independent operator or engineer can manually fulfill the operator-follower control rod pattern conformance function of the RWM. In this case, procedural control is exercised by verifying all control rod positions after the withdrawal of each group, prior to proceeding to the next group. Allowing substitution of a second independent operator or engineer in case of RWM inoperability recognizes the capability to adequately monitor proper rod sequencing in an alternate manner without unduly restricting plant operations. Above 10% power, there is no requirement that the RWM be operable since the control rod drop accident with out-of-sequence rods will result in a peak fuel energy content of less than 280 cal/gm. To assure high RWM availability, the RWM is required to be operating during a startup for the withdrawal of a significant number of control rods for any startup after May 1, 1974.

3.3.3.5 Xenon Stability

The maximum xenon reactivity buildup on shutdown from full power and the rate of xenon reactivity burnout on return to full power when the maximum shutdown xenon buildup occurs, were calculated for representative beginning-of-life and end-of-cycle reactor conditions. The maximum rate of reactivity change is obtained by assuming an instantaneous return to full power. The results of these calculations are shown in Figure 3.3-4 for the beginning-of-life condition. From this analysis it was determined that the maximum reactivity addition caused by burnup of xenon was +0.00010 ($\Delta k/k$)/minute. Assuming a control rod worth of 0.001 $\Delta k/k$ with an insertion rate of 3 in./sec, the reactivity addition by the control rod insertion is -0.00125 ($\Delta k/k$)/minute. Therefore, a very weak control rod can easily compensate for a xenon-burnup reactivity addition. The standby liquid control system, used for emergency shutdown only, is more than adequate to compensate for the reactivity added by xenon decay.

Boiling water reactors do not have instability problems due to xenon. This has been demonstrated by operating BWRs for which xenon instabilities have never been observed (such instabilities would readily be detected by the LPRMs), by special tests which have been conducted on operating BWRs in an attempt to force the reactor into xenon instability, and by calculations. All of these indicators have proven that xenon transients are highly damped in a BWR due to the large negative power coefficient.

The analysis and experiments conducted in this area are reported in Reference 17.

Yields of I-135 and Xe-135 for the various fissionable isotopes are provided in Table 3.3-2.

3.3.4 Analytical Methods

The analytical methods and nuclear data used to determine the nuclear characteristics are similar to those used throughout the industry for water- moderated systems (Reference 18).

General Electric/Global Nuclear Fuel Physics Methods:

The nuclear evaluations of all General Electric BWR cores are performed using the analytical tools and methods described in section 3.3 of Reference 51. The nuclear evaluation procedure is best addressed as two parts: lattice analysis and core analysis.

The lattice analyses are performed during the bundle design process. The results of these single bundle calculations are reduced to "libraries" of lattice reactivities, relative rod powers, and few group cross-sections as functions of instantaneous void, exposure, exposure-void history, exposure-control history, control state, and fuel and moderator temperature, for use in the core analysis. These analyses are dependent upon fuel lattice parameters only and are, therefore, valid for all plants and cycles to which they are applied.

The core analysis is unique for each cycle. It is performed in the months preceding the cycle loading to demonstrate that the core meets all applicable safety limits. The principal tool used in the core analysis is the three-dimensional Boiling Water Reactor Simulator code, which computes power distributions, exposure, and reactor thermal-hydraulic characteristics, with spatially varying voids, control rods, burnable poisons and other variables.

Operating reactor and critical experiments compared to theoretical data provide the precision necessary for reactor design (References 24 and 25). The reactivity calculation of these analytical methods is frequently compared to the actual performance of operating reactors.

Experimental tests have also been used to verify the analytical calculations of both reactivity and isotopic composition. These tests give results nearly identical to the comparisons with the operating plants.

Reference 27 contains a complete discussion of errors, uncertainties, and calculations/data comparisons pertaining to the analytical methods used in the design of BWR cores. General Electric methods are further discussed in Reference 51. As discussed in USAR sections 3, 5, 6, 7, 8, 10, and 14 certain GE analysis is retained from EPU or MELLLA+, so the following limitations and conditions remain applicable to any GE analysis that is retained.

GE obtained NRC approval for the interim use of its analytic methods for BWR power uprate analyses until GE improves its NRC-reviewed and approved experimental and operating data bases that support the analytic methods. GE used the interim analytic approach as described in licensing topical report (LTR) NEDC-33173P-A, “Applicability of GE Methods to Expanded Operating Domains” (Reference 101). The NRC staff reviewed the LTR to verify the following:

- The analytical methods and codes used to perform the design-bases safety analyses will be applied within the applicable NRC-approved validation ranges. The calculation and measurement uncertainties applied to the thermal limit calculations and the models simulating physical phenomena will remain valid for the predicted neutronic and thermal hydraulic core and fuel conditions during steady-state, transient, and accident conditions. The qualification database supporting analytical models simulating physical phenomena remains valid and applicable to the conditions under which it is applied, including those models and key parameters in which specific uncertainties are not applied.

- If the NRC-approved analytical methods and codes are extended outside the applicability ranges, the extension of the specific models are demonstrated to be acceptable or additional margins are applied to the affected downstream safety analyses until such time the supporting qualification data is extended.

The NRC staff's SER or NEDC-33173P, “Applicability of GE Methods to Expanded Operating Domains,” dated January 17, 2008, specifies the limitations that apply to NEDC-33173P (letter from H. K. Nieh of NRC to R. E. Brown of GEH, dated January 17, 2008 (Reference 102)). The NRC staff's revised final SE for NEDC-33173P was issued in a letter dated July 21, 2009 (Reference 103).

NEDC-33173P was used to justify application of GE methods to the MNGP EPU application. Each condition specified in the NRC staff's SER for NEDC-33173P was evaluated for acceptability for MNGP EPU in Enclosure 5, Appendix A of Reference 104. The cycle-specific reload analyses that supported the initial use of MELLLA+ was based on GESTR-M with peak clad temperature (PCT) impact of PRIME used to evaluate fuel rod T/M performance. (Reference 112)

Various revisions or supplements of NEDC-33173P have been issued since the completion of the NRC review for MELLLA+. Future licensing activities must consider past NRC reviews along with any potential needs to upgrade analysis based on more recent NRC reviews associated with NEDC-33173P.

AREVA Methods:

References 125 and 120 respectively discuss the applicability of AREVA methodology to EPU and MELLLA+/EFW extended operating domain operation at Monticello. The Appendices in Reference 125 are of particular note since they include discussion of neutronic methods (App. A), stability (App. B), mixed fuel vendor cores (App. C), void-quality relationships (App. D), thermal conductivity degradation (App. E), AREVA computer code COTRANSA2 cross-sections (App. F) and the extensions of CPR correlation validity to lower reactor pressures (App. G).

The bypass void fraction is confirmed each cycle to remain below 5 percent at all LPRM levels when operating at steady-state conditions within the licensed operating domain. Limiting the bypass voiding to less than 5 percent for long-term steady-state operation ensures that instrumentation is operated within the LPRM specification. For EFW operation, the bypass voiding will be evaluated on a cycle-specific basis to confirm that the void fraction remains below 5 percent at all LPRM levels when operating at steady-state conditions within the EFW upper boundary. The highest calculated bypass voiding at any LPRM level will be provided in the reload licensing analysis.

Table 3.3-1 Physics Data for Typical Fuel Cycle

	Beginning of Cycle	End of Cycle
Exposure, MWd/t	0	13,837
Core enrichment, wt %	2.40	1.13
Delayed neutron fraction	0.00618	0.00529
Neutron lifetime, micro-sec	28.8	35.6
Total Pu, wt %	0.49	0.80
Fissile Pu, wt %	0.36	0.55

NOTE: Data is based on End-of-Cycle 24 and Beginning-of-Cycle 25 information.

Table 3.3-2 Fissionable Isotope Yields

Source	I-135	Xe-135
U-233	0.0415	0.0167
U-234	0.0588	0.0012
U-235	0.0630	0.0013
U-236	0.0588	0.0012
U-238	0.0588	0.0012
Pu-239	0.0670	0.0049
Pu-240	0.0588	0.0012
Pu-241	0.0723	0.0074
Pu-242	0.0588	0.0012
Th-232	0.0519	0.0031

3.4 Fuel Mechanical Characteristics

Monticello may use fuel comprised of a variety of designs for any given core load. A reload batch of fuel generally resides in the reactor for up to four fuel cycles. During that time, continuous improvements and changes are made to bundle designs by the plant's fuel supplier(s). The four reload batches present in the core typically differ from each other in at least some manner of material composition or fabrication process. Frequently, there are at least two product lines of fuel in the reactor with differing lattice dimensions, water rod placements, etc. Additionally, a specific pattern of enrichment and burnable absorber distributions is normally custom-designed for each reload batch. What follows is a general description of the fuel used at Monticello. Detailed descriptions of each bundle design may be found in the documents referenced in the next paragraph.

The core at Monticello contains fuel of the GE14 product line (described in detail in References 59 and 88) and of the AREVA ATRIUM 10XM line (described in detail in References 114 and 119).

3.4.1 Design Basis

The fuel assembly is designed to ensure that possible fuel damage would not result in the release of radioactive materials in excess of applicable regulations. Evaluations are made in conjunction with the core nuclear characteristics, the core hydraulic characteristics, the safety evaluations, the plant equipment characteristics and the instrumentation and protection system to assure that this requirement is met. Adequacy of the fuel assembly is demonstrated if it is shown to provide substantial fission product retention capability during all potential operational modes and sufficient structural integrity to prevent operational impairment of any reactor safety equipment. The fuel cladding and assembly components are designed to withstand:

a. the predicted thermal, pressure, and mechanical interaction loadings occurring during startup testing, normal operation, and abnormal operational transients without impairment of operational capability;

b. loading predicted to occur during handling without impairment of operational capability;

c. in-core loading predicted to occur from an operating basis earthquake (OBE), occurring during normal operating conditions, without impairment of operational capability;

and are evaluated for their capability to withstand:

a. in-core loading predicted to occur from a Safe Shutdown Earthquake (SSE) when occurring during normal operation;

b. control rod drop, pipe breaks inside and outside containment, fuel handling and one recirculation pump seizure accidents.

Determination of the capability to withstand accidents is by analysis of the specific event.

3.4.2 Description of Fuel Assemblies

3.4.2.1 General

The Monticello reactor core is comprised of 121 core cells. Each consists of a control rod and four fuel assemblies which immediately surround it (see Figure 3.4-1). Each core cell is aligned above a four-lobed fuel support piece. The four fuel assemblies are lowered into the core cell and, when seated, springs mounted at the tops of each assembly force the assembly into the corners of the cell such that the sides of the assembly contact the grid beams (see Figure 3.4-2).

A fuel assembly consists of a fuel bundle and a channel which surrounds it (see Figure 3.4-3). Descriptions and analytical results for the channel designs are given in References 28 and 121. Fuel assembly parameters for certain fuel bundle types are given in References 59 and 121. The rods of all bundle types are spaced and supported in a square array by the upper and lower tie plates and several spacers. The lower tie plate has a nose piece which has the function of supporting the fuel assembly in the reactor. The upper tie plate has a handle for transferring the fuel bundle from one location to another. The identifying assembly serial number is engraved on the top of the handle. No two assemblies bear the same serial number. A boss projects from one side of the handle to help ensure proper fuel assembly orientation. Upper and lower tie plates are fabricated from stainless steel castings. In some fuel bundle designs the lower tie plate is designed to capture debris entering the bundle from below. Zircaloy or Inconel fuel rod spacers equipped with springs are employed to maintain rod-to-rod spacing. Finger springs located between the lower tie plate and the channel are utilized to control the bypass flow through that flow path. Fuel assemblies have holes drilled in the lower tie plates which provide an alternate bypass flow path.

3.4.2.2 Fuel Rods

Each fuel rod consists of high density ceramic uranium dioxide fuel pellets stacked within Zircaloy cladding which is evacuated, backfilled with helium and sealed with Zircaloy end plugs welded in each end. For some designs, the cladding consists of the same Zircaloy base material with the inner-most part of the cladding replaced by a thin zirconium liner. This liner is mechanically bonded to the base Zircaloy material during manufacture. The purpose of this liner is to prevent pellet to clad interaction (PCI) failures.

The fuel pellets are manufactured by compacting and sintering uranium dioxide powder into right circular cylindrical pellets with flat or dished ends and chamfered edges. Ceramic uranium dioxide is chemically inert to the cladding at operating temperatures and is resistant to attack by water. Several U-235 enrichments are used in the fuel assemblies to reduce the local peak-to-average fuel rod power ratios. Selected fuel rods within each reload bundle also incorporate gadolinium as burnable poison. Gd_2O_3 is uniformly distributed in the UO_2 pellet and forms a solid solution.

The fuel rod cladding thickness is adequate to be essentially free-standing under the approximately 1000 psia BWR environment. Adequate free volume is provided within each fuel rod in the form of a pellet-to-cladding gap and a plenum region at the top of the fuel rod to accommodate thermal and irradiation expansion of the UO_2 and the internal pressures resulting from the helium fill gas, impurities, and gaseous fission products liberated over the design life of the fuel. A plenum spring, or retainer, is provided in the plenum space to minimize movement of the fuel column inside the fuel rod during fuel shipping and handling. A hydrogen getter may be provided in the plenum space as assurance against chemical attack from the inadvertent admission of moisture or hydrogenous impurities into a fuel rod during manufacturing of earlier fuel types. Improvements in eliminating moisture introduction during the manufacturing process and a reduction in the hydriding susceptibility of the clad materials have allowed elimination of the hydrogen getters.

Three types of fuel rods may be used in a fuel bundle: tie rods, standard rods, and part-length rods. The tie rods in each bundle have lower end plugs which thread into the lower tie plate casting and upper ends which are fastened to the upper tie plate. These tie rods support the weight of the bundle only during fuel handling operations when the assembly is lifted by the handle. Some fuel vendor designs replace tie rods with a “load chain” that uses the central water rod to bear bundle weight while being handled. During operation, the fuel assembly is supported by the lower tie plate. The end plugs of the standard rods have shanks which fit into bosses in the tie plates. For fuel designs that use tie rods, an expansion spring is located over the upper end plug shank of each full-length rod in the assembly to keep the rods seated in the lower tie plate while allowing independent axial expansion by sliding within the holes of the upper tie plate.

Some fuel designs incorporate part-length rods which extend from the lower tie plate to an intermediate point in the assembly. These rods are supported laterally by a number of spacers.

3.4.2.3 Water Rods

Water rods are hollow circular Zircaloy tubes with several holes located at each end to facilitate coolant flow through the assembly. Some fuel vendor designs have square water rods (typically known as "water channels"). Fuel assemblies generally contain one or two water rods and these water rods are generally larger than the fuel rods, each displacing several fuel rods.

One water rod in each bundle positions the fuel spacers axially. This spacer-positioning water rod is equipped with spacer-positioning tabs which are welded to the exterior. Once in position the spacer-positioning rod is prevented from disengaging by engagement of its lower end plug with the lower tie plate hole.

3.4.2.4 Other Fuel Assembly Components

The primary function of the fuel spacer is to provide lateral support and spacing of the fuel rods, with consideration of thermal-hydraulic performance, fretting wear, strength, and neutron economy. The spacer represents an optimization of all these considerations.

Finger springs are employed to control the bypass flow through the channel-to- lower tieplate flow path.

These finger spring seals, located between the lower tie plate and the channel, provide control over the flow through this path due to channel wall deflections by maintaining a nearly constant flow area as the channel wall deforms.

The upper and lower tieplates serve the functions of supporting the weight of the fuel and positioning the rod ends during all phases of operation and handling. Both the upper and lower tieplates are shown in Figure 3.4-3. The lower tieplates have holes drilled through them which provide an alternate bypass flow path.

3.4.2.5 Channels

The BWR Zircaloy fuel channel performs the following functions:

a. forms the fuel bundle flow path outer periphery for bundle coolant flow;

b. provides surfaces for control rod guidance in the reactor core;

c. provides structural stiffness to the fuel bundle during lateral loadings applied from fuel rods through the fuel spacers;

d. minimizes, in conjunction with the finger springs and bundle lower tieplate, coolant flow leakage at the channel/lower tieplate interface;

e. transmits fuel assembly seismic loadings to the top guide and fuel support of the core internal structures;

f. provides a heat sink during loss-of-coolant accident (LOCA); and

g. provides a stagnation envelope for in-core fuel sipping.

The channel is open at the bottom and makes a sliding seal fit on the lower tieplate surface. The upper ends of the fuel assemblies in a four-bundle cell are positioned in the corners of the cell against the top guide beams by the channel fastener springs. At the top of the channel, two diagonally opposite corners have welded tabs, one of which supports the weight of the channel from a threaded raised post on the upper tieplate. One of these raised posts has a threaded hole. The channel is attached using the threaded channel fastener assembly, which also includes the fuel assembly positioning spring. Channel-to-channel spacing is provided for by means of spacer buttons located on the upper portion of the channel adjacent to the control rod passage area (Reference 59).

In 1988, a foreign facility identified channel box bowing as a contributory cause of actual fuel failures. Bowing of the channel boxes away from the control blade increases the water gap between assemblies. The increased neutron moderation associated with the increased water gap widths led to very high localized power peaking. Due to erroneous MCPR calculations, some of the fuel rods were operated beyond the MCPR safety limit. The NRC issued Information Notice 89-69 (Reference 64) and Bulletin 90-02 (Reference 65) in response to this event.

The channel boxes bow as they are exposed to a flux gradient. Generally, one channel box remains on an assembly through its life in the reactor. The channel box could then be reused on a fresh fuel assembly. Channel bow tends to increase with increased exposure. Expected channel bow is accounted for in the reload licensing analysis done for each operating cycle. According to NRC Bulletin 90-02, reuse of channel boxes must receive prior review and approval by the NRC staff. Monticello generally elects to install new channels on fresh fuel rather than reusing channels.

3.4.3 Design Evaluation

3.4.3.1 Material Properties

The basic materials used in fuel assemblies are Zircaloy-2 and Zircaloy-4, stainless steel, Inconel and ceramic uranium dioxide and gadolinia. These materials have been proven through years of reactor experience to be compatible with BWR conditions and to retain their design function capability during reactor operation. Typical material properties used in the analysis of the fuel are given in Reference 29.

3.4.3.2 Fuel Rod Thermal-Mechanical Design

A 1% plastic strain limit is used as a safety limit for the Zircaloy-2 fuel rod cladding. Below this safety limit, perforation of the cladding, due to overstraining, is not expected to occur.

The fuel vendor establishes elastic stress limits for the fuel rod mechanical design during normal and abnormal operating reactor conditions which are based on the stress categories presented in the ASME Boiler and Pressure Vessel Code, Section III. The cladding is also designed to be freestanding during the fuel design lifetime. A fatigue analysis was performed to assure that the cladding will not fail as a result of cumulative fatigue damage. A thermal-mechanical evaluation is performed to calculate the local linear heat generation rate (LHGR) corresponding to a fuel rod thermal expansion that induces 1% plastic strain on the cladding material. This equivalent LHGR is established as the fuel cladding integrity safety limit for abnormal operational transients. Pellet cladding interaction, waterlogging, fretting-corrosion, hydriding, and lateral deflection have also been considered in the fuel rod mechanical design. References 51, 59, and 88 for GNF fuel designs and References 114 and 119 through 122 for AREVA designs demonstrate compliance with the applicable design limits.

3.4.3.2.1 Cladding Stress Analysis

The effects of various stresses on the fuel cladding have been evaluated by the fuel bundle supplier for Monticello. The cladding is evaluated to ensure that the fuel will not fail due to stresses or strains exceeding the fuel component mechanical capability. Operating conditions assumed in the analysis are taken to bound conditions anticipated during normal steady state operations and anticipated operational occurrences.

Compliance with acceptance criteria is evaluated based on calculated design ratios. The limiting stresses used in these evaluations were patterned after ANSI/ANS-57.5-1981 (Reference 86). Stress and strain evaluations are performed for each fuel product line.

Compliance with the defined limits (References 51 and 122) has been demonstrated for the fuel product lines currently loaded in the Monticello core (References 59, 88, 114, and 121).

3.4.3.2.2 Cladding Collapse Analysis

The fuel rod design is evaluated to ensure that fuel rod failure due to a cladding collapse into a fuel column axial gap will not occur. The analysis performed by the fuel supplier demonstrates cladding structural instability will not occur during normal operations.

Cladding creep analyses are performed at exposures through end of life. A cladding overpressure transient is assumed to occur at the most conservative exposure. The ability of the cladding to withstand the pressurization transient without collapse due to structural instability demonstrates that applicable limits for cladding collapse are met.

Compliance with the defined limits (References 51 and 122) has been demonstrated for the fuel product lines currently loaded in the Monticello core (References 59, 88, 114, and 121).

3.4.3.2.3 Fatigue Analysis

The effects of cladding fatigue resulting from cyclic loading have been evaluated by the fuel bundle supplier for Monticello to ensure that fatigue loading capability will not be exceeded. The fatigue analysis accounts for internal and external pressure changes, cladding temperature changes, and loading changes resulting from pellet-clad contact.

Compliance with the acceptance criteria is evaluated based on calculated design ratios of fatigue relative to material fatigue capability. The fatigue evaluations are performed for each fuel product line.

Compliance with the defined limits (References 51 and 122) has been demonstrated for the fuel product lines currently loaded in the Monticello core (References 59, 88, 114, and 121).

3.4.3.2.4 Fuel Cladding Integrity Safety Limit LHGR

In order to avoid fuel rod rupture due to excessive cladding strain caused by rapid thermal expansion of the fuel pellet, Monticello's fuel supplier has established a cladding plastic strain limit of 1%. Using the previously accepted methods for calculating cladding strains, exposure-dependent linear heat generation rates (LHGRs) corresponding to 1% cladding plastic strain were determined by each fuel supplier.

3.4.3.2.5 Waterlogging

The safety aspects of waterlogging failures that could result from pellet cladding interaction (PCI) was reviewed. A survey of the available information, which includes: (1) test results from SPERT and NSRR (Reference 73) in Japan and (2) observations of waterlogging failures in commercial reactors, indicates that rupture of a waterlogged fuel rod should not result in failure propagation or significant fuel assembly damage that would affect coolability of the fuel rod assembly.

3.4.3.2.6 Fretting-Corrosion Wear

Fuel designs are evaluated by the vendor to ensure that a loss of fuel integrity will not occur due to fretting wear when the fuel is operated in an environment free from foreign material. This evaluation includes consideration of flow induced vibration at the points of contact between the spacers and fuel rods which have the potential to increase fretting wear. In order to achieve the design basis described above, fuel bundle designs are evaluated with respect to their potential for fretting wear on the basis of testing and significant operating experience with similar fuel designs.

Metal thinning of Zircaloy components due to corrosion will result in higher stresses being calculated at the end of life if the loading conditions do not change. The increase in stress is more than offset by the increase in material strength due to irradiation. However, the fatigue strength of the Zircaloy components is not increased with irradiation. Where load cycling is potentially significant, the effects of corrosion are explicitly addressed.

Compliance with the defined limits (References 51 and 122) has been demonstrated for the fuel product lines currently loaded in the Monticello core (References 59, 88, 114, and 121).

3.4.3.2.7 Lateral Deflection

The fuel rod is evaluated to ensure that fuel rod bowing does not result in fuel failure due to boiling transition. The extent of fuel rod to fuel rod gap closure resulting from rod bowing caused by fuel rod growth is determined by visual inspection of the peripheral fuel rods. This visual inspection is performed as a part of the vendor's fuel surveillance programs and other inspections (References 51 and 122).

The design limit for fuel rod lateral deflection is that contact between rods, fuel rods and water rods, and fuel rods and the channel will not result in failure from transition boiling. This operational fuel rod deflection evaluation performed by the fuel vendor includes consideration of manufacturing tolerances, thermal effects, and axial loads.

Compliance with the defined limits (References 51 and 122) has been demonstrated for the fuel product lines currently loaded in the Monticello core (References 59, 88, 114, and 121).

3.4.3.2.8 Pellet Cladding Interaction

The fuel rods are evaluated to ensure that fuel rod failure due to pellet-cladding mechanical interaction (PCI) will not occur. To meet this design basis, the fuel rod is evaluated to show that calculated cladding circumferential plastic strain will not exceed 1% during anticipated operational occurrences.

Fuel vendor evaluations to demonstrate that fuel failure does not occur due to PCI consider fuel thermal expansion, fuel phase change resulting from fuel melt, and power spiking caused by fuel densification. Calculations are performed for the most limiting transient expected to occur during the fuel rod life, assuming the most conservative combination of fuel rod dimensions allowed by manufacturing tolerances.

In addition, the fuel product line used in the MNGP core utilizes a zirconium cladding liner whose purpose is to prevent pellet to clad interaction (PCI) failures (USAR Section 3.4.2.2).

Compliance with the defined limits (References 51 and 122) has been demonstrated for the fuel product lines currently loaded in the Monticello core (References 59, 88, 114, and 121).

3.4.3.2.9 Fuel Densification

The effects of fuel densification on the fuel rod are to increase the stored energy, increase the linear thermal output and increase the probability of local power spikes from axial gaps.

The primary effects of densification on the fuel rod mechanical design are manifested in the calculation for fuel/cladding gap conductance, cladding collapse time and fuel duty (stress and fatigue evaluations). The approved analytical model incorporates time-dependent gap closure and cladding creepdown for the calculation of gap conductance. The cladding collapse time calculation also includes the effect of local gaps on cladding temperature. Finally, cladding collapse has never been observed in BWR fuels.

Fuel densification analyses submitted by GE (Reference 42) and approved by the staff (Reference 43) have addressed the effects of increased densification in gadolinia-urania fuels. The stored energy effects of increased densification in gadolinia-urania fuels are offset by the significantly lower LHGR in the gadolinia bearing fuel rods compared to the non-gadolinia bearing fuel rods in the bundle. With regard to densification power spiking effects, GE has shown that the offsetting effects of excess thermal expansion and axial heat transfer, not previously taken credit for, more than offsets the adverse spiking effects associated with gadolinia. AREVA evaluations further note that fuel densification and swelling are limited by the design criteria for fuel temperature, cladding strain, cladding collapse, and rod internal pressure criteria. Although there are no explicit criteria for fuel densification and swelling, the effects of these phenomena are included in the fuel rod performance code used in evaluations (Reference 114).

3.4.3.2.10 Fission Gas Release

Cladding creep rate due to internal pressurization from fission gas release has been evaluated by the fuel vendor. The fuel rod is evaluated to ensure that the effects of fuel rod internal pressure during normal steady-state operation will not result in fuel rod failure due to excessive cladding pressure loading.

The design basis is achieved by conservatively limiting the rate of cladding outward creep due to internal gas pressure during normal steady state operation such that it does not exceed the instantaneous fuel rod irradiation swelling rate.

Compliance with the defined limits (References 51 and 122) has been demonstrated for the fuel product lines currently loaded in the Monticello core (References 59, 88, 114, and 121).

3.4.3.2.11 Thermal Conductivity Degradation

GE/GNF Methods:

The PRIME code was developed to address a number of concerns, including Thermal Conductivity Degradation. PRIME replaces the GESTR-M code. The change to the PRIME model is principally seen by the ECCS-LOCA analysis in terms of changes of pellet thermal conductivity and changes in conductivity of the gas in the gap. The documented effect is that initial fuel temperature on average is slightly higher using the PRIME model compared to GESTR-M. As regards ECCS-LOCA analysis, this is characterized as a small increase in stored energy in the fuel as an initial condition. The LOCA analysis and other analyses (e.g., transient analyses) used for licensing of EPU were performed using GESTR-M fuel thermal mechanical properties. While the Monticello LOCA analysis was not performed using PRIME, the PCT and metal-water reaction percentage have been adjusted to account for the impact of PRIME. The use of PRIME for evaluation of ATWS PCT and maximum bulk suppression pool temperature results in slight temperature increases, but no effect on maximum vessel pressure. The fuel thermal mechanical design incorporates a 350 psi penalty on fuel rod critical pressure due to the use of GESTR-M. For analyses other than the LOCA, ATWS, fuel thermal mechanical design, the use of GESTR-M is an insignificant difference. Both GESTR-M and PRIME are acceptable methods per GESTAR II. GESTR-M is used for cycle specific analyses for the duration of Cycle 27, but subsequently the cycle specific analysis will be based on PRIME. (Reference 107)

AREVA Methods:

AREVA's RODEX4 (Reference 124) is a best-estimate, state-of-the-art fuel code that fully accounts for burnup degradation of fuel thermal conductivity. RODEX4 can therefore be used to quantify the impact of burnup-dependent fuel thermal conductivity degradation and its effect on key analysis parameters.

Thermal-mechanical licensing safety analyses for the Monticello ATRIUM 10XM fuel are performed with RODEX4 and therefore explicitly account for thermal conductivity degradation. No additional assessment is needed for those analyses.

AREVA has evaluated the impact of Thermal Conductivity Degradation (TCD) on thermal-hydraulic and safety analyses that do not include TCD explicitly. These included analyses of anticipated operational occurrences (AOOs), loss of coolant accidents (LOCAs), overpressurization, stability, and fire events. Results of these evaluations were acceptable and are further discussed in Reference 125.

3.4.3.3 Fuel Assembly Structural Design

The fuel assemblies used at Monticello are designed to withstand the predicted thermal, pressure, and mechanical interaction loadings that can occur during handling, startup, normal operation, and abnormal operational transients without impairment of functional capability. The fuel assemblies are designed to sustain predicted loadings from an operating basis earthquake. The design-analysis of the fuel assembly also shows that the functional capabilities will not be exceeded as a result of a safe-shutdown earthquake. The ability of the fuel assemblies and their components to meet these capabilities has been evaluated by the fuel supplier for Monticello (References 51, 59, 88, and 121).

The adequacy of the fuel assembly structure during normal operations and normal operating transients is based principally on stress limits and stress formulations which are consistent with the requirements of the ASME Boiler and Pressure Vessel Code Section III. A detailed description of the stress categories is given in Table 2.5.3-1 of Reference 51, US Supplement, Appendix B for GE fuel and sections 3.2.7 and 3.3.1 of Reference 122 for AREVA fuel.

USAR Section 14 addresses the capability of the fuel assembly to withstand the control rod drop accident, pipe breaks inside and outside of containment, the fuel handling accident, and the recirculation pump seizure transient.

3.4.3.4 Application of the Generic Mechanical Design Evaluation to Reloads

Design parameters which vary from one fuel type (e.g., fuel stack length) to another, or from one operating BWR plant to another, have been considered to the greatest extent possible in the generic mechanical design evaluation. This evaluation assumed the most limiting combination of tolerances for all critical fuel dimensions together with plant design conditions (e.g., core operating pressure, maximum power vs. exposure for the peak duty fuel rod) which were expected to be bounding for all future reload cycle. The continued conservatism of the generically assumed design parameter values are verified for each particular reload application. GE/GNF internal procedures for the validation process together with design parameters reviewed for each reload application are summarized in Reference 51. AREVA's use of generic evaluations is summarized in Reference 114.

3.4.3.5 Overheating of Fuel Pellets

In order to avoid fuel rod cladding failure due to overheating, AREVA analysis precludes fuel centerline melting for normal operation and AOOs. RODEX4 (Reference 124) is used to determine maximum possible fuel centerline temperatures, which are compared to the limit of 2780°F for pellets containing only UO_2 and 2680°F for pellets containing Gd_2O_3.

3.4.4 Surveillance and Testing

3.4.4.1 Unirradiated Fuel

Monticello's fuel suppliers enforce rigid quality control requirements at every stage of fuel manufacturing to ensure that the design specifications are met. Written manufacturing procedures and quality control plans define the steps in the manufacturing process. The operator of the Monticello plant routinely inspects and audits the fuel design and fabrication activities of the plant's fuel supplier to ensure that a quality assurance program in accordance with 10CFR50 Appendix B is being implemented effectively. Dimensional measurements and visual inspections of critical areas such as fuel rod-to-rod clearances are performed after assembly and after arrival at the reactor site.

Prototype testing is utilized and, for example, is an important element of AREVA's methodology for demonstrating compliance with structural design requirements. Results from design verification testing may directly demonstrate compliance with criteria or may be used as input to design analyses. Testing performed to qualify the mechanical design or evaluate assembly characteristics includes fuel assembly axial load structural strength testing, spacer grid lateral impact strength testing, tie plate lateral load strength tests and LTP axial compression testing, debris filter efficiency testing, fuel assembly fretting testing, fuel assembly static lateral deflection testing, fuel assembly lateral vibration testing, and fuel assembly impact testing (Reference 122).

3.4.4.2 Irradiated Fuel Rods

The Monticello plant benefits from its fuel suppliers' ongoing programs of surveillance of BWR fuel, both production and developmental, which operates beyond current experience. The schedule of inspection is, of course, contingent on the availability of the fuel as influenced by plant operation.

Full-length, lead use fuel rods selected with respect to exposure, linear heat generation rate, and the combination of both are inspected. Inspection techniques used may include:

a. Leak detection tests, such as "sipping."

b. Visual inspection with various aids such as binoculars, borescope, periscope, and/or underwater TV with a photographic record of observations as appropriate.

c. Nondestructive testing of selected fuel rods by ultrasonic test techniques.

d. Dimensional measurements of selected fuel rods.

Unexpected conditions or abnormalities which may arise, such as distortions, cladding perforation, or surface disturbances are analyzed. Resolution of specific technical questions indicated by site examinations may require examination of selected fuel rods in Radioactive Material Laboratory (RML) facilities.

The results of these programs are used to evaluate the boiling water reactor fuel design methods and criteria used by fuel suppliers.

In addition to fuel bundle inspection, the fuel channels are under indirect surveillance in continuing programs which typically investigate channels showing anomalous characteristics developed during operation. These surveillance programs are designed not only for the evaluation of present day designs but are also providing data in the areas of alternate materials and design modeling.

3.5 Reactivity Control Mechanical Characteristics

3.5.1 Design Basis

The reactivity control system is designed such that under conditions of normal operation (a) sufficient reactivity compensation is always available to make the reactor adequately subcritical from its most reactive condition, and (b) means are provided for continuous regulation of the core excess reactivity.

For gross or local reactor power disturbances resulting from operator error or equipment malfunctions, the reactor control system responds upon signal of the reactor protection system to prevent fuel damage.

The inherent safety features of the reactor design as described in Section 3.2 in combination with reactivity control system devices are such that the consequences of a potential nuclear excursion accident, caused by any single component failure within the reactivity control system itself, cannot result in damage either by motion or rupture to the reactor primary coolant system.

3.5.2 Control Methods

Control of reactivity is accomplished by control rod movement. The control system accommodates fuel burnup and long-term reactivity changes. A standby liquid control system is provided as a back-up shutdown system.

3.5.2.1 Description of Control Rods

3.5.2.1.1 Standard Control Rods

The control rod is shown in Figure 3.5-1. The cruciform-shaped control rods contain a number of vertical stainless steel tubes filled with boron carbide powder, compacted to approximately 70% of theoretical density. A free volume of approximately 30% is provided in each tube as a plenum for helium from the B(n,$\propto$) Li reaction. Plugs are welded into the ends of the tubes to seal them.

The tubes are held in cruciform array by a stainless steel sheath extending the full length of the poison section. A cruciform shaped top casting and handle aligns the tubes and provides structural rigidity at the top of the control rod. Rollers attached to the top casting maintain the spacing between the control rod and the fuel assembly channels. A similar connector casting which incorporates the rod velocity limiter is located at the bottom of the control rod and contains rollers to position the lower part of the control rod in the control rod guide tube located below the core. These bottom rollers always remain in the guide tube during operation. A coupling at the bottom of the control rod is connected and locked to the control rod drive index tube by an expandable ball and socket joint.

The lifetime of a control rod is determined by both mechanical (absorber tube stress due to internal gas pressure) and nuclear (Boron-10 depletion) considerations and is dependent upon the performance history of an individual rod. The performance history of each control rod is monitored during operation of the reactor. The lifetime of a control rod is based on the lifetime of the limiting absorber tube in the control rod. Based on the operating history of a control rod, the boron depletion and the build-up of internal helium gas pressure in the limiting absorber tube in a control rod can be determined. As the limiting absorber tube in each control rod reaches the design limit based on either mechanical or nuclear considerations, the control rod is removed from the core.

It should be noted that actual mechanical failure of a single absorber tube; i.e., perforation, would not prevent the control rod from performing its design function. Also, loss of absorber characteristics in a single absorber tube due to depletion of B-10 would not prevent the control rod from performing its design functions. Since control rod replacement is determined by actual performance, any replacement schedule proposed prior to operation is at best an estimate which is only of use in economic evaluations.

The effect of irradiation of material properties is taken into consideration by the use of irradiated material properties in the mechanical design of the control rod and in determining control rod mechanical lifetime. The buildup of activation products is considered as it affects the absorber tube internal gas pressure. When evaluating replacement during operation, the material properties, internal gas pressure and boron depletion are based on measured core fluxes, and correspondent integrated flux for individual control rods.

3.5.2.1.2 Advance Design Control Rods

Hybrid I Control Rod (HICR/D-160) Assemblies contain 12 Hafnium absorber rods in place of 12 B4C rods (See Figure 3.5-2a) and use improved cladding material for the remaining B4C rods. The Hafnium rods will increase blade life and the improved B4C absorber rod tube material will eliminate cracking during the lifetime of the control rod assembly.

Duralife-230 Control Rod Assemblies (D-230) contain a hafnium plate in the upper portion of each blade wing, resulting in shorter tubes of B4C absorber. The absorber tubes are slightly larger diameter than previous designs, resulting in a longer nuclear lifetime. To account for the increased absorber weight, the velocity limiter has been redesigned (see Figure 3.5-1a). The D-230 blades use a low-cobalt material for the upper roller bearings. The outer absorber tubes of each blade wing are replaced by a hafnium strip, and use the improved absorber tube material of the HICR.

Duralife-120 Control Rod Assemblies (D-120) differ from the original control rod design by having a thinner sheath thickness, improved resistance to stress corrosion cracking, elimination of structural crevices, and reduction of cobalt-bearing material. Duralife-140A Control Rod Assemblies (D-140A) add a hafnium plate like the D-230 design, as well as replacing the outer absorber tube in each wing with a hafnium rod. The general configuration of both of these designs is the same as that shown in Figure 3.5-1.

The weight of the advanced designs is the same or less than the weight of the original control rod assemblies. The mechanical and nuclear properties do not differ from those of the original control rod assemblies in any manner that would be significant in a safety evaluation during normal or accident conditions. Rod worth and scram time of these blades will be the same as original control rod assemblies. No thermal limits changes will be needed.

Marathon control rods differ from the most recent preceding approved design (Duralife-230) by replacing the absorber tube and sheath arrangement with an array of square tubes, which results in reduced weight and increased absorber volume. GE’s Technical Evaluation Report of the Topical Report NEDE-31758P (GE Marathon Control Rod Assembly), presents the information required to support the licensing basis for the implementation of the new GE Marathon control rod assembly in GE boiling water reactor cores. The NRC issued Safety Evaluation Report “GE Marathon Control Rod Assembly” concluding that NEDE-31758P provides an acceptable basis for the mechanical design for boilng water reactor control rods. The SER was issued under letter from Ashok C. Thadani to J.S. Charnley dated July 1, 1991.

General Electric report NEDE-22290 (Reference 74 and 76) presents a safety evaluation of the advanced design blades which has been reviewed and approved by the NRC (Reference 75). The NRC has also reviewed and approved the GE safety evaluations for the HICR (Reference 79) and D-230 (Reference 80) designs. The D-120 and D-140A designs incorporate only features that have already been approved by the NRC in their review of other control rod designs and thus did not require a separate unique NRC review and approval (Reference 81 and 82).

Marathon-Ultra control blades differ from the previous Marathon design with a new absorber tube geometry, B4C capsule length, method of fabrication of the velocity limiter, and use of a full-length tie rod instead of a multi-segment tie rod. The NRC has reviewed and approved the GEH safety evaluations for the Marathon-Ultra control blades, as identified in (Reference 133).

3.5.2.2 Mechanical Design of Control Rods

Design stress intensity limits for control poison tubes are given in the following table.

	Stress Intensity Limits in Terms of:	
Strength Categories	Yield Strength (S_y)	Ultimate (S_u)
General Primary Membrane Stress Intensity	2/3 S_y	1/2 S_u
Local Primary Membrane Stress Intensity	S_y	3/4 S_u
Primary Membrane plus Bending Stress Intensity	S_y	3/4 S_u
Primary plus Secondary Stress Intensity	2 S_y	1.5 S_u

A stress analysis was performed on a control rod similar to that for this reactor. It was assumed that all control rod neutron absorptions were in B-10. Based on experimental data a value of 18% was used for the fraction of He gas generated by the B-10 (n,$\propto$) Li-7 which is released from the B-10 to cause internal pressure within the poison tubes. When the nuclear life due to depletion of B-10 was reached, the internal pressure in the most highly exposed poison tube was 13,000 psi, and the resultant maximum general primary membrane stress was less then 50,000 psi compared to a design limit of 51,500 psi for irradiated material.

Operating experience has shown that the materials used in the control blades are not susceptible to dimensional distortion in service.

Central rod tubing is internally supported and can withstand external pressures far in excess of that experienced under accident conditions.

3.5.3 Control Rod Drive System

The reactivity control system is designed such that under conditions of normal operations means are provided for regulation of the core excess reactivity.

Movable control rods are used to control the fission rate. The control rods are capable of being positioned in 6-in. steps to control neutron flux distribution in the reactor core. They are moved individually at an average rate of approximately 3 ips. The movement of control rods does not perturb the reactor beyond the capability of an operator to respond to the disturbance. This requirement prevents unnecessary operation of the reactor protection system. The maximum rate at which the rods can be moved and the incremental distance between control drive notches is such that under normal operating conditions a single notch increment of control withdrawn at the maximum withdrawal rate results in a stable reactor period of no less than 20 sec.

3.5.3.1 Rate of Response

Under conditions of expected abnormal reactor system disturbances, the reactivity control system provides a sufficient rate of negative reactivity insertion, upon a signal of the reactor protection system to prevent fuel damage. Expected abnormal reactivity disturbances and resulting power transients in the core can derive from any of three sources.

These are:

a. Reactor system induced disturbances of core parameters such as coolant flow or pressure.

b. Single operator errors or procedural violations

c. Single equipment malfunctions.

The reactor protection system described in Section 7.6 senses the disturbances and under certain specified conditions initiates a scram signal. Upon receipt of a scram signal the reactivity control system is required to render the reactor subcritical at a rate sufficient to prevent the initiating disturbance from causing fuel damage. Extensive tests and many hours of reactor service have been accumulated on control rod drives of this design. Analysis of these indicates the system response is sufficient to meet this scram requirement.

3.5.3.2 System Description

3.5.3.2.1 General Description

The basic drive mechanism is a double-acting, mechanically latched, hydraulic cylinder, using water as the operating fluid. The individual drives are mounted below the reactor primary vessel, where they position the control rods in the reactor core. Bottom-entry control rods are used because they provide axial flux shaping for greater reactor fuel economy. Being bottom-mounted, the drives do not interfere with refueling and are operative even when the head is removed from the reactor primary vessel. The use of water as the operating fluid eliminates the need for special hydraulic fluids. The drive mechanisms are able to utilize simple piston seals with normal leakage contained within the reactor primary system, thus minimizing contamination. The fluid also helps to cool the mechanisms.

The drive is capable of inserting or withdrawing the control rod at a slow, controlled rate as well as providing rapid insertion upon scram initiation. A locking mechanism (the collet) allows a drive mechanism to be positioned at short increments of stroke (6 in.) and will hold the control rod in that fixed position indefinitely.

Each drive is an integral unit, entirely contained in a housing (actually a reactor primary vessel extension) extending below the reactor primary vessel. The lower end of each drive housing terminates in a flange which mates with the drive flange. In order to allow removal of the drive without disturbing the external hydraulic system connectors, hydraulic lines are welded into the housing flange, where they are sealed with static face seals. These seals, together with the reactor static seal, are compressed by the eight mounting bolts used to attach the drive to the housing flange. Three uniformly distributed mounting bolts can support CRD loads and remain within the stress limits set forth in ASME codes.

The following improvements over the design of earlier plants are incorporated in the Monticello drive design.

a. Nitrided Type-304 stainless steel is used for the index tube, replacing 17-4-PH-1100. Nitrided 304 has superior resistance to galling.

b. The guide sleeve, a part which has been the source of friction and abrasion in some drive mechanisms, is eliminated.

c. The design includes additional screens to prevent the entrance of foreign material into the drive.

d. The operating forces and collet return forces are higher.

e. The units are longer, to accommodate the 144-in. control rod travel.

f. All tubular members which are subject to column loading are larger in diameter for greater column strength.

g. Other material changes and refinements in material processing and structural improvements have been made.

3.5.3.2.2 Principle of Drive Operation

(Refer to Figures 3.5-3 and 3.5-4)

3.5.3.2.2.1 General

The drives use demineralized water from the condensate system (as the primary source) or from the condensate storage and transfer system tank (secondary source) as the actuating hydraulic medium. Normal charging water pressure is throttled to approximately 1500 psig and is delivered by the control rod drive pumps for scram accumulator charging. Normal drive water pressure is provided at about 265 psig above reactor pressure. Normally, each drive receives approximately 0.4 gpm for cooling and about 4 gpm when moving at “notching” speed. The additional pump capacity is an allowance for increased requirements for cooling, for regulation, and to provide for scram accumulator charging.

The basic principles of drive operation and construction are shown in Figure 3.5-4. This figure, used to illustrate the following explanation, is not the actual mechanical arrangement, but it illustrates the functional elements of the drive and hydraulic systems.

The four valves labeled “insert valves” and “withdraw valves” make up a four way, closed center, reversing valve which can accomplish the following modes of drive operation:

a. To apply driving pressure below the piston and connect the above-piston area to the exhaust header for control rod insertion.

b. To apply driving pressure over the piston and connect the below-piston area to the exhaust header for control rod withdrawal.

c. To shut off all driving pressure when no motion is required.

3.5.3.2.2.2 Control Rod Insertion

Drive insertion is accomplished by opening the two “insert” valves. This applies the “reactor plus 265 psi” driving pressure to the bottom of the piston, and opens the chamber above the drive piston to the exhaust header. The 265 psi differential acting on the drive piston area of 4 square inches exerts an upward force of over 1000 lb. This force is greater than the drive friction force (normally less than 100 lb.) plus the weight of the control rod and index tube (normally 186 lb., wet) so the drive inserts the control rod.

As illustrated, the construction of the latch is such that it is cammed open and acts as a ratchet during rod insertion. The speed at which the drive moves is determined by the pressure drop through the insert speed control valve. During normal motion, this pressure drop accounts for all but 80 to 90 psi of the operating differential pressure. However, if the drive slows down for any reason, the full differential pressure is available to cause continued insertion.

3.5.3.2.2.3 Control Rod Withdrawal

Control rod withdrawal is, by design, more involved. First, in the actual drive design, the latch must be raised to reach the unlocked position (rather than withdrawn horizontally as the Figure 3.5-4 indicates). The latch piston (or collet piston) area is small enough that it is impossible to raise the latch when opposed by the latch return spring, drive line weight, and the force of the driving pressure applied to the area above the drive piston. Second, the notches in the index tube and the latch mechanism are shaped so that downward forces on the index tube hold the latch in place. The index tube, therefore, must be lifted before the latch can be released. This is done by opening the drive “insert” valves (in the manner described in the preceding paragraph) for approximately 1 second using an automatic sequence timer. The “withdraw” valves are then opened (by the sequencing timer mechanism) applying driving pressure above the main piston and opening the area below the piston to the exhaust header. Pressure is simultaneously applied to the latch piston to release the latch.

This pressure must be set and maintained high enough to overcome the force of the latch return spring plus the force of reactor pressure opposing movement of the latch piston. When this occurs, the drive is unlatched and free to move in the “withdraw” direction. Water displaced by the drive piston flows out through the withdraw speed control valve, determining the speed at which the drive moves. Two speed control valves are used to provide separate insert and withdraw speed adjustments. The entire valving sequence is automatically controlled and is initiated by a single operation of the operating switch.

3.5.3.2.2.4 Scram Actuation

During a scram, a separate set of valves comes into play. These valves, the inlet and exhaust scram valves, open, admitting the water pressure in the accumulator (approximately 1400 psi) under the main drive piston and venting the area over this piston to the scram discharge header. This header is maintained at atmospheric pressure during normal plant operation. The differential pressure across the main drive piston (initially about 1400 psi and always several hundred psi--depending on reactor pressure) produces a large upward force on the index tube and control rod, giving the control rod a high initial acceleration and providing a large margin of force to overcome any possible friction or binding. This initial scram force is a maximum of 5600 pounds under cold reactor conditions with CRD accumulator charging water in service with fully charged accumulators and 2800 pounds when the reactor is at operating pressure. The characteristics of the hydraulic system are such that after the initial acceleration (less than 30 milliseconds after start of motion) the desired scram velocity of about 5 ft/sec is achieved and the drive then travels at a fairly constant velocity. This characteristic provides a high initial control rod insertion rate and a high operating force margin that cannot be achieved by a drive designed to utilize gravity forces. As the drive piston nears the top of its stroke, the piston seals close off the buffer holes in the exhaust line and the drive is slowed down. Figure 3.5-4 shows only two buffer holes; in the drive mechanism there are eight which are progressively closed, providing a more gradual deceleration.

Each drive requires about 2.5 gal of water during the full scram stroke. There is adequate water capacity in each drive’s accumulator to complete a scram in the required time at low pressures. At higher reactor pressures, the accumulator is assisted by reactor pressure reaching the drive through the ball check valve. As water is drawn from the accumulator, the accumulator discharge pressure falls below reactor pressure. This causes the check valve to shift its position to admit reactor pressure under the drive piston. Thus, reactor pressure furnishes the force needed to complete the scram stroke at higher reactor pressures, while the accumulator alone accommodates the low pressure scrams. When the reactor is up to full operating pressure, the accumulator actually is not needed to meet the scram time requirement. With the reactor at 1000 psig, the scram force is still over 1000 lb. without an accumulator.

3.5.3.2.2.5 Mechanical Arrangement

The actual mechanical arrangement of the drive is discussed in the next section and shown isometrically in Figure 3.5-3. In comparing this arrangement with the illustration in Figure 3.5-4, one should note the following:

a. A conventional hydraulic cylinder, such as is shown in Figure 3.5-3, is normally operated with a fixed cylinder and a moving piston and piston rod. To be double acting, the piston rod must pass through a seal or piston rod packing. The locking grooves shown in the Figure 3.5-3 obviously cannot be passed through a seal, so the normal arrangement is reversed in the actual drive. The fixed stop piston and piston tube correspond to piston and piston rod. The index tube and drive piston correspond to cylinder and rod seal, with these being the moving members. Because of column loading and water flow considerations, external seal rings and an outer cylinder have been added to the “conventional” arrangement. These allow driving pressure to be routed through the flange to the area below the drive piston for control rod insertion. The area inside the index tube and above the stop piston is open to reactor pressure in the actual drive rather than utilized for driving, as illustrated in Figure 3.5-3.

b. The stationary piston rod (piston tube) is hollow. A hydraulic passage is provided inside this tube to carry water to and from the area above the drive piston. The progressive orifice drilling for scram deceleration is in this member.

c. The latch mechanism is made up of six fingers attached to an annular piston operating in an area at the upper end of the drive. Spring action in the fingers themselves holds them against the index tube, except when pressure is applied to the latch (or collet) piston to hold them in the unlocked position.

d. The annular space between the drive and the housing becomes the hydraulic passage which connects reactor pressure to the ball check valve. This assures that reactor pressure is always available at the lower end of the piston (for a scram), and that the drive can be actuated in the withdraw direction only by pressures higher than reactor pressure. The integrity of this passage is vital to the fail-safe properties of the drive. A second passage is provided in the outer or drive cylinder structure, which is a double-walled tube. This passage carries the operating pressures below the collet piston, which is open to the reactor pressure on the upper side (rather than a separate line to reactor as shown on the schematic).

e. The illustration in Figure 3.5-4 does not show the position indicator probe, nor the filters which are located in all passages through which reactor water flows to enter the drive mechanism. These and other details are shown in Figure 3.5-3 and explained below.

3.5.3.2.2.6 Drive Piston and Index Tube

The main drive piston is mounted at the lower end of the index tube, which functions as a piston rod. These parts (drive piston and index tube) make up the main moving assembly in the drive. The drive piston operates between positive end stops, with a hydraulic cushion provided at the upper end only. The piston has both inside and outside seal rings, operating in an annular space between an inner and an outer cylinder. The inner piston rings are conventional radial-tangential Graphitar 14 packing sets with coil springs of Inconel 750. The upper seal set is used for cushioning the drive at the upper end of the stroke. As this type of seal is effective in only one direction, the lower sets of seal rings are mounted with one set sealing in each direction. A pair of Graphitar 14 bushings is provided to prevent metal- to-metal contact between the piston assembly and the inner cylinder surface. The outer piston rings are segmented step-cut Graphitar 14 seals with Inconel 750 expander springs holding the segments against the cylinder surface. A pair of split Graphitar 14 bushings on the outside of the piston prevents contact with the cylinder wall. The effective area for "down" travel or "withdraw" is about 1.2 square inches versus 4.0 square inches for "insertion." The difference in driving area tends to balance out the control rod weight and makes it possible always to have higher "insert" forces than "withdraw" forces.

The upper end of the index tube is threaded to receive a coupling spud. The coupling, shown on Figure 3.5-2, is designed to accommodate a small amount of angular misalignment between the drive and the control rod. Six (6) spring fingers allow the coupling spud to enter the mating socket on the control rod. A plug then enters the spud and prevents uncoupling. Two means of uncoupling are provided. The lock plug may be raised, against the spring force of approximately 50 lb., by a rod extending up the center of the control rod to an unlocking handle located above the control rod velocity limiter. The control rod, with the lock plug raised, can then be lifted from the drive. The lock plug may also be lifted from below, if it is desired to uncouple a drive without removing the reactor primary vessel head for access. In this case, the central portion of the drive mechanism is raised to lift the uncoupling rod assembly. The uncoupled rod assembly lifts the lock plug and allows the coupling spud to disengage the socket as the drive piston and index tube are driven down. Note that a control rod weight of 100 lb. or higher is sufficient to force the spud fingers to enter the socket and push the lock plug up, allowing the spud to enter the socket completely and the plug to snap back into place. Therefore, the drive can be coupled to the control rod using only the weight of the control rod. However, with the lock plug in place, a force in excess of 50,000 lb. is required to pull the coupling apart.

The index tube is a long hollow shaft made of nitrided Type-304 stainless steel. This tube has locking grooves spaced every 6 in. along the outer surface. These grooves transmit the weight of the control rod to the locking device. The inside of the index tube above the stop piston is open to reactor pressure through the coupling spud, thus allowing the effect of reactor pressure to be confined to a small area (roughly the cross-sectional area of the index tube.) A closely woven stainless screen attached to the top of the stop piston prevents the entry of foreign particles from the reactor vessel to protect the stop piston seals from abrasion.

3.5.3.2.2.7 Locking Mechanism

The ratchet-type locking device is located in the upper end of the drive mechanism. This device requires a hydraulic pressure higher than reactor pressure to unlock for “down” movement. Due to the cam action of the index tube locking grooves, no unlocking signal is needed for “up” movement.

Locking is accomplished by 6 fingers mounted on the collet piston at the top of the drive cylinder. In the locked or latched position the fingers engage a locking groove in the index tube and thus carry the weight from the index tube to the outer drive cylinder. The collet fingers are made of Inconel 750 and hard surfaced for wear resistance. The collet piston is normally held in this position by a force of approximately 150 lb. supplied by an Inconel 750 spring. Metal piston rings, made of Haynes 25 alloy, are used to seal the collet piston from reactor pressure. A pressure approximately 100 psi above reactor pressure is required to overcome spring force, slide the collet up against the conical surface in the guide cap, and spread the fingers out so that they disengage the locking groove. The collet piston is nitrided to allow rubbing against the surrounding cylinder surfaces.

Fixed in the upper end of the drive assembly is a guide cap. This member provides the unlocking cam surface for the collet. It also serves as the upper bushing for the index tube and is nitrided to provide a compatible bearing surface for the index tube. Mounted on the guide cap is a filter through which water passes when it is drawn down into the drive during a scram at elevated reactor pressures.

3.5.3.2.2.8 Piston Tube and Stop Piston

Extending up inside the drive piston and index tube is an inner cylinder or column called the piston tube. This cylinder, a Type-304 stainless steel tube, is fixed to the bottom flange of the drive and remains stationary during control rod movement. Water is brought to the upper side of the drive piston through this tube. A series of orifices at the top of the tube provides a progressive water shutoff, thus cushioning the drive piston at the upper end of its scram stroke.

A stationary piston, called the stop piston, is mounted on the upper end of the piston tube. The piston provides the seal between reactor pressure and the area above the drive piston. It also functions as a positive end stop at the upper limit of control rod travel. A stack of Inconel 750 spring washers just below the stop piston helps absorb the final mechanical shock at end of travel. The piston rings are similar to the outer drive piston seals, being segmented, step-cut, Graphitar 14 seal rings. The Inconel 750 spring used to expand the seal is, in effect, a seal ring also, sealing the gaps between ring segments. The piston rings are arranged in two pairs, with a bleed-off passage to the center of the piston tube. This arrangement allows seal leakage from the reactor (during a scram) to be bled directly to the discharge line, rather than to the critical area above the drive piston. The lower pair of seals is used only during the cushioning of the drive piston at the upper end of the stroke.

3.5.3.2.2.9 Position Indicator

The center tube of the drive mechanism is a well containing the position indicator probe. The position indicator probe is an aluminum extrusion attached to a cast aluminum housing. Mounted on the extrusion are hermetically sealed, magnetically operated position indicator switches held by spring clips. Each switch is sheathed in a braided glass sleeve, and the entire probe assembly is protected by a thin-walled stainless tube. The switches are actuated by an Alnico 5 ring magnet carried at the bottom of the drive piston. The drive piston, piston tube and indicator tube or well are all nonmagnetic stainless steel, allowing the individual switches to be operated by the magnet as the piston passes. One switch is located at each position corresponding to an index tube groove, thus allowing indication at each latching point. An additional switch is located at each midpoint between latching points, allowing indication of this intermediate point during drive motion. Duplicate switches are provided for full-in and full-out. One additional switch (an over-travel switch) is located at a level below the normal full-out position. As the limit of “down” travel is normally provided by the control rod as it reaches the backseat position, a drive can pass this position and actuate the over-travel switch only if it is uncoupled. A convenient means is thus provided to verify that the drive and control rod are coupled after installation of a drive or at any time during plant operation.

3.5.3.2.2.10 Flange and Cylinder Assembly

Welded to the drive cylinder is a heavy flange. A sealing surface on the upper face of this flange is used in making a static seal to the drive housing flange. Teflon-coated, stainless steel “O” rings are used for these seals. In addition to the reactor vessel seal, two hydraulic control lines to the drive are sealed at this face. A drive can thus be replaced without removing the control lines, which are permanently welded into the housing flange. The drive flange contains the integral ball or two-way check valve. This valve is so situated as to direct reactor pressure or driving pressure, whichever is higher; to the underside of the drive piston. Reactor pressure is admitted to this valve from the annular space between the drive and the housing through passages (not shown) in the flange. An additional screen is provided to intercept foreign material at this point.

The outer cylinder is double-walled to provide an annular passage for water used to operate the collet piston. The inner tube is honed to provide the surface required for the drive piston seals.

Both the cylinder tube and outer shell are welded to the drive flange, but the top of the tubes have a sliding fit to allow differential expansion to take place. The latch housing, welded to the outer shell, is provided with ports to allow free passage of water from the clearance space between index tube and cylinder wall.

3.5.3.2.2.11 Materials of Construction

All drive components exposed to the reactor coolant are made of 300 series stainless steel except the following:

a. Seals and bushings on the drive piston and stop piston are Graphitar 14.

b. All springs and members requiring spring-action (collet fingers, coupling spud, and spring washers) are made of Inconel 750.

c. The ball check valve is a Haynes Stellite cobalt-base alloy.

d. Elastomeric O-ring seals are ethylene propylene.

e. Collet piston rings are Haynes 25 alloy.

f. Certain wear surfaces are hard faced with Colmonoy 6.

g. Nitriding by a proprietary New Malcomizing process, Electrolyzing (a vapor deposition of chromium), and chromium plating are used in certain areas where resistance to abrasion is necessary.

h. The piston head is made of Inconel 750.

All portions of the drive forming the external pressure shell or barrier are designed according to ASME codes; materials used conform to the appropriate ASME material specifications. Drive parts not in contact with coolant, chiefly the position indicator probe, are constructed of materials meeting the peculiar design requirements of the part. The probe, for instance, must be non-magnetic, hence aluminum extrusions, beryllium copper clips, and 300 series stainless steel sheath are employed.

Significant drive parts and the factors determining the choice of materials are listed below.

a. The index tube must withstand the locking and unlocking action of the collet fingers. A compatible bearing combination must be provided which is able to withstand moderate misalignment forces. The reactor environment seriously limits the choice of materials suitable for corrosion resistance. The column and tensile loads can be satisfied by an annealed 300 series stainless steel. The wear and bearing requirements are provided by Malcomizing the completed tube. To obtain suitable corrosion resistance, a carefully controlled process of surface preparation is employed.

b. The coupling spud is subjected to severe service conditions. Inconel 750, aged to produce maximum physical strength, is used to provide the required strength and corrosion resistance. As misalignments tend to produce a chafing in the semi-spherical contact area, the entire part is protected by a thin vapor-deposited chromium plating (Electrolyzing). This plating also serves to prevent galling of the threads attaching the coupling spud to the index tube.

c. Inconel 750 is used for the collet fingers, which must function as leaf springs when cammed open to the unlocked position. A hard facing must be applied to the area contacting the index tube and unlocking cam surface of the guide cap. Colmonoy 6 hard facing provides a long-wearing surface adequate for design life.

d. Graphitar 14 has been selected for seals and bushings on the drive piston and stop piston. The material is inert and has a low friction coefficient when water lubricated. Some loss of strength is experienced at higher temperatures, so the drive is normally supplied with cooling water to hold temperatures below 250°F. The graphitar is relatively soft, which is advantageous when an occasional particle of dirt reaches a seal. Resulting scratches reduce sealing efficiency until “worn in” again, but the drive design allows for considerable leakage. These seals determine the practical service life of a drive mechanism, and the frequency of maintenance is based on average seal life.

3.5.3.2.3 Drive Mechanism Tests

3.5.3.2.3.1 General

Applicable results from tests and operation of similar units in the field and in production form a part of the technical background for the design. Tests on production prototypes are run on each significant model change to evaluate performance and operation characteristics and to obtain statistical data on main performance parameters. In addition, a thorough design evaluation test has been run on a development model drive which is similar to the drive design for this unit (Model 7R-DB-144A-1) in general arrangement, construction, and materials, and is identical to it in stroke length, column member size, coupling details, and the majority of component details. The following paragraphs briefly describe the test programs.

3.5.3.2.3.2 Development Drive Tests

The development drive (one prototype) testing included scrams and latching cycles during exposure to simulated operating conditions. These tests have demonstrated the following:

a. That the design withstands the forces, pressures, and temperatures imposed without difficulty.

b. That wear, abrasion, and corrosion of the nitrided Type-304 stainless parts are negligible, and that mechanical performance of the nitrided surface is superior to materials used in earlier operating reactors.

c. That the basic scram speed of the drive has a satisfactory margin above minimum plant requirements at any reactor pressure.

d. That the stepping response of the drive is satisfactory.

e. That usable seal lifetimes greater than 100 scram cycles may be expected.

f. That, based upon observed wear rates, the actual life of other drive components greatly exceeds design life.

3.5.3.2.3.3 Production Prototype Tests

Production prototype testing was conducted on a sampling of drives from each significant model change. Drives were subjected to extensive operational testing at reactor pressure and temperature conditions and at various abnormal conditions such as reactor vessel overpressure. The test program, run on drives which had completed factory quality control tests, included:

a. Zero vessel pressure calibration tests--friction, leakage, etc.;

b. Operating pressure characteristics such as speed, stepping performance, leakage, friction, scram times with and without accumulator, hot scrams, and scram time consistency;

c. Disassembly and inspection.

In addition, one of the sample drives was tested for approximately 4500 shim and scram cycles in a design and endurance test. Included in the operation was an evaluation of misalignment effects. Testing was done at various reactor pressures with frequent disassembly and inspection checks.

3.5.3.2.3.4 Factory Quality Control Tests

Each drive mechanism, including the sampling assigned for prototype testing, was subjected to a standard quality control test at reactor pressure conditions. Drive shim motion and latching, including proper position indication, was checked. After completion of this test, drive friction was determined to assure proper operation and to check alignment, concentricity, etc. Each drive was then subjected to cold scram tests to determine scram times at various reactor pressures and to verify stepping performance.

In addition to normal dimensional inspection, material verification, heat-treatment control weld inspection, etc., standard quality control tests and checks included:

a. Hydrostatic testing of drive to check pressure welds in accordance with ASME Codes.

b. Electrical components are checked for electrical continuity and resistance to ground.

c. All drive parts which cannot be visually inspected for dirt are flushed with filtered water at high velocity. No foreign material is permissible in effluent water

d. Seal leakage tests are performed to demonstrate proper drive assembly.

3.5.3.2.3.5 Reactor Pre-Operational Tests

After the drives were installed in the reactor, preoperational tests were performed by qualified personnel to make final adjustments in the hydraulic system and to assure proper installation of both the hydraulic system and the drives. Readings and observations at this time constituted the bases for evaluating performance changes in actual reactor service and their relationship to maintenance life.

3.5.3.3 Control Rod Drive Hydraulic System

3.5.3.3.1 System Description

(Refer to Section 15 Drawings NH-36244 and NH-36245)

The control rod drive hydraulic system of the control rod drive system which supplies and controls the pressure and flow combinations to the drives consists of 3 subsystems:

a. Supply subsystem

b. Scram subsystem

c. Cooling subsystem

There is one supply subsystem for all the control rod drives but each drive has a separate and independent scram subsystem and cooling subsystem.

3.5.3.3.2 Supply Subsystem

3.5.3.3.2.1 General

The supply subsystem is made up of supply pumps, filters, control valves, and associated instrumentation and controllers. In general, the supply subsystem takes water from the condensate system (as the primary source) or from the condensate storage and transfer system tank (secondary source), pressurizes it, filters it, and with the pressure control subsystem regulates its three output pressures. The pressure control subsystem consists of the flow control station, drive water pressure control station, cooling water pressure control station (which is not used with the return line isolated) and the hydraulic system exhaust line. The flow control station maintains a constant flow in the hydraulic system supply. Because the flow from the flow control station ultimately exhausts to the reactor vessel, drive water pressure and cooling water pressure are influenced by reactor pressure. The drive water pressure control station is adjusted to maintain a differential approximately 265 psi greater than reactor pressure and supply water to the drive water header for normal control rod drive insertion and withdrawal. The cooling water pressure is adjusted to maintain a differential ranging from 15 to 33 psi greater than reactor pressure, as required for control rod drive cooling.

The three supply pressures described above, together with reactor vessel pressure in the hydraulic system exhaust header, are the four operating pressures required by the control rod drive hydraulic system.

The CRD hydraulic system supplies the RPV Reference Leg Backfill System from a connection on the CRD charging water header.

3.5.3.3.2.2 Control Rod Drive (CRD) Pumps

The supply pump pressurizes the system. The spare pump is of 100% capacity. Changeover from one unit to the other is manually initiated from the main control room. Each pump is installed with a suction strainer, two isolation valves for pump maintenance, and a discharge check valve to prevent bypassing flow backwards through the nonoperating pump. Two check valves with test connections are installed on the CRD discharge common header to reduce the potential for backflow from the reactor control rod hydraulic units to a location outside secondary containment. The check valves assure that any flow path outside secondary containment is protected by at least two check valves. This includes the CRD pump bypass line.

A minimum flow bypass connection between the discharge and the condensate storage and transfer system tank prevents overheating of the pump in the event that the pump discharge is inadvertently closed. An additional CRD pump bypass line connected between the common discharge header and the condensate storage and transfer system is provided to allow increased flow to improve the hydraulic stability of the CRD pumps.

3.5.3.3.2.3 Filters

Two (100% capacity each) parallel filters located downstream of the CRD pumps remove foreign material larger than 25 microns from the hydraulic system water. The isolated filter can be drained, cleaned, and vented for reuse while the other is in service. A differential pressure indicator and alarm monitor the filter element as it collects foreign material. Strainers in the filter discharge lines guard the hydraulic system in the event of a filter element failure.

Two (100% capacity each) 5 micron filters located on the suction side of the CRD pumps provide full flow filtration for both CRD pumps with the normal suction head of the water supply source. Local indication and controls as well as remote alarm features prompt manual selection of a clean filter or automatically initiate a filter bypass. A relief valve is provided ensuring suction side relief protection. Pressure switches sensing CRD pump suction pressure are furnished to open the filter bypass on low pump suction pressure. Respective differential pressure indications are utilized to sense filter differential pressure and actuate a remote alarm on a high differential pressure.

3.5.3.3.2.4 Flow Control Station

The flow control station maintains flow at a nominal 48 to 56 gpm by a flow sensing element and controller and air-operated flow control valves. By throttling either valve so as to maintain constant flow through the flow element, the pump is caused to operate at the point on its characteristic curve which corresponds to the required pressure. A parallel spare valve is provided with isolation valves to permit maintenance of the non-controlling valve. The flow control valve reacts to the flow deviation sensed by the flow element and makes the necessary adjustments to maintain a constant flow in the hydraulic system supply and, thereby, some constant pressure of between 1380-1510 psi in the charging water header. The pressure in the charging header is monitored in the reactor control room with a pressure indicator and low-pressure alarm.

3.5.3.3.2.5 Drive Water Pressure Control Station

Pressure in the drive water header is manually adjusted to approximately 265 psi above the reactor primary vessel pressure by the operation of a drive water pressure control valve. The pressure control valve is a motor-operated valve which is manually adjusted from the reactor control room. The stabilizing valves as shown in Section 15 Drawing NH-36244, are no longer valved in service. It was determined by test that their operation is not required. The flow through the pressure control valve is substantially constant, and the required pressure is maintained in the drive header. The variation in flow requirements between drives is small enough that the corresponding pressure variation is within acceptable limits without using the stabilizing valves.

A manual valve is provided to allow for temporary local pressure control during maintenance on the motor-operated valve.

The flow elements and flow indicators located in the drive water header are used to measure flow to the drives for adjustments and testing. A differential pressure indicator in the main control room shows the differential pressure between the reactor primary vessel and drive water header. This is used when adjusting the drive water pressure with the motor-operated pressure control valve.

3.5.3.3.2.6 Cooling Water Pressure Control Station

Because there is no flow downstream of the cooling water header, cooling water pressure is dependent on the flow control valve and throttling valve MO-3-20. Adequate cooling water flow is provided when cooling header pressure is 15 to 33 psi greater than reactor pressure. If CRD return flow is restored to the vessel, the cooling water pressure control station is required to maintain the proper cooling water header with the variations in reactor pressure. This pressure control station operates as discussed below.

3.5.3.3.2.7 Exhaust Header

When a drive is being inserted, driving water pressure is applied to the bottom of the drive piston which causes displacement of the over piston water into the exhaust header. This water is then dispersed into the reactor vessel via the reverse flow path (leakage) available through valves SV-121, directional control solenoid valves of the HCUs, associated with the rods not being moved. When a drive is being withdrawn, it is the under piston water that is displaced into the exhaust header.

Pressure in the system return line is indicated by local pressure indicator, which is normally isolated from the system. This pressure indicator, together with the pump bypass line, permits checking the drive water pump pressures for maintenance or test purposes.

3.5.3.3.2.8 Emergency Source of High-Pressure Water to the Core

This system has not been directly assumed in safety analyses. However, during the 1975 Browns Ferry Unit 1 fire, this system was at times the only high pressure water injection system available. By Generic Letter 80-095, the NRC required licensees to demonstrate the injection capability of the CRD System for a Browns Ferry Scenario (Reference 96).

Modifications made to the control rod drive return flow (Reference 48) required analysis and testing to ensure this source of high-pressure water flow was not reduced below a water boil off rate due to decay heat generation 40 min. following shutdown from rated power and the maximum leakage rate from the primary system. The analysis was redone (Reference 97) at 2004 MWt. This analysis indicates that a flow rate of >116 gpm (Reference 97) is required to maintain the water level above the top of the active fuel. Additional flow to the vessel can be obtained by opening the two outboard isolation valves to the Reactor Water Cleanup return line. In this mode of operation, one CRD pump can be used to add as much as 150 gpm to reactor vessel.

3.5.3.3.3 Scram Subsystem

(Refer to Section 15 Drawing NH-36245)

3.5.3.3.3.1 General

The scram subsystem is made up of the following components:

Accumulators charged from the charging header
Scram valves and their pilot valves
Drain and vent valves, and their pilot valves
Scram discharge volumes
Associated instrumentation and controllers.

The nitrogen precharge system, scram pilot valve, air supply system, and reactor protection system operate in conjunction with the scram subsystem, but are discussed elsewhere. (Refer to Figure 3.5-7.)

3.5.3.3.3.2 Accumulator

The accumulator on each drive is an independent source of stored energy to scram that drive. The top of the accumulator contains water while the bottom is precharged with nitrogen.

To ensure that the accumulator is always capable of producing a scram, it is continuously monitored for water and nitrogen leakage. A float-type level switch actuates and alarms if water leaks past the barrier and collects in the bottom of the accumulator. A pressure indicator and pressure switch are connected to monitor nitrogen pressure. With the charging water pressure greater than the nitrogen pressure, the barrier is caused to move onto the bottom flange during the initial accumulator charging process. Any subsequent loss of nitrogen causes a decrease in pressure since the accumulator barrier will not move down, beyond the stop, to compress the reduced amount of gas back up to pressure. The decrease in nitrogen pressure actuates the pressure switch and sounds an alarm. An isolation valve allows all of the instruments associated with each drive to be isolated and serviced.

The stop and check valves in the charging line allow isolation of the accumulator for maintenance and prevent backflow from the accumulator to the header. The check valve assures that the accumulator retains its charge even if the supply subsystem fails or the connecting pipe ruptures.

3.5.3.3.3.3 Scram Pilot Valves

During normal plant operation, each of the dual logic channels of the reactor protective system energizes one of the two solenoids on the three-way solenoid scram pilot valves. When energized, these pilot valves supply instrument air to the operators of both the inlet scram valve and the outlet scram valve, causing both scram valves to close. During a scram, both of the dual logic channels of the reactor protection system are de-energized and both pilot valves open, venting the scram valves and allowing them to open. To protect against spurious scrams, the pilot valves are interconnected so that both pilot valves must be de-energized for the scram valves to vent. On the other hand, failure of either station electric power to both solenoids or station instrument air produces a scram. The design of the pilot valves is selected based on simplicity, a minimum of moving parts, fast opening time (approximately 0.050 sec) and statistical operating history on similar units.

For added protection, the instrument air header to all the pilot valves has two back-up scram pilot valves. Upon a scram signal, these solenoid three-way valves close off the air supply and vent this section of the station instrument air system header. This vents the air of the scram valve operators should its scram pilot valves malfunction.

3.5.3.3.3.4 Scram Valves

The inlet scram valve is a globe valve which is opened by the force of an internal spring and closes when air pressure is applied on top of the diaphragm operator. The opening force of the spring is approximately 700 lb. Each valve has a position indicator switch. Both valve switches per drive are required to energize a common light in the main control room as soon as the valves start to open. The scram valve is selected based on high operating force, fast opening time (approximately 0.1 sec) and operating history on similar units.

The outlet scram valve is identical to the inlet scram valve except that it is smaller.

3.5.3.3.3.5 Scram Discharge Volumes

The purpose of the Scram Discharge Volumes is to contain the water exhausted from the 121 control rod drives during a scram.

During normal plant operation, the discharge volumes are empty and all the vent and drain valves are open. These valves are maintained in this position by air, through four pilot valves, two for the inboard valves and two for the outboard valves. Each set is pneumatically inter-connected and each pilot valve of a set is energized by one of the two logic channels of the reactor protection system. Vent lines installed on the discharge headers for both the east and west hydraulic control unit groups are independent from each other and each line is equipped with two control valves and a check valve in series. The check valve prevents backflow when a scram is reset. Drain lines installed on each volume are also independent of each other and each line is equipped with two control valves. A series of liquid - level switches are connected to each discharge volume to monitor the water level and guard against an abnormal amount of water in the volumes when a reactor scram occurs. If water starts to accumulate in either discharge volume an annunciator in the control room is activated. If the water level increases an interlock is activated to prevent control rod withdrawal. If water continues to accumulate in either volume, four high level switches connected in a one-of-two-twice logic to the reactor protection system will initiate a reactor scram, see Reference 50.

With a scram signal the reactor protection system is de-energized and the four pilot valves vent permitting the vent and drain valves to close. Position indicator switches on the valves indicate with lights in the control room the position of each valve. Each discharge volume accepts the scram discharge water from its respective hydraulic control unit groups. While scrammed, the control rod drive seal leakage continues to flow to the respective discharge volume until each discharge volumes’ pressure equals reactor vessel pressure.

When the reactor protection system is cleared of all scram signals and reset, the drain and vent valves of both discharge volumes and the scram valves in the hydraulic control units return to their normal operating position. When the drain and vent valves open, the water accumulated in the discharge volumes drain through their dedicated drain lines and into the radwaste system. Control rod withdrawal, due to the interlock mentioned earlier, is not possible until the accumulated water in both discharge volumes has drained to below the rod block setpoint.

The drain and vent valves can be tested without disturbing the reactor protection system with the use of the test pilot valve which is controlled by a hand switch in the control room. Also, closing these valves allows the outlet scram valve seats to be leak tested.

3.5.3.3.4 Cooling Subsystem

The cooling subsystem is made up of the cooling water header, and the check valve which admits water to the under side of the drive piston. Although the drive can function without cooling water, the life of the Graphitar seals and elastomer O-rings is shortened by exposure to reactor temperatures, and cooling water is provided to protect these members. When a drive is in motion, the pressure under the piston is higher than the cooling water pressure, and the check valve is closed. It opens to admit cooling water when the drive is stationary.

3.5.3.3.5 Directional Control

3.5.3.3.5.1 General

Four solenoid directional control valves are used for switching the drive water and exhaust headers to the two drive ports. By energizing and opening two valves at a time the drive water header can be connected under or over the control rod drive piston while the exhaust header is connected to the opposite side. Two directional control valves, in addition to the speed control valves, are connected so that they always pass the flow to or from the area under the piston. This is approximately 4 gpm when the drive is moving at the normal speed of 3 ips. The balance of forces in the drive mechanism is such that the pressure under the piston is approximately 90 psi when the drive is inserting or withdrawing. Proper speed is obtained when the directional control valve speed control element is set, so that 4 gpm produces a pressure drop of 175 psi (265-90) when inserting; similarly, the other speed control element is adjusted so that 4 gpm produces a pressure drop of 85 psi (90-5) when withdrawing. The directional control valves are protected from dirt by filters.

The cooling, control, and scram subsystem for each drive use common piping to the drive; therefore the directional control valves are periodically subjected to scram pressure. The directional control valve connected to the drive water header can be opened by this higher pressure on its outlet port. The check valve prevents significant loss of water to the drive water header during scram, similarly another check valve provides the identical function for the cooling water header.

3.5.3.3.5.2 Directional Control Valve Sequencing

As described in preceding paragraphs, insert motion is obtained by opening the proper pair of valves. To unload the collet so it can be unlocked, this pair of valves is also opened for approximately 1 sec during a withdraw operation, after which the withdraw pair of valves are opened and the insert valves are closed. This is accomplished by electrical sequence timer, and occurs automatically when the rod withdraw operating switch is closed.

"Jogging" is accomplished in a similar manner. When this mode of operation is selected by the operator, the proper pair of valves is energized electrically long enough to allow the drive to move to the next notch position, at which time the valves are automatically de-energized, even if the operator holds the switch closed. This feature relieves the operator of having to estimate the time required to accomplish a single notch movement.

If all four directional control valves are closed while the drive is in a position between notches, water displaced by the drive piston must leak past the drive seals in order for the drive to "settle" into latched position. With normal seals - including those well worn - this settling speed is a fraction of normal withdraw speed. To speed up settling and latching, the "settle" circuit delays the closing of the directional control valve for approximately 5 sec. This allows the drive to withdraw at about 1/2 normal speed to the next latch position. The "jog" withdraw time interval is shortened so that the settle cycle begins before the drive has withdrawn a full notch.

3.5.4 Control Rod Drive Housing Design

The General Electric company has intensively investigated the potential modes of control rod drive housing failure. Particular attention is given in design and fabrication to minimize the probability for failure of the housing, including the following:

a. The reactor vessel and drives are designed to Section III of the ASME Code (Reference 72).

   Two bolted flanged joints are made on each control rod drive. The major bolted joint is the flange-to-housing connection. Eight 1-in. bolts are used for this joint. The other bolted joint on each control rod drive is the position indication equipment flange. Six 1/2-in. bolts are used for this joint. On each of these joints, each bolt is stressed to less than 1/6 of its ultimate strength by the reactor system pressure at the relief valve set pressure.

   The stress levels and the potential for cyclic stress fatigue in the reactor vessel and control rod drive housings have been evaluated. It has been determined that the most critical area is the welded joint between the housing and the nozzle. General Electric has performed an intensive testing program on this connection, including thermal and pressure cycling to determine the applicability of design and analytical techniques. The results from these tests are as follows:

   1. This welded joint withstands twice the maximum design stress (that is applied during operation) for 10 times the predicted number of cycles (conservative estimate of total cycles during plant life) before cracking is detected.

2. The joint withstands four times the maximum design stress (that is applied during plant operation) for more than the predicted number of cycles before it fails.

b. The piping used for each housing was hydrostatically tested to 1800 psig and ultrasonically tested. The flanges are ultrasonic and dye penetrant tested. The housing tubes are dye penetrant tested. The flange-to-housing welds are X-ray and dye penetrant tested. The housing-to-vessel welds are dye penetrant tested. Additionally, the vessel with all control rod drive housings in place is hydrostatically tested to 1.25 times the reactor design pressure as required by Section III of the ASME code (Reference 72).

c. The control rod drive housings are in a very low neutron flux region, resulting in a negligible increase in the nil ductility transition (NDT) temperature.

The intensive design evaluation and testing, the methods for preventing reactor overpressure, the low neutron flux, and the potential for detection of initiation of a rupture prevent a control rod housing or hydraulic system failure that could cause a control rod ejection. Nevertheless, additional plant protection is provided by the control rod drive housing support structure (see Section 6.5). This equipment is positioned below the control rod drives and is designed for the maximum force which could be imposed by a ruptured control rod drive housing, so that axial motion would be limited.

Thus, even in the event of a circumferential housing rupture, the control rod would not be ejected from the reactor core.

3.5.5 Operation and Performance Analysis

3.5.5.1 Normal Withdrawal Speed

Normal withdrawal speed is determined by differential pressures at the drive, and set for a nominal value of 3 ips. The characteristics of the pressure regulating system are such that this speed is maintained independent of reactor pressure. Tests have determined that accidental opening of the speed control valve to the full open position produces a velocity of approximately 6 ips. Should this system fail so as to produce maximum available pump pressure (1750 psig) to the drive system with zero reactor pressure, analysis indicates that the hydraulic resistances in the system would limit the withdraw velocity to 2 ft/sec.

The allowable operating limits on withdraw and insert speed are determined by requirements for the insert-before-withdraw motion, and for jogging, and these are lower than limits which might be set by considerations of maximum allowable reactivity variations. In fact, the jog-withdraw operation of the drive is an excellent test of the correctness of the speed setting; the drive generally will fail to withdraw if the speed is incorrectly adjusted. A pressure of approximately 80 psi higher than reactor pressure must be maintained above the main drive piston to keep the collet unlocked, and this corresponds to a pressure greater than 80 psi above reactor pressure under the main piston. Any malfunction which allows the pressure to drop below this value, a condition necessary for higher withdraw speeds, results in collet locking.

3.5.5.2 Accidental Multiple Operation

Each drive mechanism has its own complete set of electrically operated directional control valves, which are closed when de-energized. The correct operation of all four valves in the correct sequence is required to cause the drive to withdraw. Consequently, the probability of multiple simultaneous independent valve failures that could cause accidental multiple control rod withdrawal is extremely small. The electrical system which actuates the directional control valves is designed so that no credible failure can produce accidental movement of more than one control rod.

3.5.5.3 Internal Failures

The following failures have been evaluated by analyses or experiment, and are incapable of producing a high velocity withdrawal for the indicated reasons.

a. Failure of the collet to latch. The drive would continue to withdraw (after removal of the signal) at a fraction of its normal withdraw speed. There is no known means for a collet to come unlocked without some initiating signal. Failure of the drive-down inlet valve following a withdraw has the same effect as failure of the collet to latch, and would be immediately apparent to the operator. Accidental opening of the drive-down inlet valve normally does not unlock the collet, because of the characteristic of the collet to remain locked until unloaded.

b. Failure of the ball check valve to close either port. This prevents the development of pressure under the main piston, making it impossible under normal operation to unload and unlock the collet. This characteristic has been verified on test. If it is postulated that in some unspecified manner the collet is unlocked and the ball check valve is coincidentally stuck, calculations indicate that hydraulic resistance inside the drive mechanism limit the withdraw velocity to approximately 2 ft/sec.

c. Operating valve failures. Various directional control valve failures can be postulated and none is capable of producing a high velocity withdraw. Leakage through either or both of the scram valves produces a pressure which tends to insert the control rod rather than withdraw it. If the pressure in the scram dump header should exceed reactor pressure following a scram, the check valve prevents this pressure from operating the drive mechanisms.

d. Drive line separation. The maximum free fall velocity which the control rod itself can achieve is limited by the hydraulic characteristics of the velocity limiter to less than 5 ft/sec under all normal modes of reactor operation. Hence a postulated accident in which (1) there is a mechanical failure of the drive line, (2) the control rod sticks in the reactor core, (3) the drive is withdrawn and the control rod does not follow, (4) the failure to respond is not observed by the operator, (5) the control rod becomes loose and falls freely, will not produce an excessively high withdraw velocity. The probability of drive line separation is minimized through the following:

    1. The coupling members are designed for a maximum tensile stress of 1/2 the yield strength when subjected to the load imposed if there were no deceleration at the end of the scram stroke. This is a nearly impossible case, and taken as a limiting assumption.

2. The coupling is engaged and locked with forces less than the control rod weight; therefore, coupling is automatic when the drive is inserted against the control rod.

3. Manufacturing quality control procedures minimize the probability of members being made of incorrect materials.

4. The mode of failure of the coupling is that it locks, rather than unlocks.

5. The integrity of the drive line can be and is regularly verified by simple operational tests. Tests on the coupling have shown it to be capable of withstanding tensile forces of 50,000 lb. and compressive forces of 33,400 lb. without separating or becoming inoperable.

3.5.5.4 Structural and Piping Failures

The following failures can be postulated and the results have been analyzed:

a. Failure of either or both hydraulic lines to the housing flange. Failure of the line leading to the top of the drive piston or failure of both lines would result in an automatic scram if the reactor is at operating pressure, and loss of ability to obtain movement if the reactor is at zero pressure. Failure of the line leading to the bottom of the drive piston would result in loss of ability to move the drive at any pressure and loss of ability to scram at zero pressure. Failure of these lines while the drive is being withdrawn would result in loss of motion and collet engagement. If the collet failed to engage, the withdraw velocity would reach 2 ft/sec. If this pipe ruptured during withdraw and the collet did not engage and the ball check valve failed, the withdraw velocity would approach 9 ft/sec. There is no known single failure that can induce these three failures, and they must be considered independent.

   The hydraulic piping and all parts of the drive mechanism which contain reactor primary vessel pressure are designed in conformity to applicable codes, and stresses are conservatively low. The most critical hydraulic passages (those connecting the bottom of the drive piston to the ball check valve and then to the reactor) are internal to the drive mechanism and inside the drive housing.

b. Rupture of the drive housing. Unless this occurred while withdrawing, it would not result in drive motion. If it occurred while withdrawing, it is calculated that the withdraw velocity would increase to 0.6 ft/sec. Any subsequent failure which would lower the pressure in the drive would cause the collet to engage; however, should this occur (from an event such as line rupture or ball check valve failure) and if the collet failed to engage, it is calculated that the withdraw velocity would approach 10 ft/sec. As there is no single failure which can be postulated to produce failure of these three elements, (the housing, the collet, and the ball check valve), the credibility of this velocity occurring depends on the credibility of the simultaneous occurrence of all three failures.

c. Failure of the drive housing in tension. This postulated failure would allow the drive housing, drive mechanism, and control rod to withdraw a fraction of an inch until stopped by the support structure. Following this, behavior would be similar to the preceding case.

d. Failure of the bolts attaching the drive mechanism to the housing flange. This failure would be similar in consequences to the failure postulated in b. above, except that the ball check valve is bypassed, and the behavior is independent of ball check valve action.

There are no known or postulated modes of failure which are not either variations of these basic modes, or produce consequences which are considerably less severe.

3.5.5.5 Scram Reliability

High scram reliability is the object of a number of features in the system, such as the following:

a. There are two sources of scram energy (accumulator and reactor pressure) for the required number of drives when the reactor is operating.

b. Each drive mechanism has its own scram and pilot valves, so that only one drive can be affected by a scram valve failure to open, and a separate back-up valve is provided to scram a drive (after some time delay) should failure of its pilot valves occur.

c. The nature of the drive mechanism is such that it develops from 5600 pounds (at zero reactor pressure) to 2800 pounds (at rated pressure), a large margin to overcome possible friction.

d. The scram system and mechanism are designed so that the scram signal mode of operation overrides all others. The collet is designed so that it is incapable of restraining or preventing control rod insertion during a scram.

e. The scram valves are held closed by pneumatic pressure which is controlled by solenoid pilot valves. These pilot valves open when deenergized. Hence, failure of the pilot valves, the air system, or the electric system generally produces, rather than prevents, a scram. All components used in the scram hydraulic system are selected either after an extensive testing program or after millions of accumulated operating hours in actual reactor service.

3.5.5.6 Operational Reliability

High operational reliability is a notable objective in itself; in addition, it contributes generally to overall safety by minimizing the occasions when abnormal operating conditions are encountered. High operational reliability is the objective of the following features of the control rod drive system:

a. Components in the hydraulic system are selected based on established reliability. Operating valves are arranged in the plant so they are accessible for maintenance while the reactor is in operation.

b. Materials and stress levels in the drive mechanism are selected so that the operating life of the mechanism - as determined by wear, corrosion, fatigue, abrasion, etc. in a normally operating plant - is essentially unlimited. Sliding seals are the elements most subject to abrasion, a life expectancy well in excess of five years. The mechanism is designed so that removal from the reactor is possible without removing the reactor pressure vessel head.

c. All operating force margins in key components of the drive mechanism are high. The force normally available to insert the blade during a scram is 14 to 28 times the drive line weight. The force of the collet return spring (about 150 lb.) is approximately three times normal collet friction, and during a scram with the reactor at normal operating pressure this force is increased to 2150 lb. by hydraulic forces. With a drive pressure 265 psi higher than reactor pressure (a normal condition) the available operating force to withdraw a control rod is approximately 325 lb., while the available force to insert a control rod is over 1000 lb. (not considering scram conditions). Based on experiments and field observations, frictional forces of the control rod in the reactor core and moving drive parts are from 50 to 100 lb. under normal operating conditions.

d. Provisions are made to operate with a reasonable amount of foreign material in the reactor water and in the water supplied to the hydraulic system. Filters and strainers are incorporated in the drive mechanism in passages through which water is drawn into the mechanism. Filters are provided in the hydraulic system both upstream and down-stream of the supply pump and in various other positions in the hydraulic system to protect the operating valves. Seals of the type used in the main drive piston are scored rather than jammed by metal particles, but the seals can operate satisfactorily after severe scoring. Rubbing surfaces in the collet area are hardened (nitrided) to minimize the opportunity for abrasion and friction to be initiated by foreign material, which is the predominant form of contamination in BWRs.

e. Although normally cooled to less than 250°F, the mechanism can operate without cooling. Supplement 1 to SIL 173 identifies that control rod drive temperatures above 350 degrees F can adversely affect the scram time for that control rod. Continued exposure to maximum reactor temperature would eventually weaken seal rings and cause leakage, but no other damage would result. The mechanism is designed to scram without damage under conditions simulating simultaneous loss of cooling water and maximum reactor pressure, and this capability is demonstrated by tests.

3.6 Other Reactor Vessel Internals

3.6.1 Design Basis

In addition to the previously discussed fuel and control rods, the other reactor vessel internals include the following:

a. Shroud

b. Baffle plate

c. Baffle plate supports

d. Fuel support piece

e. Control rod guide tubes

f. Core top guide

g. Core support plate

h. Jet pumps

i. Feedwater sparger

j. Core spray spargers

k. Standby liquid control system sparger

l. Steam separator assembly

m. Steam dryer assembly

n. In-core nuclear instrumentation tubes

The reactor internals are designed mechanically to provide an adequate distribution of coolant flow within the reactor and maintain structural integrity during normal operations, seismic disturbances, and design basis accident conditions.

The specific design requirements for each internal component may vary due to differences in material, and location. For example, the MNGP steam dryer was originally procured and supplied as a non-safety related, non-seismic category I, non-ASME component. The significant design basis condition is that it ***SHALL NOT*** fail (i.e., ***SHALL NOT*** generate loose pieces) when subjected to the design basis events (reference 93). Each component must be able to withstand the combined loadings from differential pressures and temperature, dead weight, fluid movement, control rod motion, seismic acceleration, and vibration. Allowable stresses as defined by the ASME Code (Reference 72) are not exceeded. Allowances must be made for thermal expansion, corrosion, and crud buildup.

The shroud and jet pumps form an inner vessel which must be sufficiently leak tight, despite thermal expansion allowances, to permit reflooding the core to 2/3 of core height following a design basis loss-of-coolant accident. The reflood time is dependent on the accident assumptions used in the 10CFR50 Appendix K model. See USAR section 14.7.2.

3.6.2 Description

3.6.2.1 Shroud

The shroud is a stainless steel cylinder which surrounds the reactor core and provides a barrier to separate the upward flow of coolant through the reactor core from the downward recirculation flow. Bolted on top of the shroud is the steam separator assembly which forms the top of the core discharge plenum. This provides a mixing chamber before the steam-water mixture enters the steam separator. Refer to Figure 3.6-1 for the reactor vessel cutaway isometric for illustration of parts arrangement.

The bottom of the shroud is welded to a rim on the baffle plate. The baffle plate outer diameter is welded to the reactor vessel and the inner diameter is supported by columns extending to the bottom head.

3.6.2.2 Baffle Plate

The recirculation outlet and inlet plenum are separated by the baffle plate joining the bottom of the shroud to the vessel wall. The jet pump diffusers extend through holes in the baffle plate, and are welded to the baffle plate. A special adapter piece is used to make the transition from the pump to the plate.

The baffle plate and inner rim are of Inconel for welding to the ferritic base metal of the reactor vessel. The bottom of the shroud is welded on top of the rim, which provides for the differential expansion between the ferritic, Inconel, and stainless steel components. Inconel legs welded at intervals around the baffle plate support it from the vessel bottom head.

3.6.2.3 Baffle Plate Support

The baffle plate supports carry all the vertical weight of the shroud steam separator and dryer assembly, top and bottom core grids, peripheral fuel assemblies, and core plugs not carried on guide tubes, and jet pump components carried on the shroud. In addition, the supports must withstand the differential pressures of normal operations and blowdown accidents (either upward or downward), and for the vertical and horizontal thrusts of the seismic design.

3.6.2.4 Fuel Support Piece

The reactor fuel supports are the four-lobed, Type 304 stainless steel fuel support pieces mounted on top of the control rod guide tubes. Each support piece holds four fuel assemblies and is designed to hold the orifice plates used to obtain proper core flow distribution. The control rods pass through slots in the center of the support piece.

Each fuel support piece is removed to take out the control rod with attached velocity limiter.

3.6.2.5 Control Rod Guide Tubes

The control rod guide tubes extend up from the control rod drive housing through holes in the core support plate. Each tube is designed as a lateral guide for the control rod and as the vertical support for the fuel support piece which holds the four fuel assemblies surrounding the control rod. The guide tubes are fabricated from stainless steel with 0.165-in. nominal and 0.134-in. minimum wall thickness. The bottom of the guide tube is inserted and locked into a sleeve in the control rod drive housing.

3.6.2.6 Core Top Guide

The core top guide appears as a series of beams at right angles forming square openings which maintains the alignment of control rods and fuel bundles during normal operation, pressure transients, and seismic events. The guide provides lateral support and guidance for the fuel assemblies, thereby making it part of the core support structure. The top guide is attached to the reactor core shroud.

3.6.2.7 Core Support Plate

The core support plate consists of a perforated stainless steel plate supported on a grid beam structure, which is in turn supported on the reactor core shroud. The core plate assembly provides lateral support for the fuel bundles, control rod guide tubes, and in-core instrumentation. Sixteen fuel assemblies or core plugs at the periphery of the core, which are not adjacent to control rods, are directly supported by the core support plate. Proper orificing for coolant flow is provided in the grid for these 16 assemblies. Smaller perforations in the core plate provide guidance for the in-core neutron monitor guide tubes, between fuel assembly locations.

3.6.2.8 Jet Pumps

The 20 jet pumps are of stainless steel construction and consist of a driving nozzle, suction inlet, throat or mixing section, and diffuser. The jet pumps are arranged in two symmetric groups around the reactor core shroud in the downcomer annulus. There are 10 risers, each supplying a jet pump pair with high pressure water. Each supply line is welded to a nozzle on the outside of the reactor vessel. On the inside of the vessel, a stainless steel riser pipe terminates at the pair of jets. The riser is held in position by support arms welded to the vessel wall.

The jet nozzle, contoured inlet, and throat are joined together as a removable unit, clamped to the top piece of the riser by a nut-locking system. The joint between the throat and the diffuser is a slip fit. The throat section is supported by a clamp ring attached to the riser.

The jet pump diffuser is a gradual conical section changing to a straight cylindrical section and flanged at the lower end. The diffuser is inserted in the baffle plate, and is supported by brackets from the vessel wall. A water seal is formed by the adapter piece which is welded to the baffle plate and the diffusers.

The hydraulic and operational effects of the jet pump design are discussed in Section 4.3.3.

3.6.2.9 Feedwater Sparger

The feedwater sparger is made up of four sections each independently fed from one of the four feedwater inlets. The spargers are located approximately 4 ft below the normal water level in the core. The feedwater sparger sections each cover a 72° arc, the remaining 18° of the quarter circle is taken up by brackets clamped to the end plates. Brackets are attached at both ends of each section and are mounted to brackets welded into place on the vessel wall.

Each feedwater nozzle is provided with a double thermal sleeve which provides enhanced thermal protection. The inner thermal sleeve is welded to the safe end to eliminate any leakage of colder feedwater into the nozzle bore. The outer thermal sleeve slips over the inner thermal sleeve. It is positioned radially by a shoulder on the outboard end of the inner thermal sleeve and by lugs on the inboard end of the inner thermal sleeve. It is held in position axially by pins that are spot-welded to the outer thermal sleeve. It extends beyond the inner thermal sleeve and is provided with half-moon cutouts to accommodate the sparger arms. The sparger tee is installed inside the inner thermal sleeve using an interference fit which minimizes leakage. Any leakage past the interference fit is routed into the reactor by the outer thermal sleeve, thereby protecting the nozzle from thermal fatigue.

Feedwater sparger discharge flow exits the sparger through elbows mounted on top of the sparger. The elbows are fitted with converging discharge nozzles. This reduces temperature stratification in the sparger and flow separation around the periphery of the flow holes at low feedwater flow.

3.6.2.10 Core Spray Spargers

The reactor has two core spray spargers. Each sparger is in two halves to allow for thermal expansion, and is supported by slip-fit brackets welded just below the top of the core shroud. Each half receives spray water from a pair of supply lines routed in the reactor vessel to accommodate differential movement between the shroud and the vessel. The supply line pairs terminate at a common vessel nozzle. Each half has distribution nozzles pointed radially inward and downward at a slight angle to achieve a specified distribution pattern.

3.6.2.11 Standby Liquid Control System Sparger

The standby liquid control system sparger is a perforated pipe attached inside the bottom end of the core shroud. It discharges the sodium pentaborate solution into the cooling water which then rises upward through the reactor fuel.

3.6.2.12 Steam Separator Assembly

The steam separator assembly consists of the core top plenum head into which are welded an array of standpipes, with a steam separator attached to the top of each standpipe. The assembly is bolted on top of the core shroud by long bolts which permit removal for refueling operations. The assembly is guided into place by vertical guide tracks on the inside of the reactor vessel, and by locating pins on top of the shroud.

The fixed centrifugal type steam separators have no moving parts. In each separator, the steam-water mixture rising through the standpipe passes vanes which impart a spin to establish a vortex which separates the steam from the water. The steam exits from the top of the separator and rises up to the dryers. The separated water exits from under the separator cap and returns to the trays among the standpipes, which drain into the downcomer annulus.

3.6.2.13 Steam Dryer Assembly

The steam dryer assembly is seated on brackets on the inside of the reactor vessel wall below the steam outlet nozzle. A skirt extends down from the dryer assembly into the water to form a seal between the wet steam plenum below the dryers and the dry steam flowing out the top and down to the steam nozzles. Moisture is removed by impinging on the dryer vanes, and flows down through collecting troughs and tubes to the water trays above the downcomer annulus. The vertical tracks inside the reactor vessel are also used to guide the dryer assembly into position.

3.6.2.14 Incore Nuclear Instrumentation Tubes

There are 40 in-core nuclear instrumentation guide tubes extending up through the bottom of the reactor vessel to the core support plate. Thirty-six of these locations contain nuclear instrumentation tubes that extend to the core top guide. The four remaining guide tubes are spares.

The guide tubes are inserted into the reactor through housings that are attached to the bottom head of the reactor vessel and extend down to the same level as the drive housing flanges.

Twelve of the instrumentation tubes are closed at the top end, and are designed for the same pressure as the reactor vessel to prevent leakage of reactor water. Four of these twelve tubes are for the SRM detectors and eight for the IRM detectors.

Twenty-four of the others are for the LPRM in-core detector strings, and contain a smaller guide tube for the traveling in-core probe. Each of the 24 stainless steel tubes is about 1 in. in diameter, contains entry holes at the top for water cooling, and has a pressure seal at the bottom where the coaxial cables leave the reactor.

3.6.3 Performance Evaluation

The reactor core structural components are designed to accommodate the loadings applied during normal operation and maneuvering transients. Deflections are limited so that the normal functioning of the components under these conditions is not impaired. Where deflections are not the limiting factor, the ASME Boiler and Pressure Vessel Code, Section III (Reference 72), is used as a guide to determine limiting stress intensities and cyclic loadings for the core internal structure.

The loading conditions which occur during excursions or loss-of-coolant accidents have been examined. The reactor core shroud, shroud support, and jet pump body, which comprise the inner vessel around the core within the reactor vessel, are designed to maintain reflooding capability following design basis loss-of-coolant accidents. Reflooding the reactor core to the top of the jet pump inlets provides adequate cooling of the fuel.

The design of the jet pump parts takes into account the pressure loading both in normal and accident conditions and the reactions at the supporting brackets due to differential thermal expansion of the pump and reactor primary vessel.

The reactor internals are designed to preclude failure which would result in any part being discharged through the main steam line, in the event of a steam line break, which might block a main steam line isolation valve.

The structural components which guide the control rods are analyzed to determine the loadings which would occur in design basis loss of coolant accidents. The reactor core structural components are designed so that deformations produced by accident loadings do not prevent insertion of control rods.

The differential pressures across the reactor internal components are shown in Table 3.6-1.

3.6.3.1 Vibration Measurements

The vibration analysis and testing of BWR reactor internals has been well developed, and provides the needed assurance that the integrity of the BWR reactor internal structure is not violated as a result of flow-induced vibrations. The vibration acceptance criteria are calculated by General Electric using a lumped-mass dynamic analysis of the reactor vessel and internals. This method of analysis has been verified through experimentation, and it is in general use throughout the nuclear industry. The value of the endurance limit used in establishing the vibration criteria for BWR reactor internals with the exception of the existing Westinghouse steam dryer is 10,000 psi. This is considered to be a conservative design value; it is 250% lower than the value of the endurance limit recommended by ASME in their Code for Nuclear Vessels (Reference 72). The Westinghouse steam dryer has been qualified for high-cycle fatigue subject to acoustic loads using an endurance-strength of 13.6 Ksi based on use of ASME Code Figure I-9.2.2, Curve C. (Reference 94)

Vibration data obtained from operating BWR plants have shown conclusively that, for a broad range of BWR sizes, the conservatively chosen long term steady state vibration criteria are not violated for normal balanced flow conditions. Since all BWR jet pump plants are geometrically similar, it is not expected that there is any significant difference in vibration response of plants in various limited size ranges. Therefore, a complete series of vibration tests is not necessary for individual units. The vibration tests on an individual unit include testing of the shroud, separators and jet pump assemblies.

Additional components are included in the test program on a selective basis to assure that their vibrations are also within acceptable criteria. All vibration test data is analyzed, and the maximum amplitude of vibration is recorded. However, it should be emphasized that the indication of a maximum amplitude of vibration in no way implies that the vibration occurs continuously at that maximum amplitude and frequency for 40 years of plant operation; it merely represents the maximum value that might be expected to occur during plant lifetime.

Vibration measurements were made by General Electric on the reactor internals at Monticello during the initial startup program in 1970-71. The following components were included in the vibration testing:

Shroud Separator Assembly
Jet Pump Riser Pipe Vibration Motion (Tangential)
Jet Pump Vibration Motion (Radial, at the Top)
In-Core Guide Tube Housing
Control Rod Guide Tubes

These tests were conducted for various conditions, beginning with cold flow tests and ending with turbine trip tests from 100% power and 100% coolant flow.

3.6.3.1.1 Shroud-Separator Assembly Vibration Measurements

The maximum vibration motions of the shroud-separator assembly for all steady operating conditions, with both balanced and unbalanced flow, were 0.001” peak-to-peak at 6.0 to 7.0 Hz and .0006” peak-to-peak at 14.8 Hz. These represent 1.8% and 3.2% of the respective criteria.

The highest vibration amplitudes measured are related to the opening of a pressure relief valve and to scram when operating at and above 50% power. Transient vibrations lasting up to 1.5 sec resulted in the following maximum amplitudes:

	Amplitude Peak to Peak	Vibration Frequency	% Criteria
2 Pump Trip	0.0012”	5.5 Hz	2.2
	0.0025	15	13.1
Turbine Trip	0.005	5.6	9.1
	0.0065	15	34

3.6.3.1.2 Jet Pump Riser Pipe Vibration Motion (Tangential)

The maximum tangential vibration motions of the jet pump riser during the tests were as follows:

Criteria	Vibration Amplitude	Vibration Frequency	% of Steady State
Constant Flow, Cold			
Balanced Flow	0.004” p.p.	25 Hz	50
Unbalanced Flow	0.0066	25	83 (1) (4)
Constant Flow, Hot			
Balanced Flow	0.002	25 Hz	25
Unbalanced Flow	0.008	23.5	91 (1)
Transient Flow			
“A” Pump Trip, Cold	0.009	26	112 (2) (4)
Hot	0.008	24.8	100 (2) (3)
“B” Pump Trip, Cold	0.012	25	150 (2) (4)
Hot	0.0035	31.5	25
Turbine Trip	0.004	26.8	53 (2)

Notes: (1) Procedural limitation forbids operation with the unbalanced flow established for these tests points.
(2) The amplitudes measured occurred for less than 1.5 sec.
(3) This reading occurred during “A” pump coastdown when unbalanced flow passed through critical region (see note 1).
(4) The jet pumps cavitate under these conditions, and this mode is not permitted during plant operation.

3.6.3.1.3 Jet Pump Vibration Motion (Radial at the Top)

The maximum radial vibration motions of the jet pumps during the tests were as follows:

	Vibration Amplitude	Vibration Frequency	% Criteria
Constant Flow, Cold			
Balanced Flow	0.004” p.p.	36 Hz	30
Unbalanced	0.003	24	17
Constant Flow, Hot			
Balanced Flow	0.0015	24.8	6
Unbalanced	0.005	24.8	20
Transient Flow			
“A” Pump Trip, Cold	0.012	32	47
Turbine Trip	0.005	36	37

The cold readings also represent operation during initial cavitation, which is normally avoided.

The amplitudes listed for transient conditions last only 1.0 to 2.0 sec.

3.6.3.1.4 In-Core Guide Tube Housing Vibration Motion

The maximum vibration amplitudes of the incore guide tube housing occurred during the cold unbalanced flow test. This amplitude was 0.0098” peak to peak at 45 Hz, which is 19% of the criterion. During the hot flow tests, the amplitude never exceeded 6.6% of the criterion.

3.6.3.1.5 Control Rod Guide Tubes

The maximum vibration strain amplitude occurred during unbalanced cold flow operation. The amplitude was 69.0 micro strain peak to peak at 19 Hz, which is 9% of the criterion. All readings during the hot flow tests were below 1% of the criterion.

The GE test reports reviewed by NSP showed no vibration amplitudes or frequencies outside the acceptance criteria established by GE. In fact, the measured vibration levels were within acceptable limits established for normal operation up to 100% power and 100% flow. These test results were reviewed again by GE and found acceptable when the Increased Core Flow region was added to the Power-Flow Operating Map.

For unbalanced flow operation, procedural controls have been installed to prevent operation of recirculation pumps in areas that may result in undue vibration of the jet pump assembly.

3.6.3.1.6 Evaluation of Reactor Internals Flow Induced Vibration

At a reactor power of 2004 MWt, there would be increased steam production in the core over that for the original licensed power level of 1670 MWt. The increased steam production results in an increase in the pressure drop across the core. In a jet pump plant like Monticello, the recirculation drive flow must be increased in order to maintain the same core flow as the differential pressure across the core increases with increased power level. The increase in recirculation pump speed may increase the possibility of reactor internals vibration. An evaluation was performed to determine the effects of flow induced vibration on the reactor internals at a bounding reactor power of 2044 MWt and 105% of rated core flow. This assessment was based on an evaluation of the Monticello plant specific vibration data for the reactor internal components recorded during the startup testing and on operating experience from similar plants. The expected vibration levels at 2044 MWt were estimated by extrapolating the vibration data recorded during startup testing at MNGP and other operating experience. These expected vibration levels were then compared with the established vibration acceptance limits. The following components were evaluated.

a. Shroud head and separator

b. Fuel assembly, top guide and core plate

c. Jet pump assemblies

d. In-core guide tubes

e. Control rod guide tubes

f. Jet pump sensing lines

g. Feedwater sparger

h. Guide rods

i. Shroud head bolts

j. RPV top head nozzles

k. Core spray piping (internal to RPV)

The results of the vibration evaluation (References 98 and 100) show that operation up to bounding reactor power of 2044 MWt and 105% of rated core flow is possible without any detrimental effects on the reactor internal components.

The established vibration level acceptance limits are based on the GE criterion which limits FIV alternating stress intensity to 10,000 psi for austenitic stainless steels. The NRC staff found this criterion acceptable, as it is conservative when compared to the ASME Section III design fatigue endurance limit for austenitic stainless steel material of 13,600 psi which is further reduced for steady state vibration by a factor of 0.8 to 10,880 psi, following the guidance of Part 3 (Requirements for Preoperational and Initial Startup Vibration Testing of Nuclear

Power Plant Piping Systems) of the ASME OM-SG Code, “Standards and Guides for the Operation and Maintenance of Nuclear Plants” (Reference 106).

A high-cycle fatigue evaluation of the existing Westinghouse steam dryer for the Monticello Plant has been completed. Acoustic loads and stresses have been evaluated for high cycle fatigue and have been determined to meet the American Society of Mechanical Engineers (ASME) Boiler and Pressure Vessel (B&PV) Code Section III, Subsection NG criteria. (Reference 94)

3.6.3.2 Pressure Forces During Blowdown

In this section the internal pressure forces which would be imposed across the internal reactor components during rapid depressurizations associated with pipe breaks are discussed in detail.

3.6.3.2.1 Analytical Model

Internal reactor pressure forces are calculated for two postulated break conditions, a steam line rupture and recirculation line rupture. The steam line break is assumed to be a guillotine line severance which is located upstream of the flow limiter. This break gives the maximum break steam flow and maximum pressure forces. The conclusion of the event is complete blowdown to the drywell. The recirculation line break is assumed to be a guillotine line severance at the pressure vessel outlet. The conclusion of the event is also a complete blowdown to the drywell. In both cases reflooding of the reactor is accomplished by the emergency core cooling system. The break is assumed, in each case, to occur while the plant is at a reactor power of 2044 MWt (102% of 2004 MWt) with 60.48×10^6 (105% of 57.6×10^6) lbm/hr core recirculation flow. Internal reactor pressure forces for normal, upset, emergency and faulted conditions were reviewed and found acceptable (References 95 and 99).

When calculating internal pressure loading due to a blowdown accident, an analytical model is employed in which the pressure vessel is divided into five major chambers or nodes. Each node is connected to adjoining nodes by a flow resistance, Figure 3.6-2. The five nodes are:

a. sub-cooled lower plenum,

b. saturated core,

c. saturated upper plenum,

d. saturated mixing plenum, and

e. saturated steam dome.

The lower plenum to core resistance includes the inlet orifice, acceleration, local, and flow losses to the core mid-plane. The core-to-upper plenum resistance consists of the remaining core local losses and flow losses. The separator resistance is between the upper plenum and mixing plenum and steam dome. In the recirculation line break, one additional resistance is included, i.e., the resistance between the downcomer and the lower plenum through the open jet pumps of the broken line. Jet pumps are described in Section 4.3. Refer to Figure 3.6-2, for a schematic of the reactor vessel and internal components. Table 3.6-1 depicts the pressure forces acting on major components.

The two design basis breaks are discussed individually.

3.6.3.2.2 Recirculation Line Rupture

The recirculation line rupture (double-ended) causes high flow rates from the downcomer and plenum regions. Initially, super critical flow (high single-phase flow) exists in the blowdown lines prior to flashing of the water. After bubbles form in the lines, two-phase critical flow is established and the blowdown rate is reduced from the supercritical flow value. No credit is taken for friction losses in the broken line.

Although the flow rate from the downcomer is high, the pressure change rate in the mixing plenum is only about 20 psi/second assuming no admission valve action to maintain pressure. Because large amounts of saturated water are present in the mixing plenum, the depressurization rate is low due to the accompanying flashing.

Large pressure forces due to depressurization of the subcooled lower plenum do not develop in the current BWR plant. The principal reason in this case is that, in the event of a line break, the subcooled lower plenum does not discharge directly to the atmosphere. Instead, it discharges to the downcomer region through the inoperative jet pump diffusers, and the downcomer pressure is maintained by compression of the steam above the mixing plenum.

Thus, large pressure forces cannot develop across the diffusers and shroud support because the inoperative jet pump diffusers are open between the downcomer and lower plenum. Even though the lower plenum is subcooled, its depressurization rate is limited by the downcomer and mixing plenum depressurization rate. The fact that some water flows through the jet pump nozzles to the atmosphere is not serious since the flow would be critical or “choked” in the nozzles, and the total nozzle area is only 15% of the 28-in. outside diameter recirculation line area.

Fuel lift is affected by the reactor building seismic response and fuel bundle and control rod guide tube lift forces. Fuel lift margin for GE14 fuel was evaluated at normal, upset, emergency and faulted conditions and fuel hold down forces remain above the uplift forces (Reference 99). Fuel liftoff does not occur for AREVA fuel (Reference 121).

The calculated maximum pressure differential across the fuel channel during a DBA-LOCA would be approximately 12.9 psi outward (initial value) for the faulted condition. Core inlet flow decreases to about 40% rated flow resulting in a decrease in channel box pressure level. Since the channel differential pressure is similar to that occurring during normal operating, control rod interference will not occur. Core pressure drops are very similar between GE14 and AREVA fuel (Reference 119). Therefore channel wall pressure differences during normal and abnormal conditions are expected to be similar.

Shroud loads were evaluated to determine impact on shroud screening criteria for shroud flaw evaluations including the impact of reactor recirculation line break loads (Reference 105).

3.6.3.2.3 Steam Line Rupture

Following the instantaneous steam line (double-ended) rupture, critical flow is established in each broken line. Since the break is postulated to be upstream of the steam flow restrictor, the break area is the sum of one open steam line area plus one steam flow restrictor area at the other end of the break. This break causes the system to depressurize at about 100 psi/sec during initial steam blowdown.

The design-break is assumed to have a constant break area of 1.9 sq ft, actually the effective break area diminishes with time since the isolation valves are closing in one end of the break. When the isolation valves have been closed, the effective break area is reduced to only one steam line cross- sectional area. Rapid decompression of the subcooled lower plenum cannot occur because the decompression rate is limited by the saturated upper core regions.

Following an instantaneous steam line break, the initial differential pressure increase across the separators and shroud support is caused by the momentum effects associated with the accelerating flow into the depressurizing mixing plenum. The increased loadings at approximately 2 sec are the result of saturating the previously subcooled lower plenum inventory. The high exit mass flow rates associated with this flashing decrease as the inventory becomes depleted; as this occurs, the loadings across the various internal components are reduced. Subsequently, no means exist for sustaining large differentials between any of the vessel regions, and all differential pressures drop to low values.

The maximum vessel internal loadings have been evaluated without any consideration of the rise in coolant level that would occur after a steam line break. This level rise would in fact cause two phase blowdown from the vessel and thus reduce the depressurization rate during the time when the maximum loadings would occur. It is also assumed that the recirculation system pumps remain at full speed through the transient; since they help to sustain inter-region pressure differentials this is a conservative assumption. Similarly the assumption of continued injection of full feedwater flow is also conservative since it would contribute to the depressurization rate and thus maximize the internal loading.

3.6.3.3 Performance of Reactor Internals

An analysis has been performed to evaluate the potential leakage from within the flooded portion of the reactor vessel during the postulated recirculation line break accident.

This leakage would extend the ECC analysis reflooding time if it were not taken into account in the accident calculations.

The possible sources of leakage are the jet pump slip joint and the jet pump bolted joint. Both of these leakage points have been analyzed for possible leakage. The total leakage has been accounted for in the transient level calculations used to predict coolant levels in the emergency core cooling systems analyses of Section 6.2.

The reactor internals and primary system piping are being designed to conform with criteria as specified in Section 12.2.1.4.

The designs of the reactor internal components are sensitive primarily to the application of single rather than combination loads. Combination loads tend to produce only a secondary effect. For example, the reactor internal component which is most sensitive to the maximum seismic load is the top guide; however, the top guide is not appreciably affected by DBA loads. On the other hand, the steam dryer is predominantly affected by the blowdown pressure differentials which accompany the steam line rupture DBA whereas seismic loads are negligible in comparison. Therefore, the following discussion of stresses and deformations calculated for the reactor internals are only concerned with the specific locations in the reactor where the maximum stress or strain occurs for a given load combination. The stress or strain at every other location is less than the one cited.

During a maximum earthquake, the largest stress in the reactor internals occurs in the top guide assembly. To determine this stress, the grid work structure of the top guide assembly is modeled for computer analysis, and an earthquake loading is applied. With the load assumed to be uniformly applied along the grid members, the loading direction producing the highest stress was found by examining three independent directions, two of which acted parallel to the grid beams (i.e., first the X-direction, then the Y-direction) and one which acted at 45° to the beams. The maximum stress, which was calculated to be less than 9000 psi, occurred for a load direction of 45° and a 0.6g equivalent static load.

During the steam line rupture DBA, the sensitive component is the steam dryer assembly. The design criteria for the steam dryer requires that the structural integrity of the dryer be maintained for a steam line break which occurs beyond the main isolation valves so as to assure that no part of the dryer can become lodged in the valve and prevent its proper closure. The existing Westinghouse steam dryer has been analyzed for a main steam line rupture DBA in Reference 95.

During core reflooding following a DBA, the predominant stresses are secondary (thermal). According to the 1965 edition of ASME Section III, (Reference 72) (which is used as a guide), thermal stresses need not be calculated if they occur during emergency operation for fewer than 25 cycles. However, even though the DBA satisfies the requirements of not requiring a thermal or fatigue analysis, a thermal stress and fatigue analysis was performed to be certain that the structural integrity of the internals is retained so that the core reflooding capability can be maintained.

The most significant thermal strain in any of the reactor internal components occurs in the shroud support or baffle plate (Figure 3.6-5). The results of earlier preliminary calculations were reported in APED-5460, “Design and Performance of GE BWR Jet Pumps,” September 1968 (Reference 78).

The sensitive regions of the Dresden-2 jet pump-shroud support plate assembly have been investigated for fatigue in a refined analysis in which “normal” operating transients as well as the Design Basis Accident (DBA) have been considered. The sensitive areas are defined in Figure 3.6-5 as points A, B & C.

The largest peak strain intensity range was found to occur at point B. An “upper bound” strain range was determined to be 8.64 percent. This value is based on the following: a finite element model of the support plate-to-shroud junction in which inelastic strains are considered; the actual temperature distribution in the geometry; and conservatively defined deformation boundary conditions.

This peak strain range was found to occur for the cycle which includes the improper recirculation loop startup transient and the point in the time of the post DBA flooding (LPCI) when the shroud and support plate through-wall gradients are a maximum. This strain range corresponds to about 3 allowable fatigue cycles based on an extrapolation of the ASME Section III fatigue curve for Inconel. The other “normal” transients evaluated do not contribute to the accumulative usage; therefore, the total usage factor is about 0.33.

Referring to APED-5460 (Reference 78), it can be seen that the magnitude and location of the peak strain differ from the recently calculated values. The principal reason for this difference is that the effect of out of plane deformation was neglected in the earlier work. The major contributor to the recently calculated value of peak strain range is the strain intensity produced at the plate-to-shroud junction due to the large plate and shroud through wall temperature gradient resulting from post accident emergency flooding. Early in the LPCI flooding, cold water exists at the under side of the plate and at the inside surface of the shroud, producing a large redundant bending moment between the support plate and shroud.

The peak strain intensity was also recalculated at the minimum support plate ligament cross section (point A, in Figure 3.6-5) and was determined to be 0.875 percent. This value is also found from a refined finite element model of the support plate in which inelastic strains were considered. This model does not account for the stiffening effect of the jet pump diffuser (conservative). The reduction in strain from the previously calculated value (APED-5460) (Reference 78) may be explained as follows: 1) The early calculation considered the vessel to be rigid and the shroud to be an elastic, infinitely long cylinder; the recent calculation accounts for the elasticity of the real geometry. 2) The early analysis assumed the vessel to be at a temperature of 550oF and the shroud at a temperature of 120°F; the latest calculation considers the maximum shroud-vessel average temperature difference as obtained from a refined thermal analysis. 3) The model of the plate is more refined than that previously used; strain hardening and actual predicted plate temperatures were considered.

An “upper bound” peak strain intensity at point C has been determined to be 2.5 percent. This value is also based on the finite element model of the plate. In this evaluation, the shroud is considered disconnected from the plate I.D. while the plate O.D. is radially deformed an amount equal to the vessel thermal growth at the maximum vessel-shroud average temperature difference.

The calculations described above are specifically applicable to the Dresden 2 plant. However, since the shroud support plate for Monticello is somewhat thicker than for Dresden 2, the maximum strain would be less than the value reported for Dresden 2.

3.6.4 Inspection and Testing

Quality control methods were used during the fabrication and assembly of reactor internals to assure that the design specifications are met. The reactor coolant system was thoroughly cleaned and flushed before fuel was loaded initially. During the preoperational test program, systems such as feedwater, jet pumps, core spray, and standby liquid control spargers were tested to assure operational readiness.

Based on industry in-vessel inspection experience and safety assessments completed by the Boiling Water Reactor Vessel Internals Project (BWRVIP), various inspection and evaluation guidelines have been developed and utilized at Monticello for assuring the long term integrity of the internal vessel components.

Table 3.6-1 Reactor Internal Pressure Differentials (psid)

Component	Normal Conditions[1]	Upset Conditions[2]	Emergency Condtions[3]	Faulted Conditions[4]
Shroud Support Ring and Lower Shroud	26.63	29.03	38	45
Core Plate and Guide Tube	20.17	22.57	26.5	28
Upper Shroud	6.65	9.98	12.1	24.50
Shroud Head	7.21	10.82	12.8	25
Shroud Head to Water Level (Irreversible[5])	9.47	14.21	14.1	26
Shroud Head to Water Level (Elevation[5])	0.61	0.92	1.0	1.7
Top Guide	0.48	0.53	0.12	0.38
Fuel Channel Wall	9.67	<11.8	11.8	12.9
Steam Dryer	0.19[6]	0.32[6]	0.37[7]	0.64[8]

Notes:
1. Normal conditions are defined as steady state operating conditions. This condition assumes 100% rated thermal power (2004 MWt), 105% of rated core flow, and reactor dome pressure of 1025 psia (References 98 and 99).
2. Upset conditions are defined as anticipated plant transients (moderate frequency), which are expected to occur during the operational plant's lifetime (e.g., turbine trip). The upset condition values are based on application of bounding adders and multipliers to the normal condition values. This condition assumes 102% rated thermal power (2044 MWt), 105% of rated core flow, and reactor dome pressure of 1025 psia (References 98 and 99).
3. Emergency conditions are defined as infrequent events, which are postulated to occur once during the operational plant's lifetime. The emergency conditions are based on the most limiting non-DBA transient event postulated to occur once during the operational plant's lifetime. This condition assumes 102% rated thermal power (2044 MWt), 105% of rated core flow, and reactor dome pressure of 1040 psia (References 98 and 99).
4. Faulted conditions are defined as accidents or limiting faults, which are postulated as part of the plant's design basis. Values are the maximum results from either the cavitation interlock power and flow or the high power and 105% core flow points (References 98 and 99).
5. Irreversible loss is the loss across the separators; the elevation loss or reversible head loss is the loss between the inside shroud to the exit of the separators (References 98 and 99).
6. Values are from Reference 95 and are based on the normal and upset power, flow, and dome pressure conditions.
7. Not based on emergency conditions but on a main steam line break outside containment at rated power and core flow (Reference 95).
8. Based on main steam line break outside containment during hot standby (Reference 95).

3.7 References

1. Deleted.

2. General Electric Report, NEDE-21156, "Supplemental Information for Plant Modification to Eliminate Incore Vibration", January 1976.

3. Deleted.

4. Deleted.

5. NRC Safety Evaluation Report on the Reactor Modification to Eliminate Significant Incore Vibration in Operating Reactors with One Inch Bypass Holes in the Core Support Plate, February 1976.

6. General Electric Report, NEDO-10299, "Core Flow Distribution in a Modern Boiling Water Reactor as Measured in Monticello", H T Kim, January 1971.

7. General Electric Report, NEDO-10722, "Core Flow Distribution in a General Electric Boiling Water Reactor as Measured in Quad Cities Unit 1", H T Kim and H S Smith, December 1972.

8. General Electric Report, NEDO-21118, "Brunswick Steam Electric Plant Unit 2 Safety Analysis Report for Plant Modifications to Eliminate Significant Incore Vibrations", December 1975.

9. NRC Letter (W Butler) to General Electric (I Stuart), Topical Report Evaluation of NEDO-10722 and NEDO-10299, dated October 1, 1974.

10. General Electric Report, NEDO-20964, "Generation of Void and Doppler Reactivity Feedback for Application to BWR Design", R C Stirn, December 1975.

11. General Electric Report, NEDO-20964-1, "Generation of Void and Doppler Reactivity Feedback for Application to BWR Design (Amendment No. 1)", July 1977.

12. Deleted.

13. Deleted.

14. Deleted.

15. Deleted.

16. NSP (L O Mayer) letter to the AEC (J F O'Leary), "Additional Information Concerning Supplement No. 1 to Technical Specification Change Request No. 3", dated October 4, 1973.

17. General Electric Report, APED-5640, "Xenon Consideration in Design of Boiling Water Reactors", R L Crowther, June 1968.

18. "Status of Reactor-Physics Calculations for U.S. Power Reactors", by J Chernick, Reactor Technology, Vol. 13, No. 4, Winter 1970-1971.

19. Deleted.

20. Deleted.

21. Deleted.

22. Deleted.

23. Deleted.

24. "Physics of Operating Boiling Water Reactors", E D Fuller, Nuclear Applications and Technology, Vol. 9, November 1970.

25. "The Physics of Non-Uniform BWR Lattice", P G Aline, et. al., BNES International Conference on the Physics Problems in Thermal Reactor Design, June 1967.

26. Deleted.

27. Appendix 4A at the end of Chapter 4 of GESSAR.

28. General Electric Reports, NEDE-21354-P and NEDO-21354, "BWR Fuel Channel Mechanical Design and Deflection", September 1976.

29. General Electric Reports NEDE-20943-P and NEDO-20943, "Urania - Gadolinia Nuclear Fuel Physical and Irradiation Characteristics and Material Properties", G A Potts, January 1977.

30. Deleted.

31. Deleted.

32. Deleted.

33. Deleted.

34. Deleted.

35. Deleted.

36. Deleted.

37. Deleted.

38. Deleted.

39. Deleted.

40. Deleted.

41. Deleted.

42. General Electric Report, NEDE-21282-P, “General Electric Densification Program Status”, Revision 1, April 1977.

43. NRC (O Parr) letter to General Electric (G Sherwood), “Topical Report NEDE-21282-P, General Electric Densification Program Status”, dated January 3, 1978.

44. Deleted.

45. Deleted.

46. Deleted.

47. Deleted.

48. NSP (D M Musolf) Letter to the NRC, “BWR Control Rod Drive Return Line Nozzle Cracking Post Modification Report for NUREG-0619”, dated May 9, 1983.

49. Deleted.

50. General Electric Report, RDE No. 20-0787, “Monticello Scram Evaluation with Partially Filled Discharge Volume”, August 1987.

51. Global Nuclear Fuels - Americas Report, NEDE-24011-P-A-27, “General Electric Standard Application for Reactor Fuel”, Revision 27, August 2018, and the U.S. Supplement, NEDE-24011-P-A-27-US, August 2018. 60400000333

52. Deleted.

53. Deleted.

54. Deleted.

55. Deleted.

56. EAS-43-0789, "Increased Core Flow Analysis for Monticello Nuclear Generating Plant Cycle 14", September 1991, RRM02944-0385.

57. Deleted.

58. Deleted.

59. General Electric Report, NEDE-31152-P, “General Electric Bundle Designs”, Revision 8, April 2001 (As revised).

60. Deleted.

61. Deleted.

62. Deleted.

63. Deleted.

64. NRC Information Notice 89-69, “Loss of Thermal Margin Caused by Channel Box Bow”, September 29, 1989.

65. NRC Bulletin 90-02, “Loss of Thermal Margin Caused by Channel Box Bow”, March 20, 1990.

66. Deleted.

67. Deleted.

68. Deleted.

69. Deleted.

70. Deleted.

71. Deleted.

72. ASME Boiler and Pressure Vessel Code, Section III, 1965, with Summer 1966 Addenda.

73. Survey of test results from SPERT and NSRR and observations of waterlogging failures in commercial reactors.

74. General Electric Report, NEDE-22290, “Safety Evaluation of the GE Hybrid I Control Rod Assembly”, December 1982.

75. NRC Letter (C O Thomas) to General Electric (J F Klapproth), “Acceptance for Referencing of Licensing Topical Report NEDE-22290, Safety Evaluation of the General Electric Hybrid I Control Rod Assembly”, dated August 22, 1983.

76. General Electric Report, NEDE-22290-A, “Safety Evaluation of the GE Hybrid I Control Rod Assembly”, September 1983.

77. Deleted.

78. General Electric report, APED-5460, “Design and Performance of GE BWR Jet Pumps”, September 1968.

79. General Electric report, NEDE-22290-A, Supplement 2, “Safety Evaluation of the General Electric Advanced Longer Life Control Rod Assembly”, August 1985.

80. General Electric report, NEDE-22290-P-A, Supplement 3, “Safety Evaluation of the General Electric Duralife 230 Control Rod Assembly”, May 1988.

81. General Electric (K W Brayman) letter to NSP (H H Paustian), “Duralife 120 Control Rod Safety Evaluation”, dated January 15, 1991.

82. General Electric (G D Plotycia) letter to NSP (D G Wegener), “Safety Evaluation for Duralife Control Rods for Monticello Reload 16”, dated June 28, 1994.

83. Deleted.

84. American National Standard ANSI/ANS 5.1 - 1979, “Decay Heat Power in Light Water Reactors.”

85. Deleted.

86. American National Standard, ANSI/ANS-57.5-1981, “American National Standard for Light Water Reactor Fuel Assembly Mechanical Design and Evaluation.

87. T Sorlie, et. al., “Experiences With Operating BWR Fuel Rods Above the Critical Heat Flux”, Nucleonics, Vol. 23, No. 4, April 1965.

88. NEDC-32868P, Revision 5, “GE14 Compliance With Amendment 22 of NEDE-24011-P-A (GESTAR II)”, May 2013.

89. NEDE-31758P-A, GE Nuclear Energy, GE Marathon Control Rod Assembly, October 1991.

90. SSP-09/444-C, "Gardel BWR - Monticello NPP Power Distribution Uncertainties", July 2009.

91. General Electric Report, NEDO-21231, “Banked Position Withdrawal Sequence” C J Paone, January 1977.

92. General Electric Report, NEDO-33091-A, “Improved BPWS Control Rod Insertion Process” J Tuttle, July 2004.

93. General Electric correspondence, GE-MNGP-AEP-125, “Comment Resolution for Monticello EPU Task Scoping Document T0305A - Steam Dryer Structural Integrity”, June 11, 2007.

94. Westinghouse document WCAP-17549-P, "Monticello Replacement Steam Dryer Structural Evaluation for High-Cycle Acoustic Loads Using ACE. (Monticello calculation number 12-032)

95. Westinghouse Report SES 09-127-P, Rev. 2, “Monticello Steam Dryer Replacement - Structural Verification of Steam Dryer”, June 28, 2010. (Monticello calculation number 10-176)

96. NRC Letter (D G Eisenhut) to Licensee, November 13, 1980 (Issuance of NUREG-0619 via Generic Letter 80-95).

97. Monticello calculation 97-249, Revision 1, "Use of CRD System to Maintain Reactor Water Level".

98. GE Hitachi Report NEDC-33322P, Revision 3, "Safety Analysis Report for Monticello Constant Pressure Power Uprate," October 2008.

99. GE Hitachi EPU Project Task Report GE-NE-0000-0060-9039-TR-R1, Revision 1, "Task T0304: Reactor Internal Pressure Difference, Fuel Lift Margin, CRGT Lift force, Acoustic and Flow Induced Loads," November 2008 (Monticello calculation number 11-225).

100. GE Hitachi Project Task Report GE-NE-0000-0063-3152-TR-R0, Revision 0, "Task T0305, RPV Flow Induced Vibration," February 2008 (Monticello calculation number 11-226).

101. GE Hitachi Licensing Topical Report NEDC-33173P-A, “Applicability of GE Methods to Expanded Operating Domains.” (ADAMS Accession No. ML060450677).

102. NRC Letter (H K Nieh) to GE Hitachi (R E Brown), "Final Safety Evaluation for General Electric (GE) - Hitachi Nuclear Energy Americas, LLC (GHNE) Licensing Topical Report (LTR) NEDC-33173P, 'Applicability of GE Methods for Expanded Operating Domains' (TAC No. MD0277)," dated January 17, 2008 (ADAMS Accession No. ML073340231).

103. NRC Letter (T B Blount) to GE Hitachi (J G Head), "Final Safety Evaluation for GE Hitachi Nuclear Energy Americas, LLC Licensing Topical Report NEDC-33173P, 'Applicability of GE Methods to Expanded Operating Domains' (TAC No. MD0277)”, dated July 21, 2009 (ADAMS Accession No. ML083530224).

104. NSPM letter L-MT-08-052 (T J O'Connor) to NRC, "License Amendment Request: Extended Power Uprate (TAC MD9990)," dated November 5, 2008 (ADAMS Accession No. ML083230111).

105. NSPM letter L-MT-12-114 (M A Schimmel) to NRC, “Monticello Extended Power Uprate (EPU): Supplement to Gap Analysis Updates (TAC MD9990)”, dated January 21, 2013 (ADAMS Accession No. ML130390220).

106. ASME OM-SG Code, Standards and Guides for the Operation and Maintenance of Nuclear Plants.

107. NSPM Letter L-MT-13-053 (Mark A. Schimmel) to NRC, "Monticello Extended Power Uprate and Maximum Extended Load Line Limit Analysis Plus License Amendment Requests: Supplement for Analytical Methods Used to Address Thermal Conductivity Degradation and Analytical Methods Limitations (TAC Nos. MD9990 and ME3145)", dated July 8, 2013.

108. GE Nuclear Energy Service Information Letter 653, "MELLLA Upper Boundary Analytical Bases", December 15, 2003.

109. NSPM Letter L-MT-09-017 (T J O'Connor) to NRC, "Monticello Extended Power Uprate: Response to NRC Reactor Systems Branch and Nuclear Performance & Code Review Branch Request for Additional Information (RAI) dated January 16, 2009 (TAC No. MD9990)", dated March 19, 2009

110. NSPM Letter L-MT-13-092 (K D Fili) to NRC, "Monticello Extended Power Uprate (EPU): Completion of EPU Commitments, Proposed License Conditions and Revised Power Ascension Test Plan (TAC MD9990)", dated September 30, 2013

111. Letter from NRC (T A Beltz) to NSPM (K D Fili), "Monticello Nuclear Generating Plant - Issuance of Amendment No. 176 to Renewed Facility Operating License Regarding Extended Power Uprate (TAC No. MD9990)", dated December 9, 2013

112. NSPM Letter L-MT-13-126 (Karen D. Fili) to NRC, "Maximum Extended Load Line Limit Analysis Plus: Cycle 27 Safety Reload Licensing Report and Request for Additional Information Response (TAC ME3145)", dated December 20, 2013

113. NEDO-33173 Supplement 4-A, Rev. 1, "Implementation of PRIME Models and Data in Downstream Methods," November 2012.

114. ANP-3519P, Revision 0, "Fuel Rod Thermal-Mechanical Design for Monticello ATRIUM 10XM Fuel Assemblies, Cycle 29", November 2016.

115. ANP-2637, Revision 6, "Boiling Water Reactor Licensing Methodology Compendium", October 2014.

116. EMF-2209(P)(A) Revision 3, "SPCB Critical Power Correlation", September 2009.

117. ANP-10298PA, Revision 1, "ACE/ATRIUM 10XM Critical Power Correlation", March 2014.

118. EMF-2245(P)(A), Revision 0, "Application of Siemens Power Corporation's Critical Power Correlations to Co-Resident Fuel", August 2000.

119. ANP-3092P Revision 1, "Monticello Thermal-Hydraulic Design Report for ATRIUM™ 10-XM Fuel Assemblies," June 2016.

120. ANP-3135P, Revision 0, "Applicability of AREVA BWR Methods to Extended Flow Window for Monticello", April 2014.

121. ANP-3119P, Revision 1, "Mechanical Design Report for Monticello ATRIUM™ 10XM Fuel Assemblies", October 2016.

122. ANF-89-98(P)(A), Revision 1 and Supplement 1, "Generic Mechanical Design Criteria for BWR Fuel Designs," May 1995.

123. EMF-93-177(P)(A), Revision 1, "Mechanical Design for BWR Fuel Channels," August 2005.

124. BAW-10247PA Revision 0, "Realistic Thermal-Mechanical Fuel Rod Methodology for Boiling Water Reactors", April 2008.

125. ANP-3224P, Revision 2, "Applicability of AREVA NP BWR Methods to Monticello", June 2013.

126. XN-NF-80-19(P)(A) Volume 1 and Supplements 1 and 2, "Exxon Nuclear Methodology for Boiling Water Reactors - Neutronic Methods for Design and Analysis," Exxon Nuclear Company, March 1983

127. EMF-2158(P)(A) Revision 0, Siemens Power Corporation Methodology for Boiling Water Reactors: Evaluation and Validation of CASMO-4/MICROBURN-B2, October 1999.

128. XN-NF-79-59(P)(A), Methodology for Calculation of Pressure Drop in BWR Fuel Assemblies, November 1983.

129. ANP-10307PA Revision 0, AREVA MCPR Safety Limit Methodology for Boiling Water Reactors, June 2011.

130. XN-NF-80-19(P)(A) Volume 3 Revision 2, Exxon Nuclear Methodology for Boiling Water Reactors, THERMEX: Thermal Limits Methodology Summary Description, January 1987.

131. ANP-3295 Revision 3, "Monticello Licensing Analysis for EFW (EPU/MELLLA+)," February 2016.

132. ANP-3213 Rev 1, "Monticello Fuel Transition Cycle 28 Reload Licensing Analysis (EPU/MELLLA)," June 2013.

133. NEDE-33284 Supplement 1P-A, Revision 1, "Marathon-Ultra Control Rod Assembly", March 2012.

FIGURES

Figure 3.2-1 Power Flow Operating Map

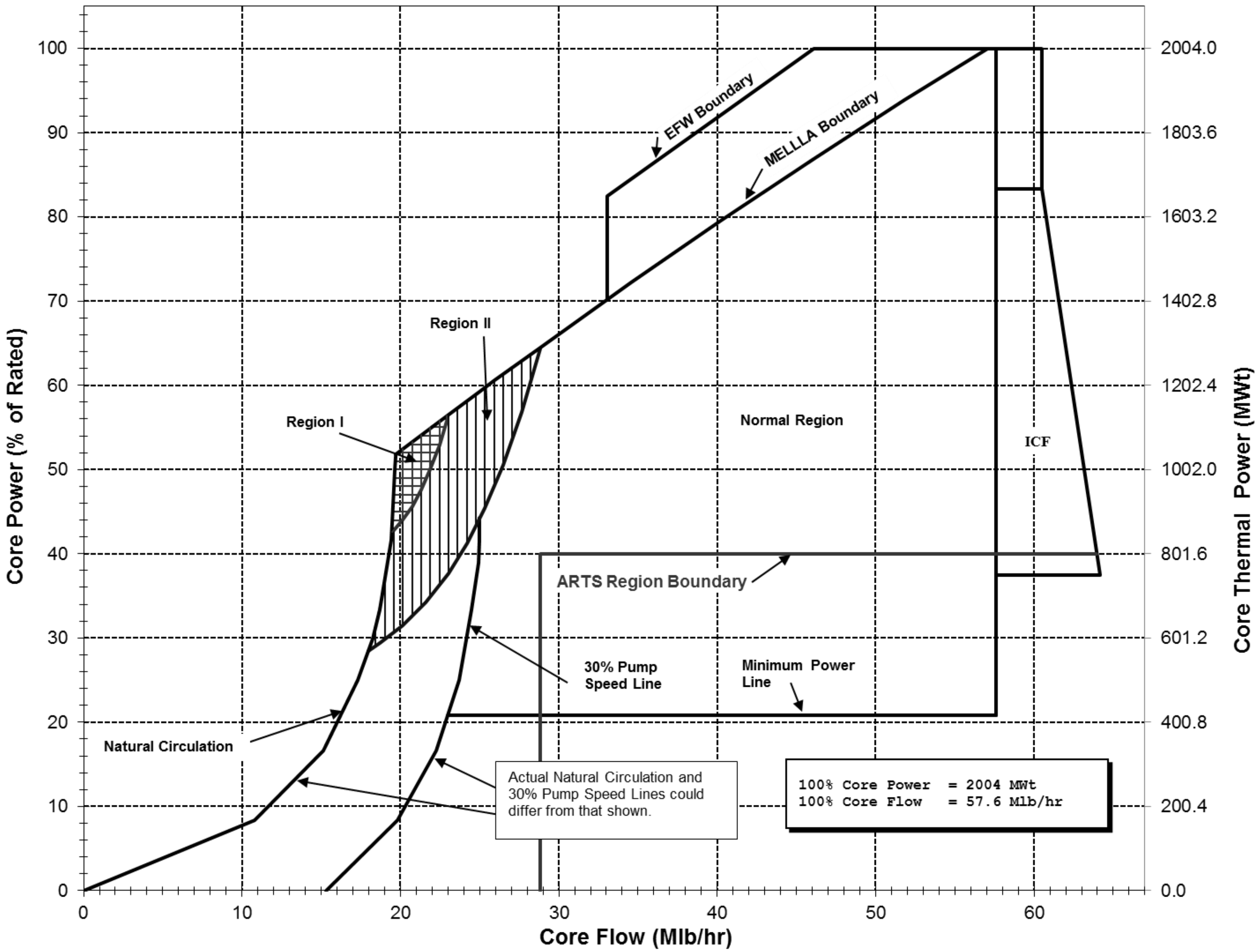

Figure 3.3-1 Envelope of Doppler Coefficient Versus Temperature, E= 200 MWd/t

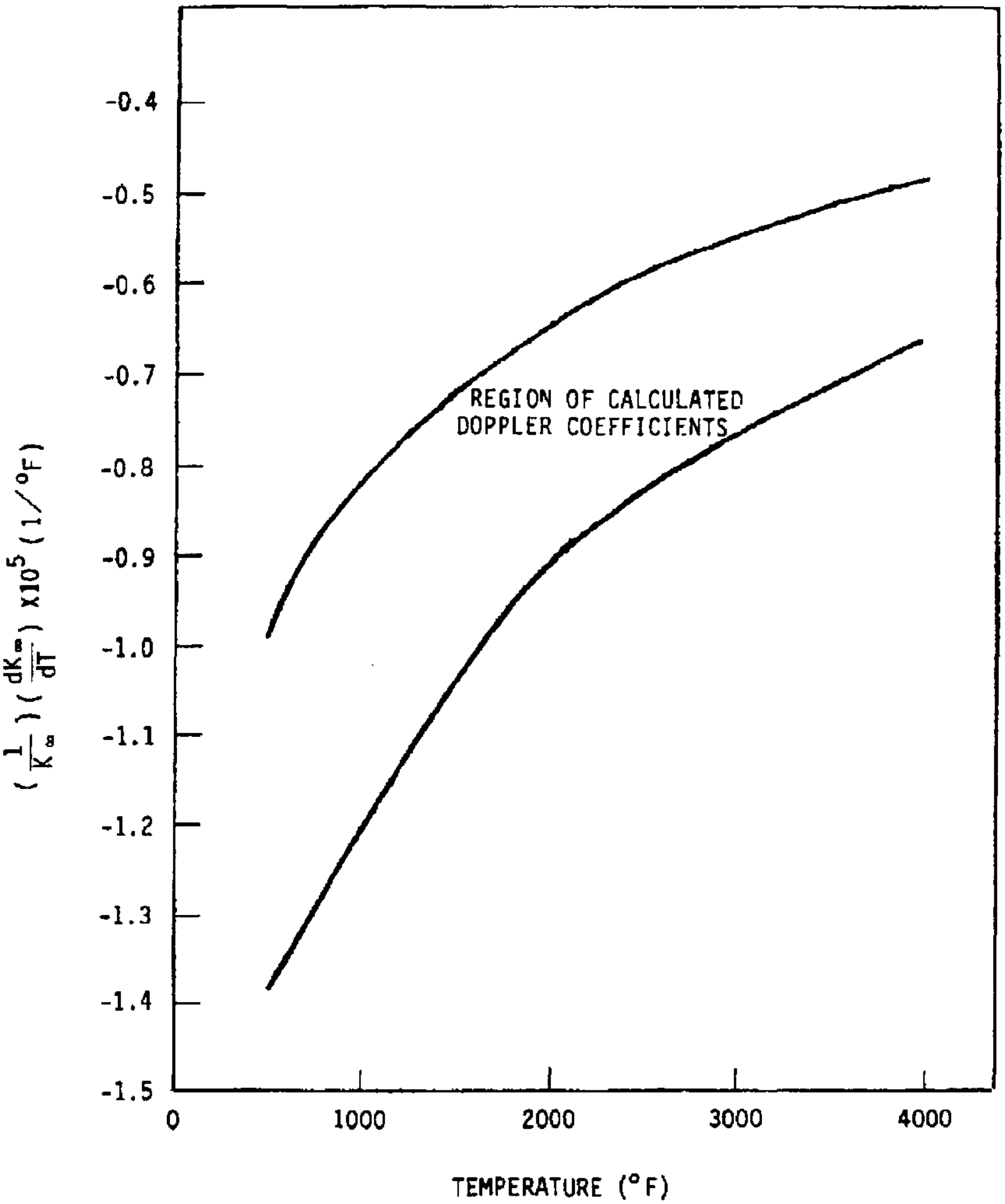

Figure 3.3-2 Envelope of Doppler Coefficient Versus Temperature, E= 15,000 MWd/t

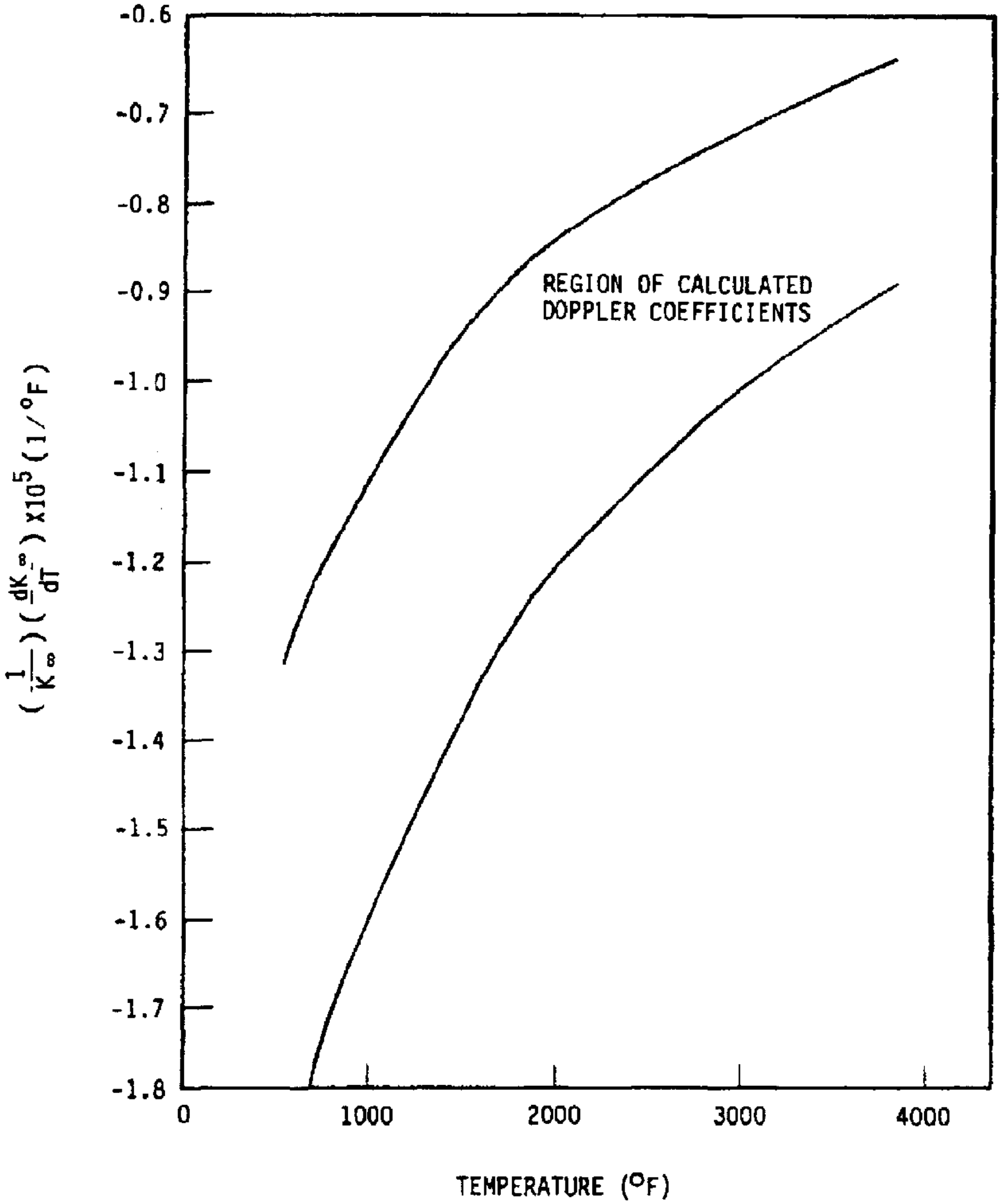

Figure 3.3-3 Moderator Void Reactivity Coefficient as a Function of Void Percentage and Time of Life

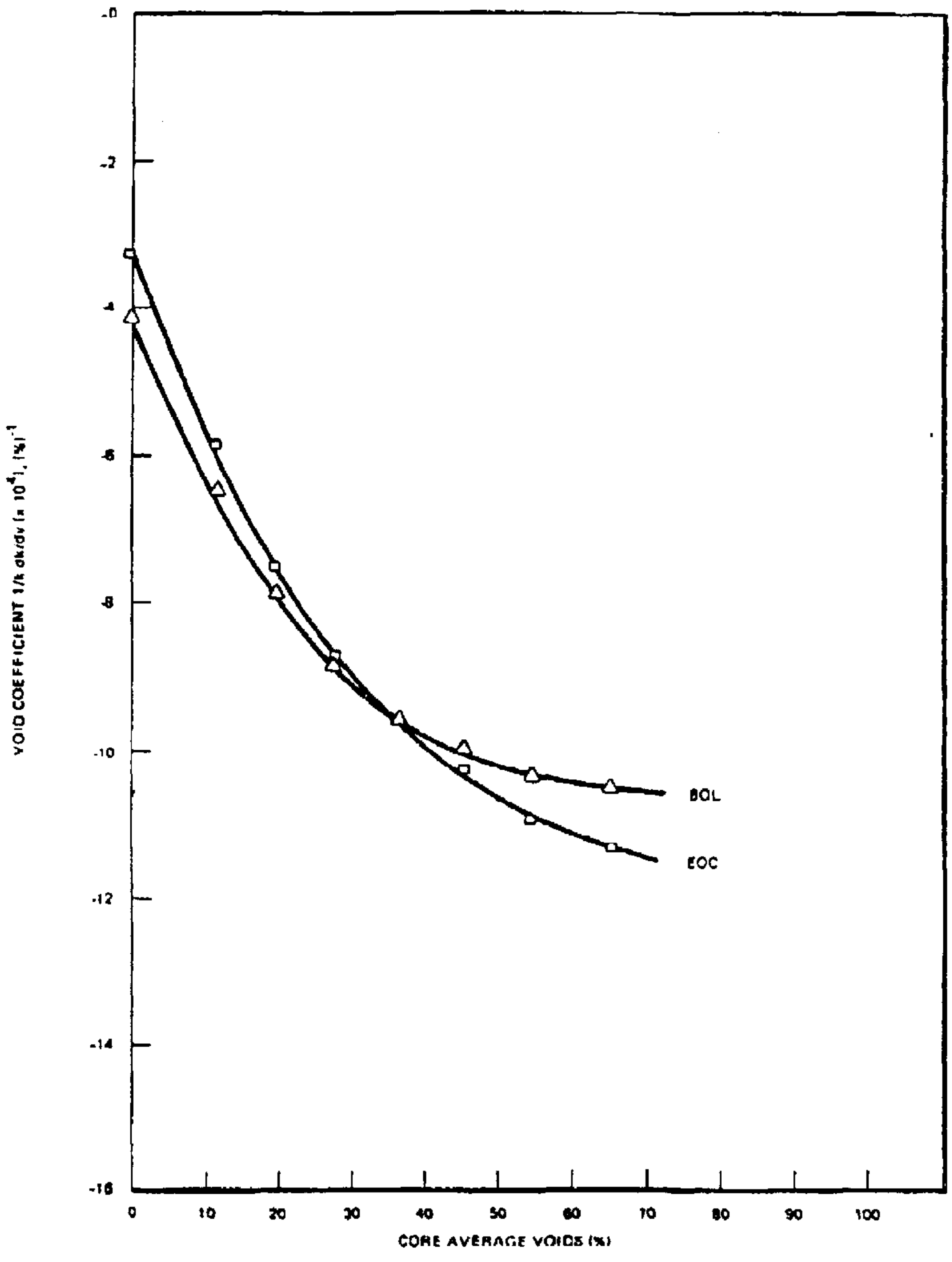

Figure 3.3-4 Xenon Reactivity Buildup After Shutdown, Beginning of Life

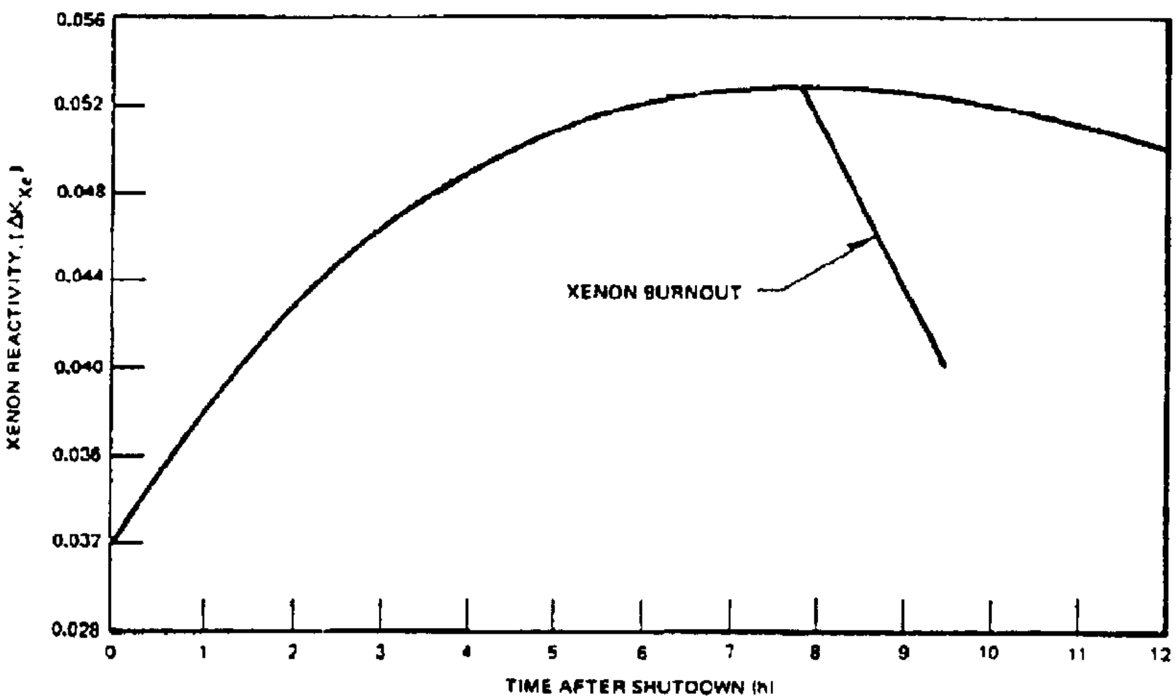

Figure 3.4-1 Typical Core Cell

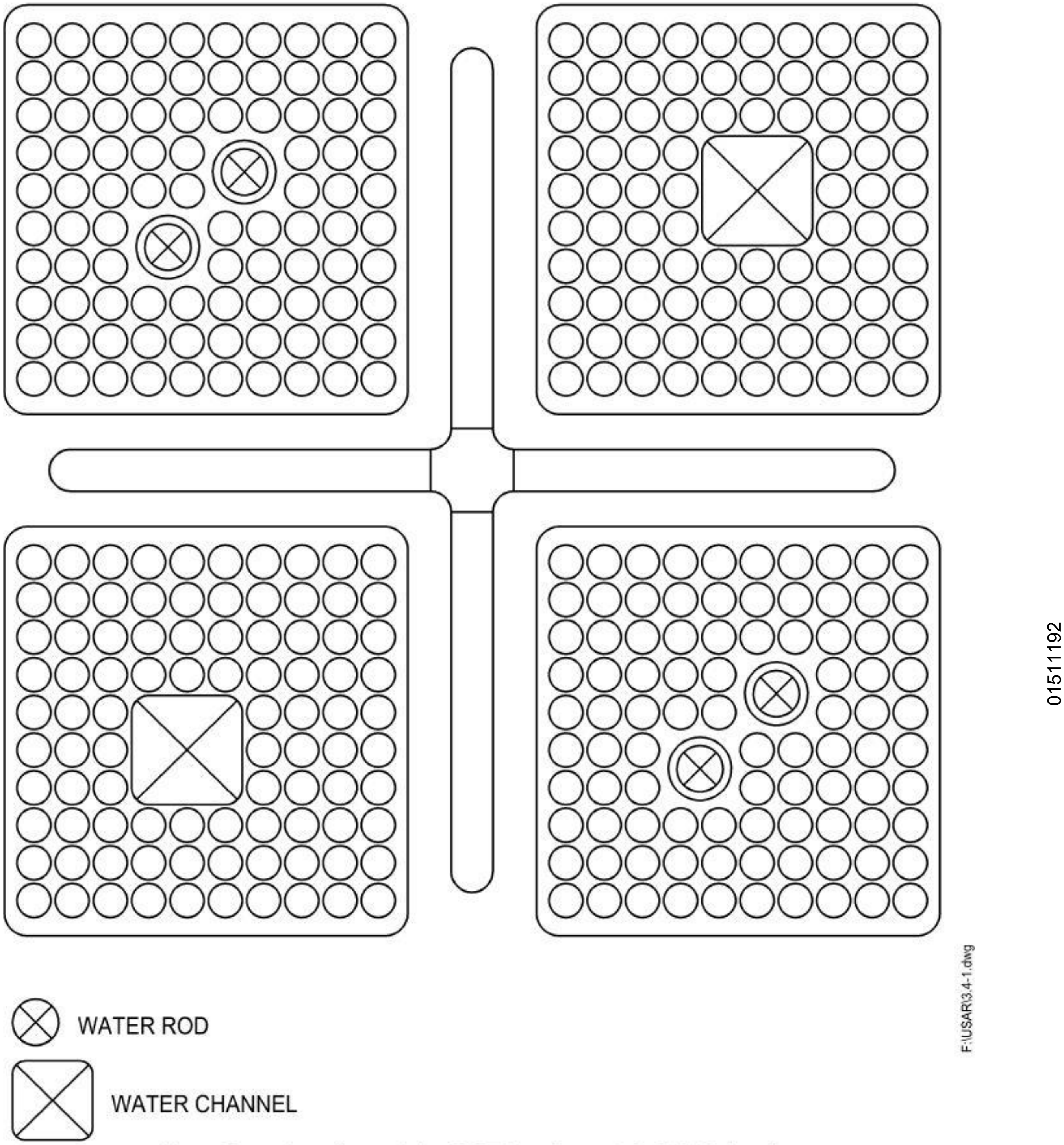

Note: Example cell containing 2 GE bundles and 2 AREVA bundles.

Figure 3.4-2 Schematic of Four Bundle Cell Arrangement

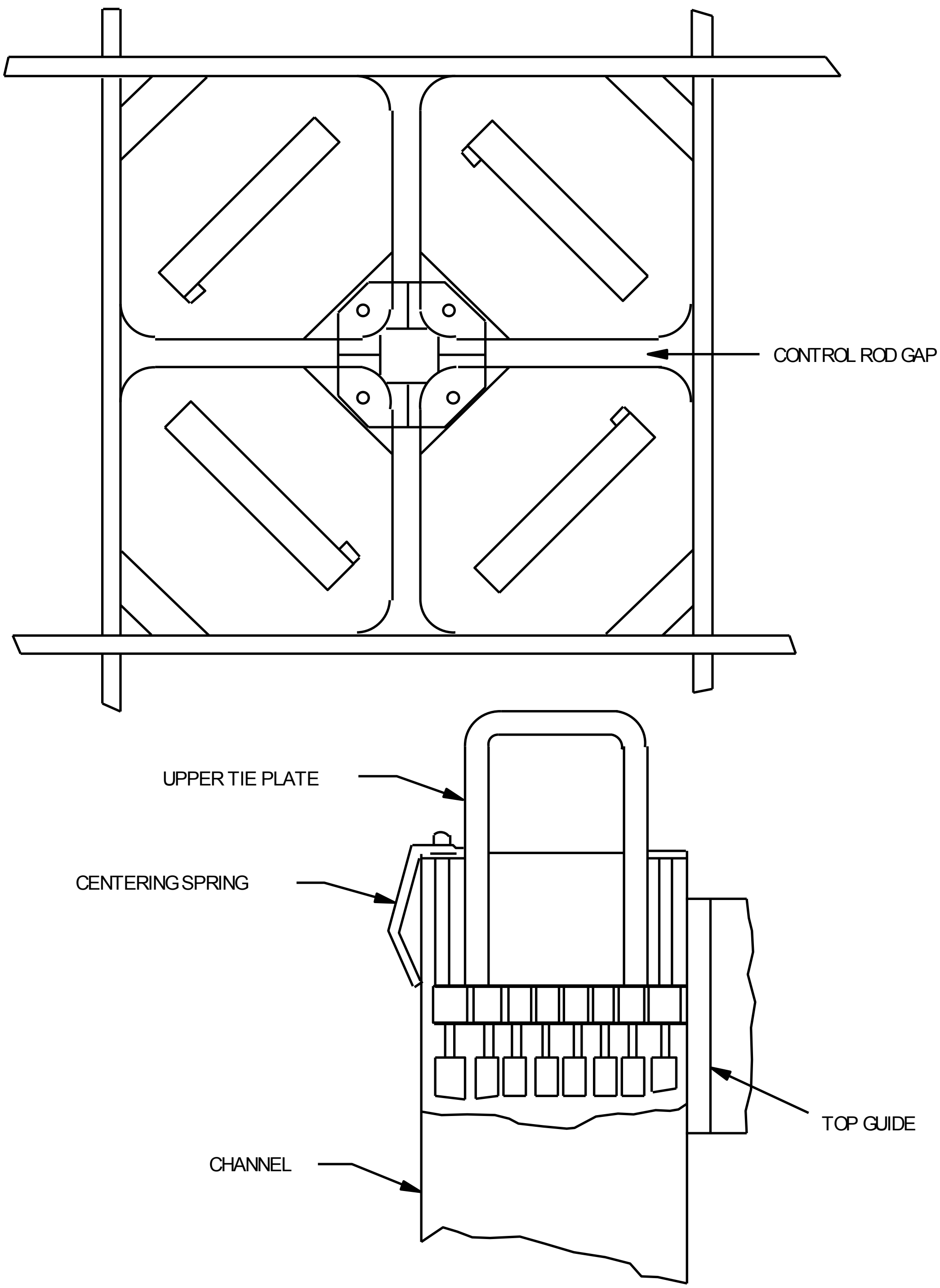

usar3.4-2

Figure 3.4-3 Typical GE BWR Fuel Assembly

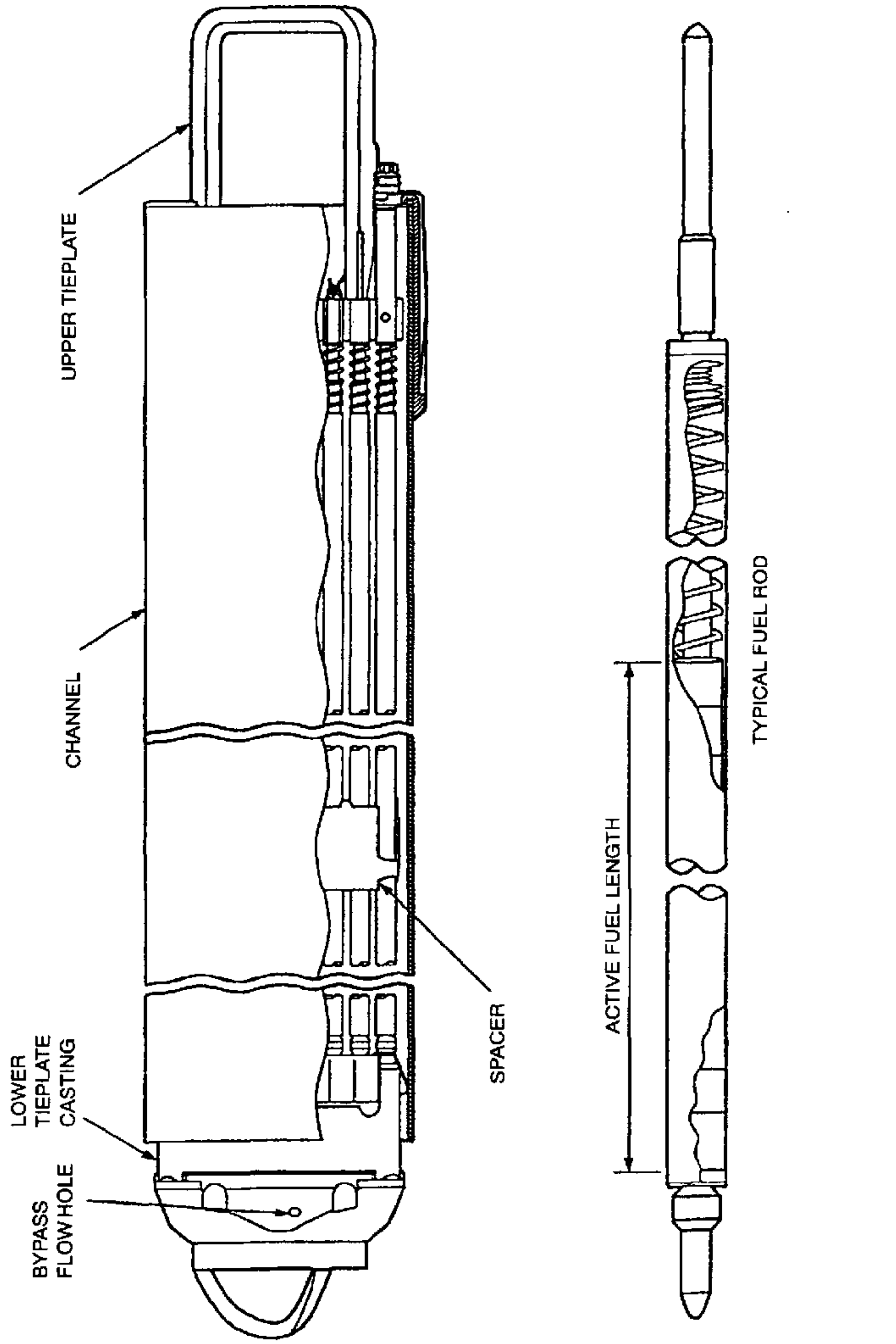

Figure 3.4-4 AREVA 10XM Fuel Assembly

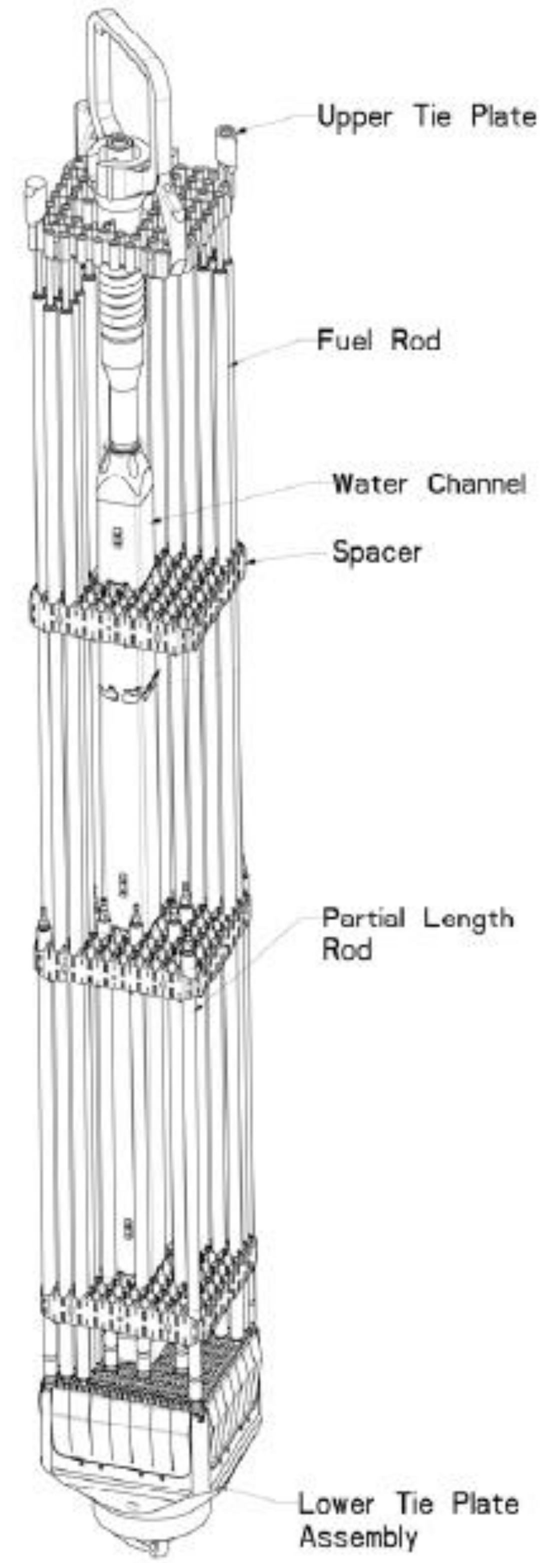

01511192

Figure 3.5-1 Control Rod Assembly Isometric

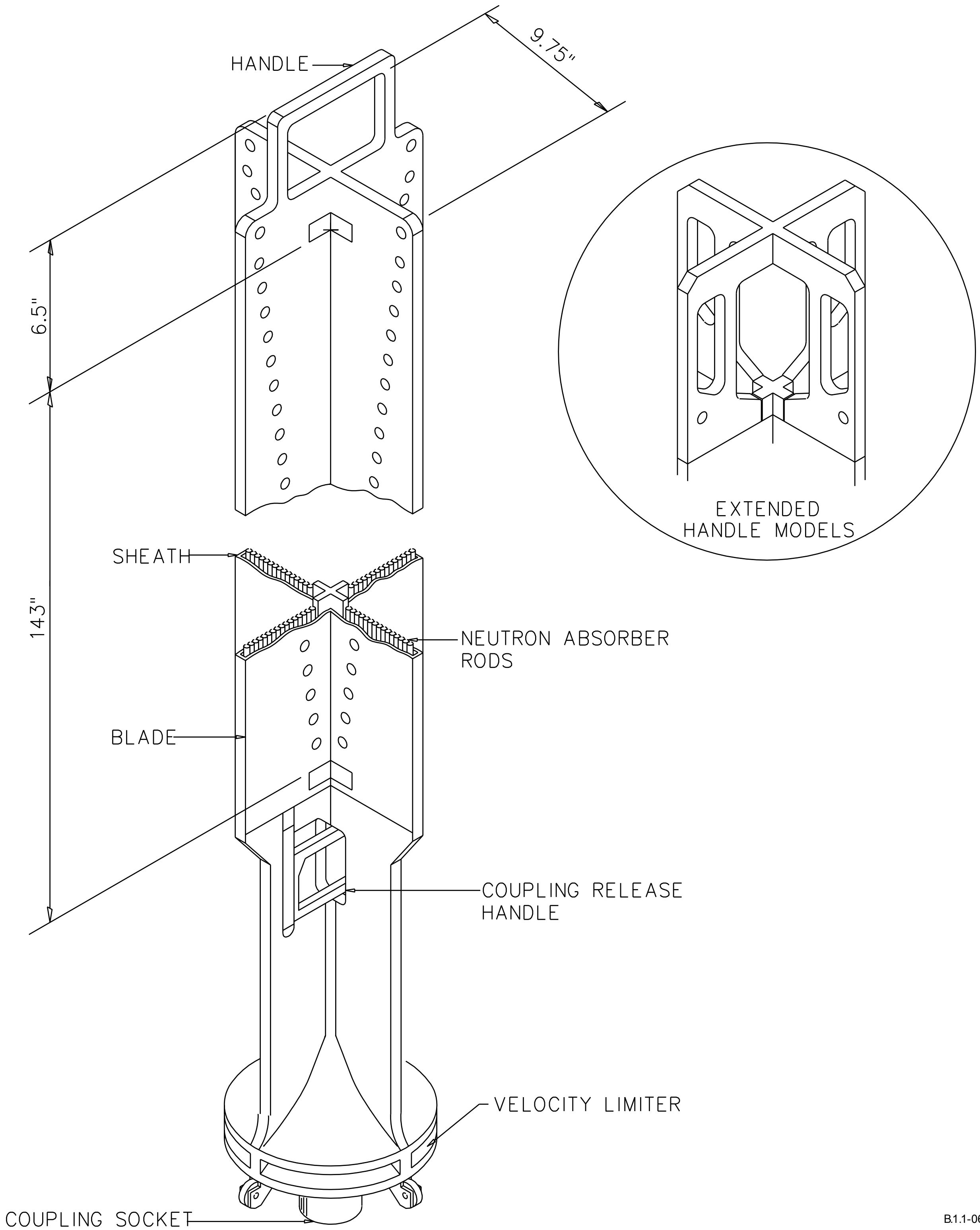

B.1.1-06.02-3

Figure 3.5-1a Duralife - 230 Control Blade

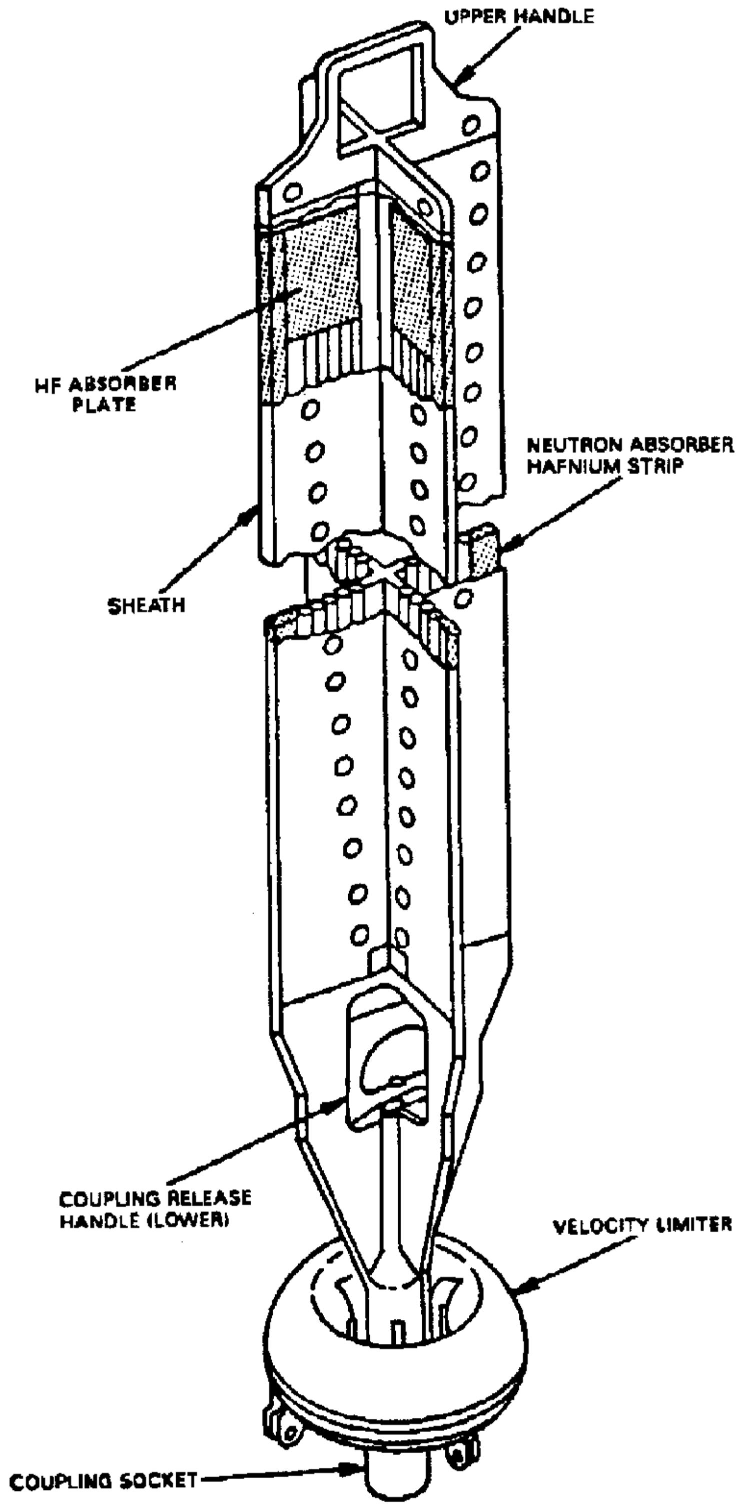

Figure 3.5-2 Control Rod Assembly and Drive Coupling Isometric

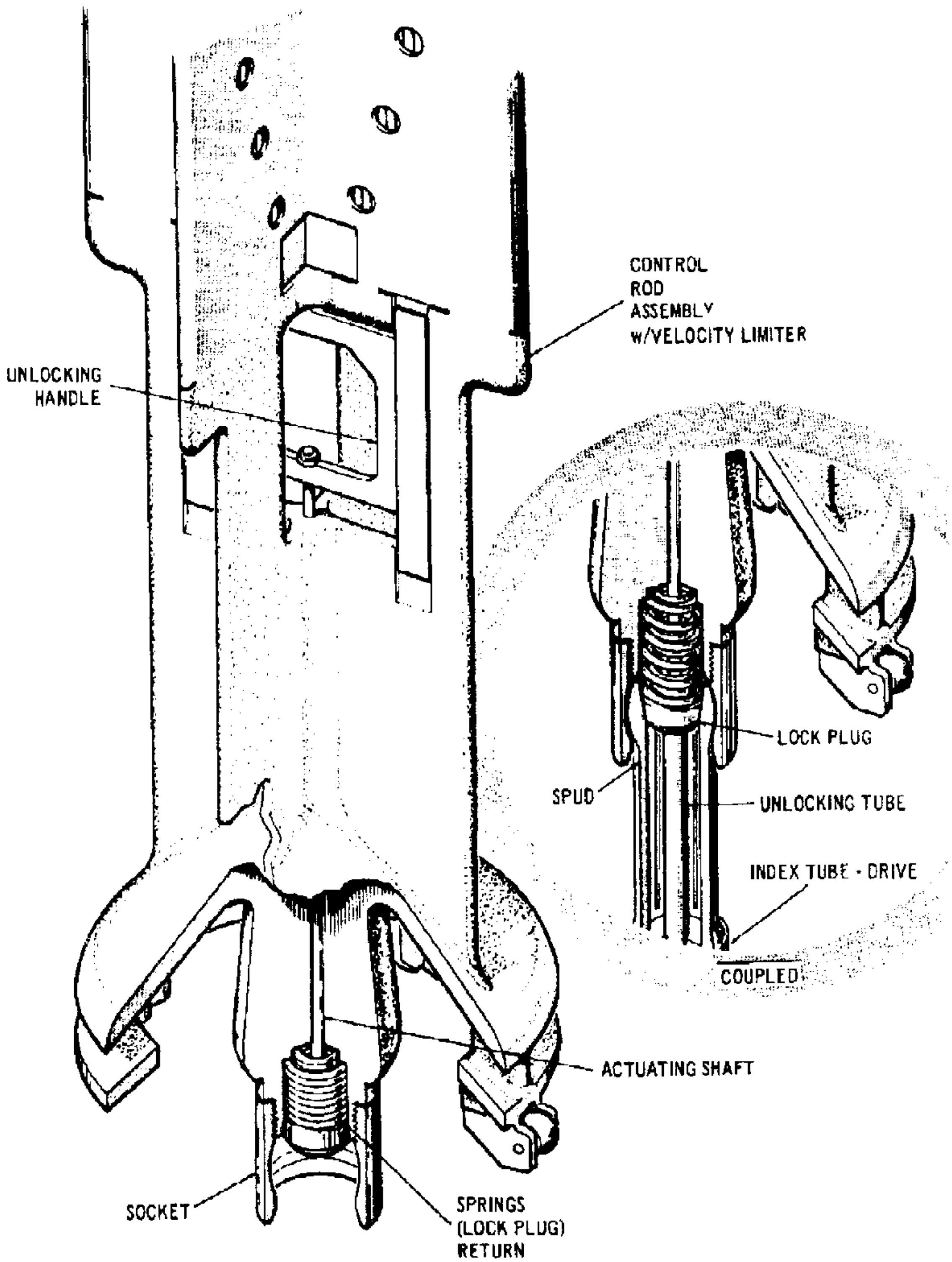

Figure 3.5-2a Hybrid I Control Rod (D-160) Assembly

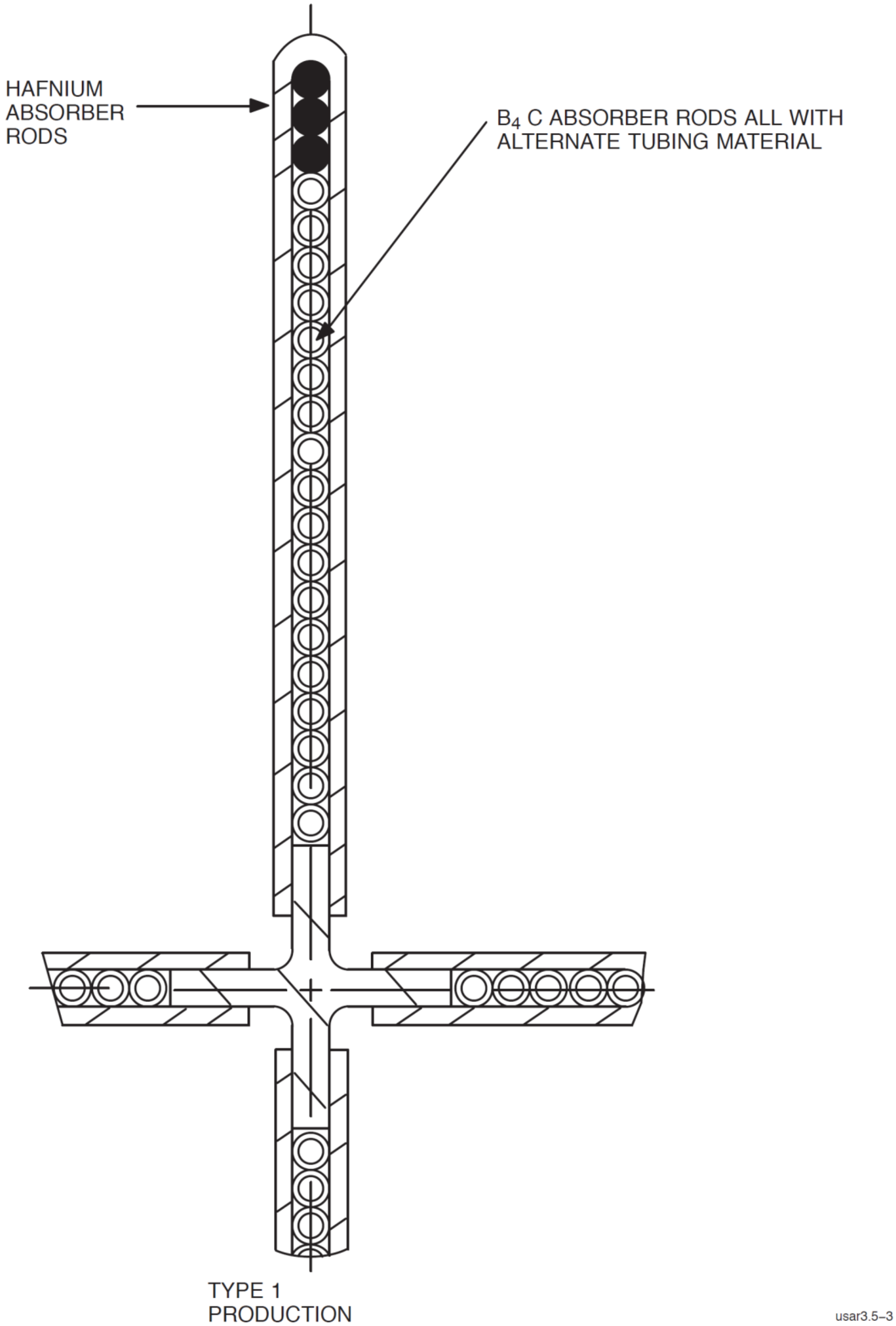

Figure 3.5-3 Control Rod Drive Mechanism Isometric

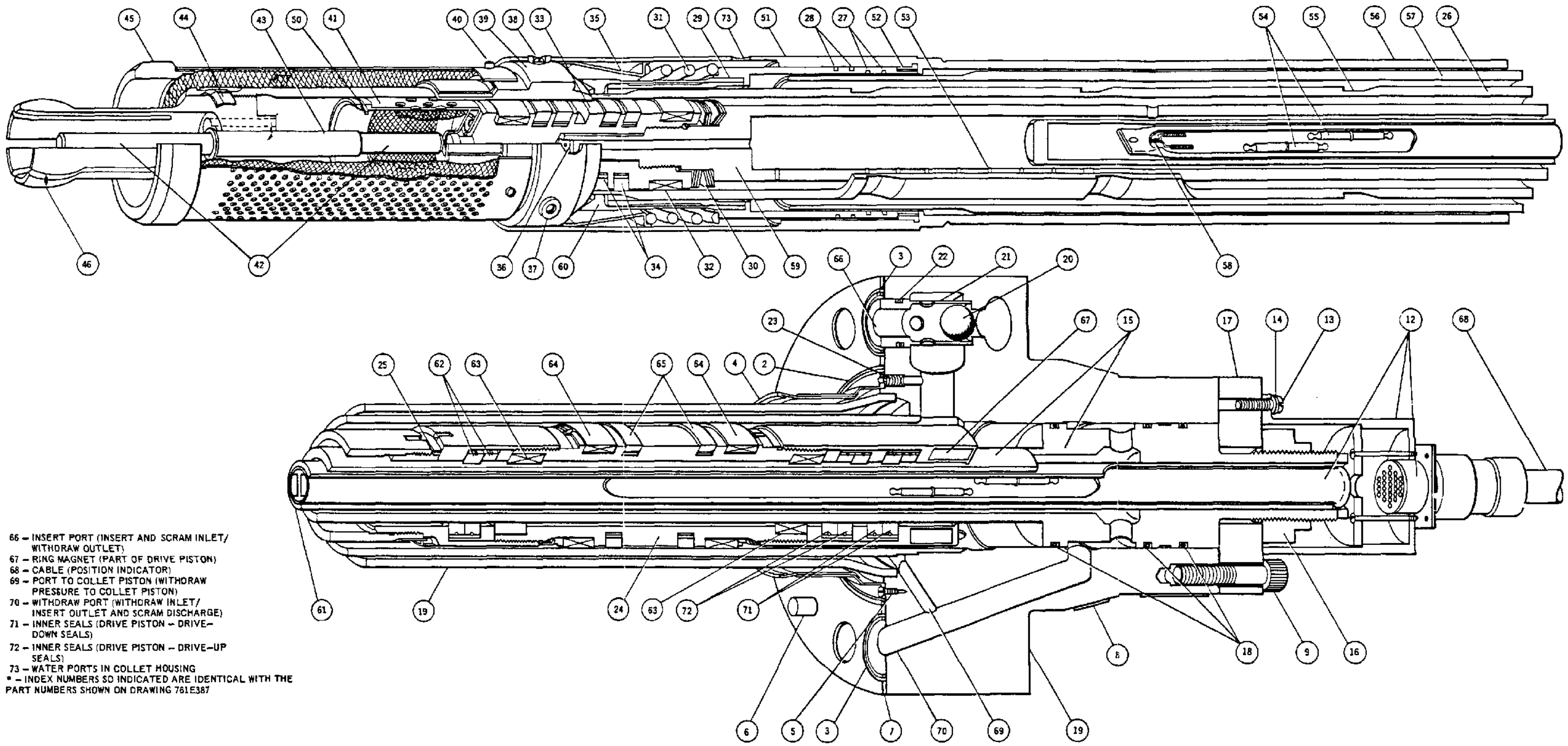

*2 – O–RING (CRD FLANGE FACE)
*3 – O–RING (INSERT AND WITHDRAW PORTS)
*4 – STRAINER
*5 – FLAT HEAD SCREW (STRAINER–MOUNTING)
*6 – DOWEL ALIGNMENT PIN
*7 – O–RING SPACER
*8 – NAMEPLATE
*9 – SOCKET–HEAD CAP SCREW (RING FLANGE MOUNTING)
*12 – POSITION INDICATOR PROBE
*13 – FILLISTER–HEAD SCREW (POSITION INDICATOR PROBE MOUNTING)
*14 – LOCKWASHER (FOR PART 13)
*15 – PISTON TUBE
*16 – NUT (PISTON TUBE)
*17 – RING FLANGE
*18 – O–RING (PISTON TUBE)
*19 – CYLINDER, TUBE, AND FLANGE
*20 – BALL (CHECK VALVE)
*21 – BALL RETAINER
*22 – O–RING (BALL RETAINER)
*23 – SET SCREW PLUG (COOLING WATER ORIFICE)
*24 – DRIVE PISTON
*25 – BAND
*26 – INDEX TUBE
*27 – SEAL RING (COLLET PISTON – INTERNAL)
*28 – SEAL RING (COLLET PISTON – EXTERNAL)
*29 – COLLET AND PISTON
*30 – SPRING WASHERS
*31 – COLLET SPRING
*32 – SPLIT BUSHING (STOP PISTON)
*33 – STOP PISTON
*34 – SEAL RING (STOP PISTON)
*35 – BARREL
*36 – COTTER PIN (STOP PISTON)
*37 – PLUG (GUIDE CAP)
*38 – FILLISTER–HEAD SCREW (GUIDE CAP PLUG MOUNTING)
*39 – GUIDE CAP
*40 – DRILLED FILLISTER–HEAD SCREW (OUTER FILTER MOUNTING)
*41 – INNER FILTER
*42 – ROD
*43 – TUBE
*44 – BAND
*45 – FILTER (OUTER)
*46 – SPUD
*50 – SEAL RING (INNER FILTER)
51 – COLLET HOUSING (PORTION OF OUTER TUBE)
52 – SPACER (PART OF CYLINDER, TUBE, AND FLANGE)
53 – BUFFER ORIFICES IN PISTON TUBE (TYPICAL)
54 – POSITION INDICATOR SWITCHES
55 – INDEX TUBE NOTCH
56 – OUTER TUBE (PART OF CYLINDER, TUBE, AND FLANGE)
57 – INNER CYLINDER (PART OF CYLINDER, TUBE, AND FLANGE)
58 – THERMOCOUPLE (PART OF POSITION INDICATOR PROBE)
59 – STUD (PORTION OF PISTON TUBE)
60 – COLLET FINGER (PART OF COLLET AND PISTON)
61 – INDICATOR TUBE (PART OF PISTON TUBE)
62 – INNER SEALS (DRIVE PISTON–BUFFER SEALS)
63 – INTERNAL BUSHING (DRIVE PISTON)
64 – EXTERNAL BUSHING (DRIVE PISTON)
65 – OUTER SEALS (DRIVE PISTON)
66 – INSERT PORT (INSERT AND SCRAM INLET/WITHDRAW OUTLET)
67 – RING MAGNET (PART OF DRIVE PISTON)
68 – CABLE (POSITION INDICATOR)
69 – PORT TO COLLET PISTON (WITHDRAW PRESSURE TO COLLET PISTON)
70 – WITHDRAW PORT (WITHDRAW INLET/INSERT OUTLET AND SCRAM DISCHARGE)
71 – INNER SEALS (DRIVE PISTON – DRIVE–DOWN SEALS)
72 – INNER SEALS (DRIVE PISTON – DRIVE–UP SEALS)
73 – WATER PORTS IN COLLET HOUSING
* – INDEX NUMBERS SO INDICATED ARE IDENTICAL WITH THE PART NUMBERS SHOWN ON DRAWING 761E387

Figure 3.5-4 Control Rod Drive Simplified Component Illustration

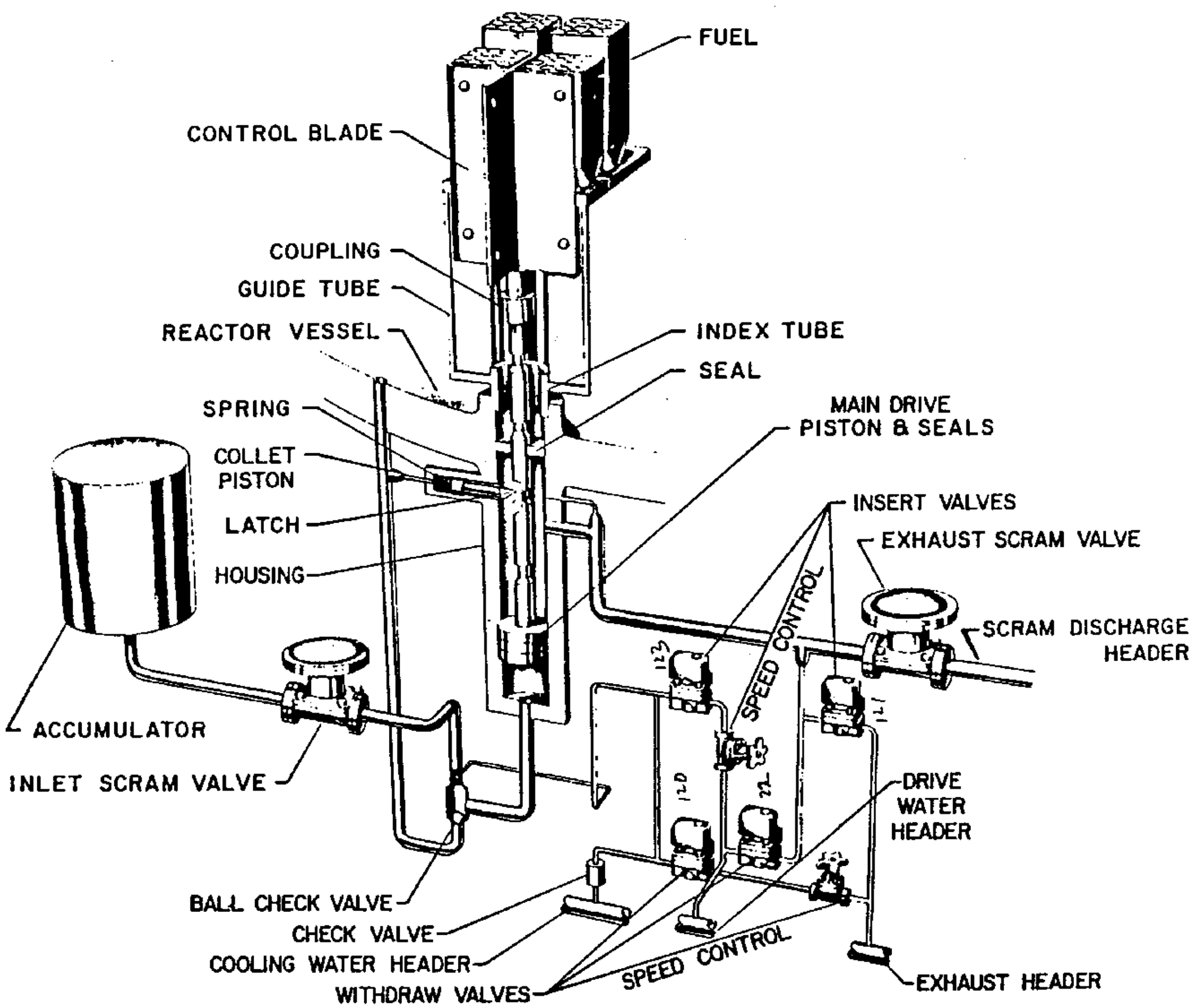

Figure 3.5-7 Hydraulic Control Unit Isometric

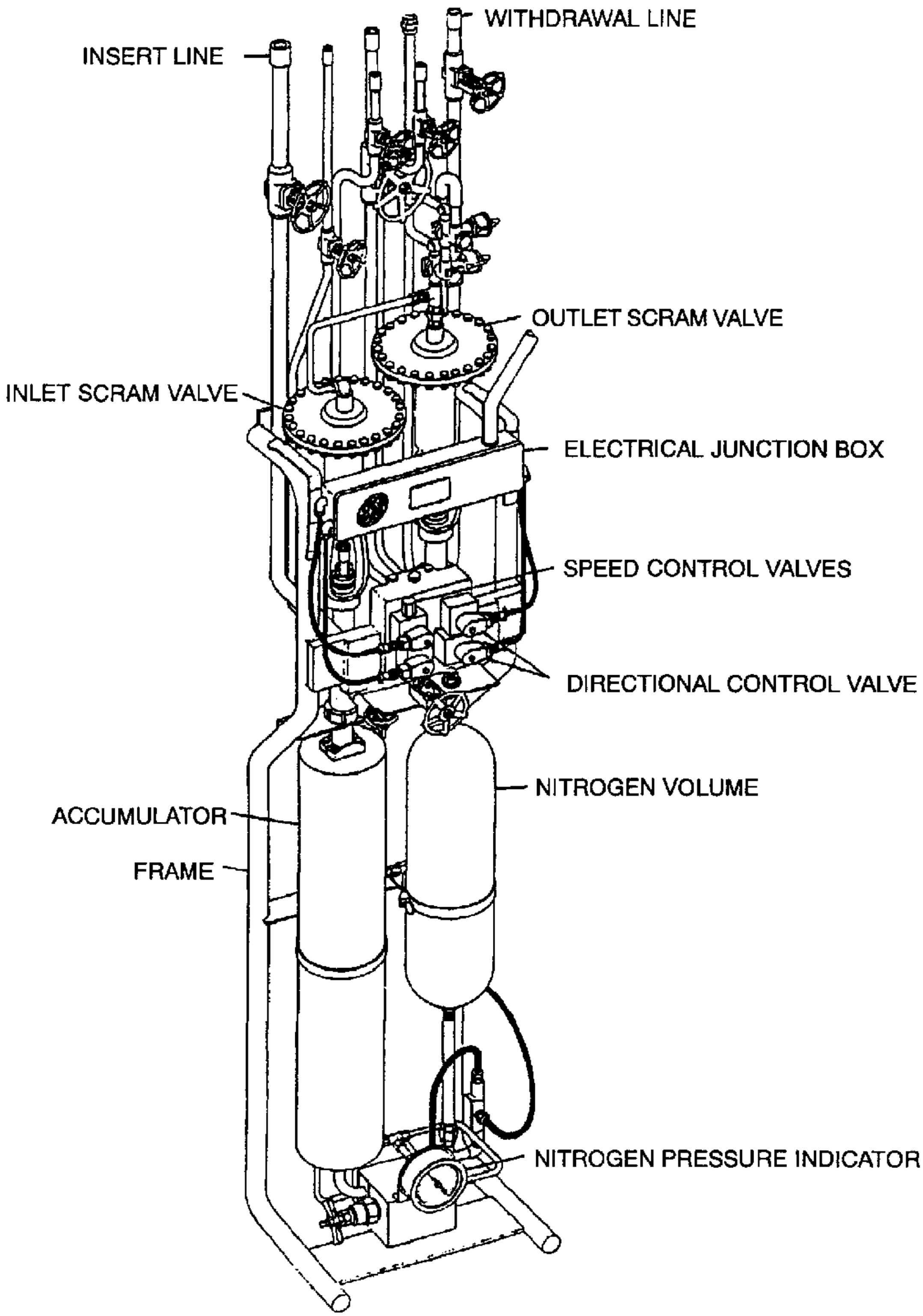

Figure 3.6-1 Reactor Vessel Internals

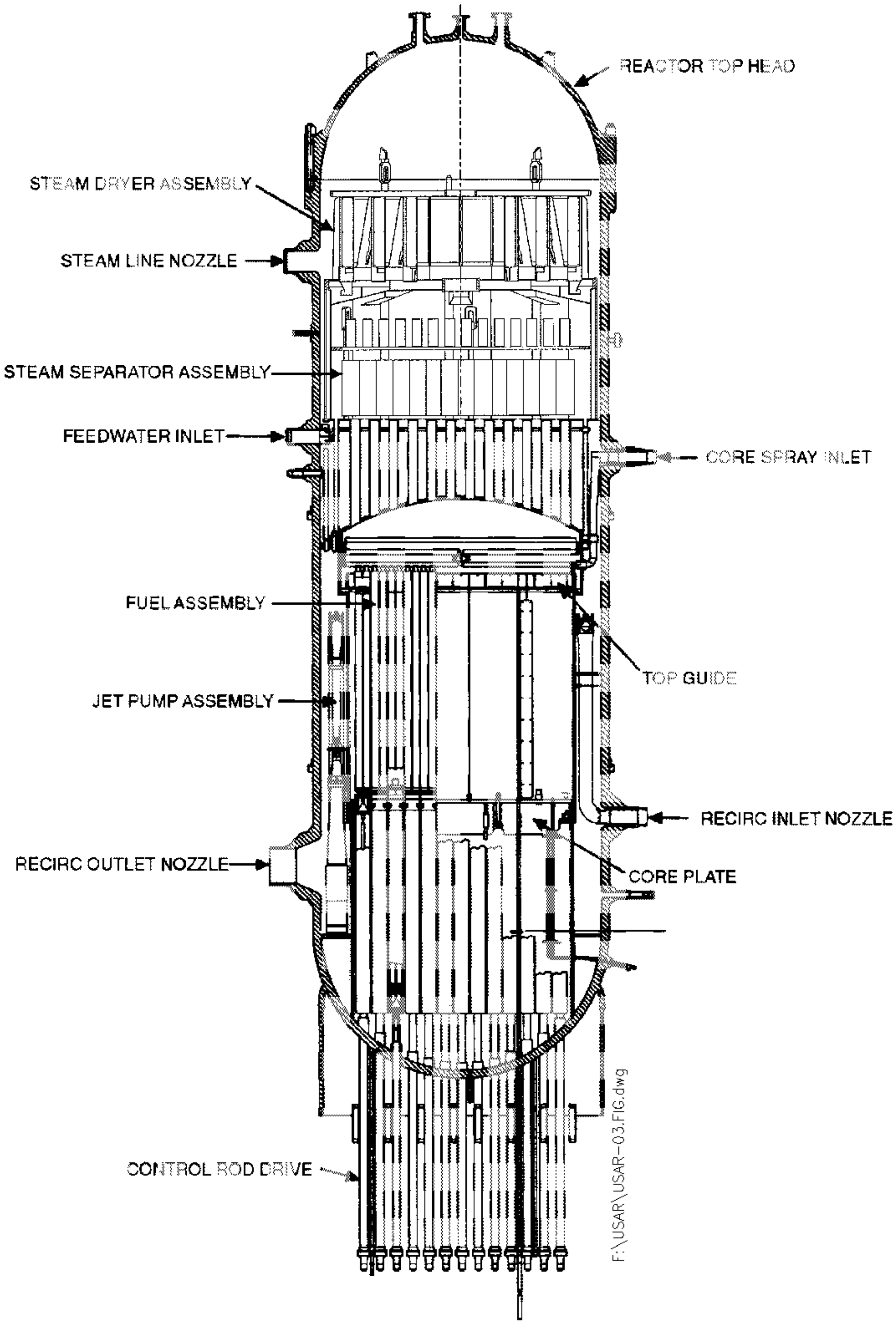

Figure 3.6-2 Reactor Vessel and Internal Components Schematic

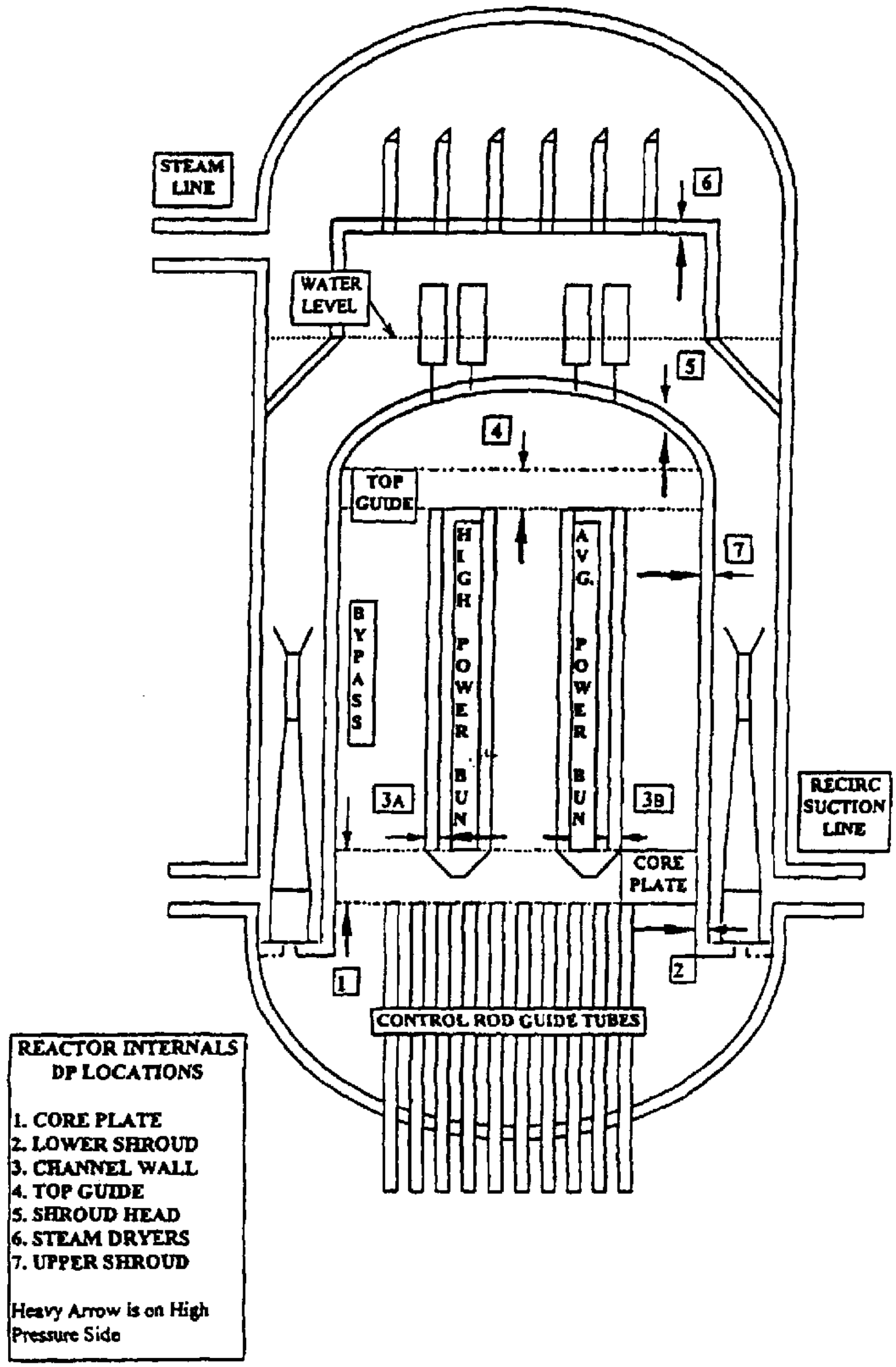

Figure 3.6-5 Dresden-2 Shroud Support Plate Segment Fatigue Analysis